



UNIVERSITEIT VAN PRETORIA
UNIVERSITY OF PRETORIA
YUNIBESITHI YA PRETORIA

The Effects of Age and Wear on the Stiffness Properties of an SUV tyre

by

Kraig Richard Shipley Wright

Submitted in partial fulfilment of the requirements for the degree

**Master of Engineering
(Mechanical Engineering)**

in the Faculty of

Engineering, Built Environment and Information Technology (EBIT)

at the

**University of Pretoria,
Pretoria**

November 2016

SUMMARY

Title: The Effects of Age and Wear on the Stiffness Properties of an SUV tyre

Author: Kraig Richard Shipley Wright

Study Leader: Prof. P. S. Els

Department: Mechanical and Aeronautical Engineering, University of Pretoria

Degree: Masters in Engineering (Mechanical Engineering)

With an increasing need for accurate full vehicle models, a sensitivity analysis of the modelling of tyres depending on their age and wear was conducted. This included a sensitivity analysis into the accuracy of acquiring the tyre stiffnesses on a static test setup.

An FTire model is developed with the aim to update this model with basic tests to give a more accurate representation of the aged or worn tyre. A well-researched and documented method is used to artificially age the tyres. During the aging process the tyre was statically tested to monitor the potential changes in characteristics. Tyres were also worn on a dynamic test setup and periodically tested to monitor the property changes. These tests included both static and dynamic measurements.

The results indicate that the vertical and longitudinal stiffnesses of the tyre have convincing dependencies on the age and wear of the tyre. While the aging process was a trustworthy method, the wear process created irregular wear across and around the tyre subsequently skewing the results. Simple methods of updating the FTire tyre model without re-parameterising the model completely, was found to be effective in accounting for age and wear

ACKNOWLEDGEMENTS

I would like to extend my gratitude to:

- Professor Els, for his guidance and teachings throughout my undergraduate and postgraduate career.
- My parents, Janine and Richard Wright, who have always supported my endeavours.
- My sister, Caryn Wright, for her support and ensuring I was always an early bird during my postgraduate studies.
- My friend and colleague, Joachim Stallmann, for his never-ending assistance and guidance.
- My work-colleagues, Peet Kruger, Wietsche Penny, Glenn Guthrie, Johann Clarke, Jacob and Khulu for their assistance in the manufacturing and assembling of the static tyre test rig.
- My friend and colleague, Gerrie Heymans for inspiring me to work hard through his own example.
- My friend, Leshanti Rajh Gopaul, for her continuous support and the amazing editing of my reports.
- My friend, Kirstin Bosch, for always believing in me.

TABLE OF CONTENTS

Summary	I
Acknowledgements	II
Table of Contents	III
List of Figures	VII
List of Tables	X
List of Abbreviations and Symbols	XI
Abbreviations	XI
Roman Symbols	XI
Greek Symbols	XII
Subscripts	XII
1 Introduction and Literature Review	1
1.1 Introduction	1
1.2 FTire Parameterisation	2
1.2.1 Parameterisation	2
1.2.2 General Data Required	4
1.2.3 Identification and Validation	6
1.2.4 Updatable Parameters	6
1.3 Aging of Tyres	7
1.3.1 Oxidation	7
1.3.2 Temperature Dependence	9
1.3.3 Effects of Aging on Forces and Moments	9
1.4 Accelerated Aging of Tyres	11
1.4.1 Oven Based Aging	12
1.4.2 Field Based	16
1.4.3 Correlation of Oven-Aged and Field Tyres	17
1.5 Wearing of Tyres	20
1.5.1 Factors Affecting Tyre Wear	20
1.5.2 Effect of Tyre Wear on Rolling Resistance	21
1.6 Method of Comparing Stiffnesses	22

TABLE OF CONTENTS

1.7	Subject Tyre	22
1.8	Concluding Remarks	23
1.9	Problem Statement	23
1.10	Hypothesis	24
1.11	Project Overview	24
1.12	Dissertation Summary	24
2	Test Setup	26
2.1	Introduction	26
2.2	Static Tyre Test Rig	26
2.2.1	Tests to be completed	26
2.2.2	Equipment	26
2.2.3	Tread Profile Measurement	31
2.3	Dynamic Tyre Test Trailer	31
2.3.1	Tests to be completed	32
2.3.2	Data Not Acquired	32
2.3.3	Equipment	32
2.3.4	Wheel Slip Calculation	34
2.4	Concluding Remarks	35
3	Testing Method Sensitivity	36
3.1	Introduction	36
3.2	Cycle Sensitivity	37
3.3	Input Waveform	37
3.4	Loading Velocity Sensitivity	38
3.5	Different Test Setup	38
3.6	Different Tyres	39
3.7	Small Temperature Variations	40
3.8	Contact Surface	40
3.9	Concluding Remarks	42
4	FTire Parameterisation	43

TABLE OF CONTENTS

4.1	Checking-in of Data	43
4.1.1	Tyre Geometrical Data	44
4.1.2	Tyre Footprints	44
4.1.3	Tyre Static and Dynamic Data	46
4.2	Initial Validation	48
4.3	Identification and Final Validation	48
4.3.1	Process	49
4.3.2	Steady-State Test Identification	49
4.3.3	Dynamic Stiffness Tests	52
4.3.4	Footprints	55
4.3.5	Additional Validation Figures	57
4.4	Concluding Remarks	57
5	Aging	58
5.1	Introduction	58
5.2	Experimental Details and Analysis	58
5.2.1	Method of Comparing Stiffnesses	58
5.2.2	Tyre Age Calculation	59
5.2.3	Tyre Aging Procedure	60
5.3	Shore A Hardness Effects	60
5.3.1	Measurement Device and Method	60
5.3.2	Results	61
5.3.3	Discussion of Results	61
5.3.4	Application in FTire	62
5.4	The Influence of Inflation Pressure	62
5.4.1	Results	62
5.5	Aging Stiffness Test Results	63
5.5.1	Vertical Stiffness on a Flat Surface	64
5.5.2	Vertical Stiffness with a Cleat	68
5.5.3	Longitudinal Stiffness	72
5.6	Discussion of Results	74
5.7	Potential FTire Model Updates	76
5.7.1	Shore A Hardness Update	76
5.8	Concluding Remarks on Aging	79
6	Wear	81

TABLE OF CONTENTS

6.1	Introduction	81
6.2	Miscellaneous Property Changes	81
6.2.1	Tread Profile	81
6.2.2	Mass	83
6.2.3	Tread Wear Assumption Effects	84
6.2.4	Application in FTire	84
6.3	Run-in Stiffness Comparison	84
6.3.1	Stiffness Test Results	84
6.3.2	Discussion of Results	86
6.4	Flat Spot Stiffness Comparison	87
6.4.1	Stiffness Test Results	87
6.4.2	Footprint Comparison	88
6.4.3	Discussion of Results	88
6.5	Tread Wear Stiffness Test Results	89
6.5.1	Vertical Stiffness on a Flat Surface	90
6.5.2	Vertical Stiffness on a Cleat	94
6.5.3	Longitudinal Stiffness	99
6.6	Discussion of Results	100
6.7	Potential FTire Model Updates	100
6.7.1	Mass and Tread Depth Update	101
6.8	Concluding Remarks	104
7	Conclusion and Recommendations	106
7.1	Conclusion	106
7.2	Recommendations	107
8	References	108
Appendix A		111
8.1	Aging Tables	111
8.2	Wearing Tables	112

LIST OF FIGURES

Figure 1.1 - Oil component as a function of time and mileage (Kataoka, et al., 2003)	8
Figure 1.2 - Percentage swelling as a function of time and mileage (Kataoka, et al., 2003)	8
Figure 1.3 - Specimen stress values as a function of time and mileage (Kataoka, et al., 2003)	10
Figure 1.4 - Specimen strain and Shore A hardness as a function of time and mileage (Kataoka, et al., 2003)	11
Figure 1.5 - Typical construction of passenger car tyre (Baldwin, et al., 2006)	12
Figure 1.6 - Tyre wedge strain data for aging at various temperatures (Baldwin, 2003)	14
Figure 1.7 - Percentage change in crosslink density between air and N ₂ /O ₂ inflation media (Baldwin, 2003)	15
Figure 1.8 - Aging rate as a function of oven temperature (Baldwin, et al., 2005)	15
Figure 1.9 - Modulus of the wedge of rubber and peel strength of the skim rubber results for field tyres (Baldwin, et al., 2006)	17
Figure 1.10 - Elongation-to-break and peel strength of oven aged tyres at various aging temperatures (Bauer, et al., 2005)	18
Figure 1.11 - Dependency of aging rate as a function of different tyres (Bauer, et al., 2005)	19
Figure 1.12 - Shift factor obtained from oven aging and field aging (Bauer, et al., 2005)	19
Figure 1.13 - Comparative histogram of the sensitivity of the parameters influencing tyre wear (Yong, et al., 2011)	21
Figure 1.14 - Change in rolling resistance between new and fully worn tyre	22
Figure 2.1 - Isometric view of STTR in position for vertical and longitudinal stiffness test	27
Figure 2.2 - Plan view of STTR in position for vertical and longitudinal stiffness test	27
Figure 2.3 - Isometric view of the STTR in position for the lateral stiffness test	28
Figure 2.4 - Side view of STTR in position for lateral stiffness test	29
Figure 2.5 - Wheel Force Transducer (WFT) mounted onto the sample tyre rim	30
Figure 2.6 - Isometric view of the Dynamic Tyre Test Trailer	33
Figure 3.1 - Comparison of input waveform at 0.5 Hz loading velocity with vertical stiffness	37
Figure 3.2 - Comparison of four consecutive cycles at 0.1 Hz with vertical stiffness	36
Figure 3.3 - Comparison of input waveform velocity with vertical stiffness	38
Figure 3.4 - Comparison of vertical stiffness measured on two different test rigs	39
Figure 3.5 - Comparison of 4 of the same tyre with the vertical stiffness at 0 and 4° camber	40
Figure 3.6 - Comparison of minor changes in the tyre temperature with the vertical stiffness on a transverse cleat at -4° camber	41
Figure 3.7 - Comparison of two different contact surface friction coefficients at 1.5 and 2.5Bar inflation pressure with the vertical stiffness	41
Figure 4.1 - FTire/fit tyre estimate and geometrical data	43
Figure 4.2 - FTire/tools tread and carcass cross-section	44
Figure 4.3 - Calibration board	45

LIST OF FIGURES

Figure 4.4 - Footprint at 100% of the LI and -4 degrees camber	45
Figure 4.5 - Final scaled black and white footprint bitmap	46
Figure 4.6 - Vertical stiffness data filtering and sub-sampling	47
Figure 4.7 - Side force vs slip angle data filtering and sub-sampling	47
Figure 4.8 - Initial validation of footprints at 50% of the LI: 0° camber (Left), -4° camber (Right)	48
Figure 4.9 – Final FTire Validation - Vertical stiffness at 0° camber	49
Figure 4.10 - Final FTire validation - vertical stiffness on transverse cleat at 0° camber	50
Figure 4.11 - Final FTire Validation - vertical stiffness with longitudinal cleat at 0° camber	51
Figure 4.12 - Final FTire Validation - longitudinal stiffness	51
Figure 4.13 - Final FTire Validation - lateral stiffness	52
Figure 4.14 - Final FTire Validation - longitudinal force against longitudinal slip	53
Figure 4.15 - Final FTire Validation - lateral force against lateral slip angle at 0° camber	55
Figure 4.16 - Final FTire Validation - footprints at 0° camber	56
Figure 4.17 - Final FTire Validation - Footprints at -4 degrees camber	56
Figure 5.1 - Percentile change in Shore A hardness at the tread and sidewall whilst aging	61
Figure 5.2 - Vertical stiffness comparison of inflation pressure	63
Figure 5.3 - Vertical stiffness changes on a flat surface as the tyre ages	64
Figure 5.4 - Percentile change in deflection of aged tyre on a flat surface	65
Figure 5.5 - Footprint comparison at 0° camber at 100% of the LI - New Tyre (Left), Aged Tyre (Right)	65
Figure 5.6 - Vertical stiffness changes on a flat surface at -4° camber as the tyre ages	66
Figure 5.7 - Percentile change in deflection on a flat surface at -4° camber	67
Figure 5.8 - Footprint comparison at 4° camber at 100% of the LI - New Tyre (Left) and Aged Tyre (Right)	67
Figure 5.9 - Footprint comparison of 2.5 Bar Inflation at 4° camber at 50 % of the LI - New Tyre (Left) and Aged Tyre (Right)	68
Figure 5.10 - Vertical stiffness changes on a transverse cleat at 0° camber as the tyre ages	69
Figure 5.11 - Percentile change in deflection on a transverse cleat at 0° camber	70
Figure 5.12 - Vertical stiffness changes on a transverse cleat at -4 degrees camber as the tyre ages	70
Figure 5.13 - Vertical stiffness changes on a longitudinal cleat as the tyre ages	71
Figure 5.14 - Percentile change in deflection on a longitudinal cleat as the tyre ages	72
Figure 5.15 - Changes in longitudinal stiffness as the tyre ages	73
Figure 5.16 - Percentile change in longitudinal deflection as the tyre ages	73
Figure 5.17 - Percentile change in deflection of all test data with averages and a line of best fit	74
Figure 5.18 - Change in the hysteresis loop on a longitudinal cleat at different inflation pressures as the tyre ages	75
Figure 5.19 - Comparison of the validation of footprints with an update of the Shore A hardness in the tyre model. Left – final validation of new tyre; Middle – validation after Shore A update; Right – actual footprint after aging	77
Figure 5.20 - FTire tyre model Shore A hardness update effect on the various stiffness's tested	78
Figure 5.21 - Validation of the Shore A hardness updated tyre model on a transverse cleat at 0 and -4 degrees camber	79

LIST OF FIGURES

Figure 6.1 - Irregularity in tread profile around the tyre after final process of wearing	82
Figure 6.2 - Change in tread profile as the tyre is worn	83
Figure 6.3 - Comparison of vertical stiffness on a flat surface at 0 and -4° camber with a run-in tyre at 2.5Bar	85
Figure 6.4 - Comparison of vertical stiffness's on a longitudinal and transverse cleat at 0° camber with a run-in tyre	86
Figure 6.5 - Comparison of longitudinal stiffness with a run-in tyre	86
Figure 6.6 - Comparison of vertical stiffness's on a flat surface at 0 and -4° camber between a normally worn contact patch and a flat spot	88
Figure 6.7 - Changes in footprint shape due to flat spot at 0° camber (b) and -4° camber (d), (a) and (c) are the equivalent footprints at another location around the tyre away from the flatspot.	89
Figure 6.8 - Changes in vertical stiffness on a flat surface as the tyre is worn	91
Figure 6.9 - Percentile change in deflection on a flat surface as the tyre is worn	90
Figure 6.10 - Change in footprint at 0° camber as the tyre is worn – new to fully worn from (a) to (d)	92
Figure 6.11 - Changes in vertical stiffness on a flat surface at -4° camber as the tyre is worn	93
Figure 6.12 - Percentile change in deflection on a flat surface at -4° camber as the tyre is worn	93
Figure 6.13 - Changes in footprint at -4° camber as the tyre is worn - newest to fully worn, (a) to (d)	94
Figure 6.14 - Changes in vertical stiffness on a transverse cleat as the tyre is worn	95
Figure 6.15 - Percentile change in deflection on a transverse cleat as the tyre is worn	96
Figure 6.16 - Changes in vertical stiffness on a transverse cleat at -4° camber as the tyre is worn	97
Figure 6.17 - Percentile changes in deflection on a transverse cleat at -4° camber as the tyre is worn	97
Figure 6.18 - Changes in deflection on a longitudinal cleat as the tyre is worn	98
Figure 6.19 - Percentile change in deflection on a longitudinal cleat at 50 and 100% of the LI as the tyre is worn	98
Figure 6.20 - Changes in the longitudinal stiffness as the tyre is worn	99
Figure 6.21 - Percentile change in deflection at 50% of the maximum longitudinal force acquired	100
Figure 6.22 - Percentile change in deflection of all test data	101
Figure 6.23 - Changes in the footprint at 0° camber after model update of mass and tread depth – Left is the original model, Right is the updated model	102
Figure 6.24 - FTire tyre model mass and tread depth update effect on various stiffnesses tested	103
Figure 6.25 - FTire tyre model update validation with measured longitudinal stiffness after wearing	104

LIST OF TABLES

<i>Table 1.1 - List of parameters adjusted in the FTire tyre model</i>	2
<i>Table 1.2 - FTire Parameterisation Test Data – Tyre Basics</i>	5
<i>Table 1.3 - FTire Parameterisation Test Data – Static Tests</i>	5
<i>Table 1.4 - FTire Parameterisation Test Data – Dynamic Tests</i>	6
<i>Table 1.5 – Field Aging Rates (weeks⁻¹) (Baldwin, et al., 2006)</i>	17
<i>Table 1.6 - Comparison of aging rates (weeks⁻¹) of oven aging to field aging in Phoenix (Bauer, et al., 2005)</i>	18
<hr/>	
<i>Table 2.1 - List of data acquisition channels</i>	31
<i>Table 4.1 - Change in vertical stiffness error at 50 and 100 % of the LI</i>	49
<i>Table 4.2 - Shore A Hardness of Tyre Tread Before and After Testing - Statistical Results</i>	54
<i>Table 5.1 - Aging rates (weeks⁻¹) and acceleration factor for aging at 65°C</i>	59
<i>Table 6.1 - Change in mass of tyre as the tyre is worn</i>	83

LIST OF ABBREVIATIONS AND SYMBOLS

ABBREVIATIONS

Abbreviation	Description
ADAMS	Automated Dynamic Analysis of Mechanical Systems
BFG	BF Goodrich tyre brand
DLO	Diffusion Limited Oxidation
DTTT	Dynamic Tyre Test Trailer
FTire	Flexible Structure Tire Model
JIS	Japanese Industrial Standards
LI	Tyre Load Index
LVDT	Linear Variable Differential Transformer
MATLAB	Matrix Laboratory software
NHTSA	National Highway Traffic Safety Administration
OEM	Original Equipment Manufacturer
P80	P-grade 80 grit sandpaper
STTR	Static Tyre Test Rig
SUV	Sports Utility Vehicle
TYDEX	Tyre Data Exchange Format
ULP	Universal Low Profile
USA	United States of America
WFT	Wheel Force Transducer

ROMAN SYMBOLS

Symbol	Description
a_f	Acceleration factor
A	Rubber modulus
B	Peel strength, elongation to break
F	Force
M	Moment
N_2	Nitrogen
O_2	Oxygen
R	Radius
Sh	Shore A Hardness

LIST OF ABBREVIATIONS AND SYMBOLS

T	Temperature
t	Time
V	Velocity
X	X-axis, longitudinal direction
Y	Y-axis, lateral direction
Z	Z-axis, vertical direction

GREEK SYMBOLS

Symbol	Description
α	Oxidation rate (rubber modulus)
C_α	Cornering stiffness
β	Oxidation rate (peel strength and elongation to break)
δ	Change in displacement
ΔSh	Change in Shore A Hardness
ε	Strain
γ	Inclination angle
φ	Shift factor of the acceleration of the aging of the tyre
μ	Coefficient of friction
τ	$1000/T$
ω	Angular velocity
Φ	Longitudinal slip ratio
σ	Stress

SUBSCRIPTS

Symbol	Description
1	First reference point
2	Second reference point
200	At 200MPa
<i>break</i>	At breaking point
<i>e</i>	Effective
<i>l</i>	Loaded
<i>ref</i>	Reference
<i>u</i>	Unloaded

1 INTRODUCTION AND LITERATURE REVIEW

1.1 INTRODUCTION

In contemporary vehicle design the use of models to lower the cost of the design process and shorten the time required to find an optimal design has become a common trait for Original Equipment Manufacturers (OEMs). Due to its high non-linearity, the pneumatic tyre has always been a difficult component of a full vehicle to accurately model. As a result, a fair amount of research has been placed on the modelling of a full tyre capable of simulation in all natural vehicle environments. These efforts involve validating a proposed tyre model with real test data collected on the specific tyre being modelled.

On the other hand, it is common knowledge that a tyre's tread wears as it is used. Furthermore, although less well-known, the rubber in a tyre oxidises with the oxygen in the air used to inflate it as well as the oxygen in the air surrounding it (Baldwin, et al., 2006). The effects of these two phenomena, tread wear and tyre age, on the characteristics of a tyre, such as vertical, longitudinal and lateral stiffness, are not well understood.

These characteristics are specifically used to model tyres, especially when attempting to create an FTire model. Hence, it would be crucial to the accuracy of these tyre models if these characteristics of the tyre change as the tyre is worn or aged.

This dissertation aims to determine whether or not these characteristics change sufficiently enough to merit a current state test as the tyre is either aged or worn.

This chapter surveys whether these changes exist and if so to what extent. In the case that they do exist, the chapter also investigates the feasibility of updating the tyre model to be more representative of the aged or worn tyre.

1.2 FTIRE PARAMETERISATION

Flexible Structure Tire Model (FTire) is a physics-based three dimensional tyre model. Like most mechanical tyre models, this model consists of two parts: the structure model and the tread-road contact model (Gipser, 2005). The structure model defines the tyre's structural stiffness, damping and inertia properties whilst the tread-road contact involves road evaluation, contact pressure distribution and frictional forces. FTire is also one of the advanced tyre models used in the dynamics simulation software, MSC.ADAMS, and is becoming the major tyre model used in industry for durability, ride comfort investigations and the implication on road load (Gipser, 2005).

Topical to this dissertation is the capability of the FTire model to be easily updated. For example, if the said tyre has aged or worn significantly since it was last modelled, parameters such as the geometry and Shore A hardness of the tread in the tyre model could be updated respectively to improve the relevancy of the model to the current state of the tyre. This will be discussed further in the sections that follow.

The parameterisation of an FTire tyre model involves the use of test data acquired from the subject tyre to identify specific parameters in the tyre model. FTire/fit is the software used for this process. Specific tests are recommended for the parameterisation process in Gipser et al. (2016), these are listed and explained below.

1.2.1 Parameterisation

The parameters are those which are manipulated in FTire/fit to fit the test data of the tyre. Table 1.1 lists the commonly used parameters in an FTire tyre model. It is important to note that more parameters exist and that there are several different approaches that can be used to develop the tyre model. Each parameter fine tunes the model one step further, however, it is equally important to have trustworthy data.

Table 1.1 - List of parameters adjusted in the FTire tyre model

Parameter	Associated Tests
First deflection	Vertical stiffness on a flat plate
Second deflection	
Belt torsion stiffness	Vertical stiffness on a flat plate at camber
Belt lateral bending stiffness	Vertical stiffness on a longitudinal cleat
Belt lateral bending stiffness progressivity	Footprint at 0° camber
Relative longitudinal belt member tension	Vertical stiffness on a transverse cleat

INTRODUCTION AND LITERATURE REVIEW

Belt in plane bending stiffness	Footprint at 0° camber
Belt twist stiffness	Vertical stiffness on a transverse cleat at camber
Tyre longitudinal stiffness	Footprint at camber
Tyre longitudinal stiffness progressivity	Longitudinal stiffness
Stiffness of the tread rubber	Traction
Tyre lateral stiffness	Lateral stiffness
Tyre lateral stiffness progressivity	
Belt out of plane bending stiffness	Side force slip angle
Belt torsion stiffness	Footprint at camber
In-plane rotation damping	Dynamic cleat
In-plane translation damping	Dynamic cleat
Out-of-plane rotation damping	Dynamic oblique cleat

The tests listed in Table 1.1 are usually captured on a drum test rig where the tyre can be tested both statically and dynamically by spinning the drum.

1.2.1.1 *Vertical Stiffness*

The vertical stiffness test involves measuring the vertical displacement and vertical force applied to the tyre. Measuring these components the tyre is loaded, generally to the load index, onto a flat surface (or drum in the case of a drum test rig), as well as a cleat positioned in a lateral, oblique and longitudinal direction. The vertical stiffness is also acquired with the tyre at a prescribed camber angle.

1.2.1.2 *Lateral Stiffness*

The lateral stiffness is acquired by loading the tyre to 50% of the load index and then either by laterally pulling the contact surface or by pushing or pulling the actual tyre in its lateral direction. Here it is required to at least measure the lateral displacement and lateral force generated until the tyre starts to slip.

1.2.1.3 *Longitudinal Stiffness*

Similar to the lateral stiffness, the longitudinal stiffness is obtained by actuating and measuring in the tyre's longitudinal direction. The tyre is also loaded to 50% of the load index and the longitudinal force is measured until the tyre starts to slip on the contact surface.

INTRODUCTION AND LITERATURE REVIEW

1.2.1.4 *Footprint*

The tyre footprints are acquired at 50% and 100% of the load index as well as at a camber angle. The specific method used in this dissertation will be discussed in detail later.

1.2.1.5 *Traction*

The traction test is a dynamic test as it measures the tyre's ability to generate longitudinal force whilst rolling. There are several different methods for acquiring this data. Generally, the braking force on a tyre is slowly increased whilst maintaining the same longitudinal speed until the tyre locks up. This involves measuring the generated longitudinal force of the tyre as a function of longitudinal slip ratio. The test can also be repeated at various speeds and vertical loads.

1.2.1.6 *Side Force Slip Angle*

This dynamic test is similar to the traction test, however, a slip angle is induced on the wheel. This slip angle is measured along with the side force generated by the tyre and the test can be repeated at various speeds and vertical loads.

1.2.1.7 *Dynamic Cleat*

The dynamic cleat tests acquire the damping parameters of the tyre. This test is particularly troublesome as it requires the isolation of the damping of the tyre from the system used to capture it. Generally a cleat is mounted onto the drum of the setup and with the wheel rotating the vertical force of the tyre is measured from when it encounters the cleat until it returns to the initial vertical load applied. This is repeated at various loads and velocities and with a cleat mounted at an oblique angle.

1.2.2 **General Data Required**

These tests are expanded into specific sets of data listed in Table 1.2, Table 1.3 and Table 1.4 as the generally accepted tests required for the development of an FTire model for a passenger car tyre. They have been grouped into geometrical, static and dynamic tests respectively as per Gipser et al. (2016):

INTRODUCTION AND LITERATURE REVIEW
Table 1.2 - FTire Parameterisation Test Data – Tyre Basics

Tyre Geometrical Data			
Test Name	Camber (°)	Identified Parameter	Notes
Mass		Mass of Tyre	Without rim
Shore A Hardness		Tread Stiffness	At various locations on the tread
Profile		Footprint	Tread profile in the lateral direction at various locations
Dimensions			Actual outer dimensions

Table 1.3 - FTire Parameterisation Test Data – Static Tests

Static Tests			
Test Name	Camber (°)	Identified Parameter	Notes
Vertical Stiffness			
Flat Surface	0	First and second deflection	Test conducted on Corundum P80 surface
	4	Belt torsion stiffness	
Footprints	0	Belt lateral bending stiffness	Footprint acquired at 50 and 100% LI
		Belt in-plane bending stiffness	
	4	Belt torsion stiffness Belt twist stiffness	
Lateral Cleat	0	Longitudinal belt membrane tension	Cleat is 25x25mm in outer dimensions
		Belt in-plane bending stiffness	
	4	Belt twist stiffness	
Longitudinal Cleat	0	Belt lateral bending stiffness	Cleat is 25x25mm in outer dimensions
Oblique Cleat	0	Only used for validation	Cleat is 25x25mm in outer dimensions

INTRODUCTION AND LITERATURE REVIEW

Longitudinal Stiffness			
Longitudinal Stiffness	0	Tyre longitudinal stiffness	Test conducted on Corundum P80 surface at 50% LI
Lateral Stiffness			
Lateral Stiffness	0	Tyre lateral stiffness	Test conducted on Corundum P80 surface at 50% LI

Table 1.4 - FTire Parameterisation Test Data – Dynamic Tests

Dynamic Tests			
Test Name	Camber (°)	Identified Parameter	Notes
Longitudinal Slip	0	Tread rubber stiffness	Test conducted on concrete at 10 km/h at 50 and 100% LI
Lateral Slip	0	Belt out-of-plane bending stiffness	Test conducted on concrete at 10 km/h at 50 and 100% LI with sweeping slip angle from 0 to 16°
	4	Belt out-of-plane bending stiffness	

1.2.3 Identification and Validation

The terms, identification and validation, are commonly used in the modelling process of an FTire tyre model. The validation of a parameter or set of parameters involves simulating the tyre model under the same test conditions as are associated with that specific parameter(s) and presenting the results. Therefore the validation is simply a comparison between the test data and the tyre model.

Identification, on the other hand, also involves simulating the tyre model under the same test conditions however FTire/fit performs an optimisation process whereby the error between the tyre model's simulated result and that of the test data is reduced through the adjustment of the associated parameter. This is where the actual parameterisation of the tyre model takes place.

1.2.4 Updatable Parameters

Table 1.2, Table 1.3 and Table 1.4 illustrated the extent of the test data required to model a tyre. From this list there are several tests which are time consuming and costly would consequently not be feasible parameters to update the tyre model as a result of wear or age.

INTRODUCTION AND LITERATURE REVIEW

The geometrical set of data, however, provides this opportunity. In the FTire/fit environment these parameters are easily modified and have potential bearing on the tyre model itself. Furthermore these parameters are simple to measure and not time consuming to acquire. Shore hardness is also simple and quick to measure compared to full static tests whilst dynamic tests are the most expensive and are not feasible for periodically updating the tyre model.

1.3 AGING OF TYRES

In general, literature on the aging of tyres and the effects thereof is scarce. This section combines various sources that have discussed or attempted to explain the most influential mechanisms and effects of the age in tyres. Regarding this topic, a book entitled “The Pneumatic Tire” provided useful insight. This source was compiled by the National Highway Traffic Safety Administration (NHTSA) in 2006 under instruction from the United States Department of Transport. It constitutes a comprehensive range of chapters published by recognised authorities in their respective fields of tyre science and technology. For the purpose of the discussion in this report, each chapter relevant to the work from this book has been listed as a separate reference since each chapter has been written by a different author(s).

1.3.1 Oxidation

Oxidation is the most influential mechanism in the aging of tyres. It acts at a slightly lower rate than other aging mechanisms such as ozone attack and vulcanisation, however, all tyres exist in oxygen filled environments and are therefore subject to oxidation. This slow rate causes the oxidation to penetrate to a greater depth before reacting with the rubber according to Gent (2006). As a result the rubber doesn't necessarily crack due to the oxidation but is rather made more brittle and can crack upon flexing or deformation of the tyre. The rates of oxidation are highly dependent on the ambient temperature and can consequently range in penetration through the tyre.

The oxidation process is initiated by the “typical hydrocarbon elastomers undergo(ing) an autocatalytic reaction” (Gent, 2006). This source of catalysts in turn causes the reaction between the rubber molecules and oxygen at which point oxygen atoms are added to the rubber molecule leading to the formation of crosslinks between neighbouring molecules. Not only does this increase the hardness of the rubber but it also induces changes in the swelling of the tyre (Kataoka, et al., 2003).

This swelling is a measurable parameter which in turn allows for the measurement of the level of oxidation the tyre has undergone. The degree of swelling is determined according to JIS K6258 (Kataoka, et al., 2003). From this standard as well as JIS K6229 (Kataoka, et al., 2003) the process

INTRODUCTION AND LITERATURE REVIEW

oil, antioxidant and wax can be extracted from the rubber and is referred to as the oil component of the tyre. These traits of the tyre are used to compare the effects of storage and service on tyre performance. Figure 1.1 and Figure 1.2 illustrates these results (Kataoka, et al., 2003).

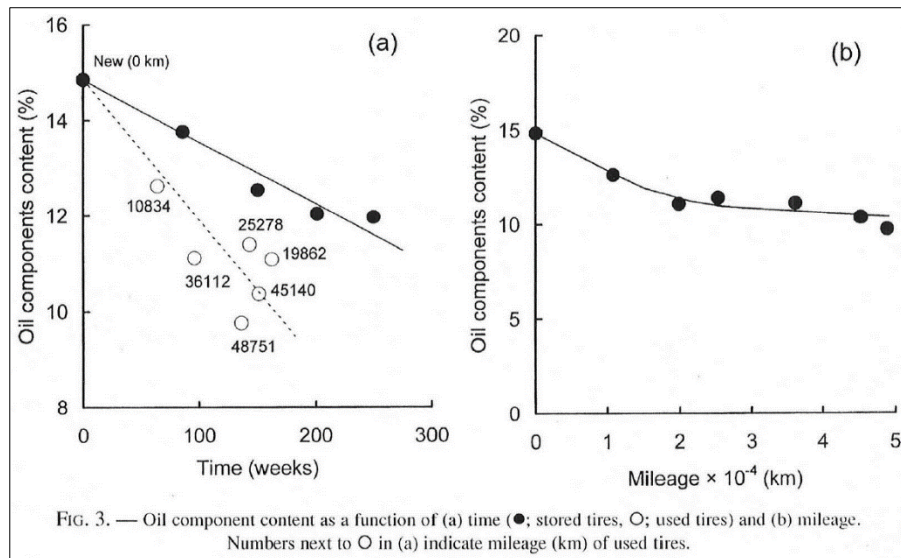


Figure 1.1 - Oil component as a function of time and mileage (Kataoka, et al., 2003)

The percentage swelling can be directly related to the level of oxidation in the respective tyres. This is confirmed in Figure 1.2 as the percentage swelling is seen to steadily decrease as a function of time left in storage. This concept is additionally reinforced in Figure 1.1.

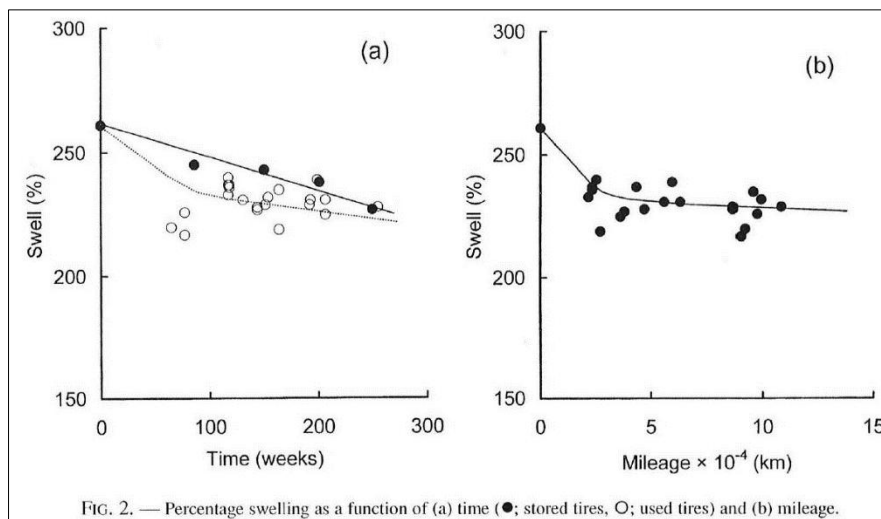


Figure 1.2 - Percentage swelling as a function of time and mileage (Kataoka, et al., 2003)

What is interesting about these graphs is the acceleration of both the percentage swelling and the oil component when the tyre is in service. The effects, however, do reach equilibrium with

INTRODUCTION AND LITERATURE REVIEW

increased mileage and are eventually found to be equivalent to tyres left in storage after a few years. This is due to an initial drop in the percentage swelling followed by a relatively constant value thereafter shown in Figure 1.2(b).

1.3.2 Temperature Dependence

The oxidation of tyres is largely dependent on the temperatures they are exposed to. Potinger (2006) indicates a noticeable difference in the cornering and aligning stiffnesses depending on the temperature at which the tyres were stored. Furthermore Potinger (2006) described this relationship as in Equation (1).

$$\left(\frac{d\alpha}{dt}\right)_2 = \left(\frac{d\alpha}{dt}\right)_1 \times 2^{0.1(T_2-T_1)} \quad (1)$$

This equation assumes a linear gradient for the change in cornering stiffness with change in the aging time. In Equation (1) the subscripts represent the respective value at the first and second temperature and C_α , the cornering stiffness coefficient. This at least shows that there exists a relationship between the change in stiffnesses of a tyre and the temperature at which it is stored.

This temperature dependence is discussed and tested extensively in Baldwin (2005) where an accelerated method for aging tyres is investigated. Specific to aging it is claimed that the aging mechanism changes depending on the storage temperature. Further discussion is detailed later on in this chapter.

1.3.3 Effects of Aging on Forces and Moments

A direct result of changes in the hardness, swelling and/or oil component content are changes in the tyre's ability to generate forces and moments. This is ultimately the desired output of any aging analysis as the resultant changes in forces and moments generated by the tyre can be inserted into a vehicle model environment. Subsequently the results of an aging analysis can be used to improve the accuracy of a dynamic vehicle model according to the age of the tyres. This is also useful for the validation of dynamic vehicle or tyre models and can improve the robustness of critical systems such as the ABS

1.3.3.1 Tyre Stiffnesses

The effects of aging on tyre stiffness are thus evident, however, the rate at which these stiffnesses change, as well as the magnitude of those changes, is less apparent. Potinger (2006) found that cornering and aligning stiffnesses increase with age and this is dependent on the storage temperature of the tyre. The effect was, however, not quantified.

On the other hand, some information on the effects of forces and moments is given by (Kataoka, et al., 2003). Rubber samples from TL 185/70R14 tyres are tested after undergoing a combination

INTRODUCTION AND LITERATURE REVIEW

of storage and service. Aspects such as manufacturing date, the temperature of the storage facility after manufacturing and the length of time under these conditions were all considered in the tests conducted. Following tests, rubber samples were removed from the tyre tread of each respective tyre. Thereafter the samples were tested in a tensile testing machine where the stress and strain required to break each specimen (σ_{break} and ϵ_{break}) and the stress required to elongate the specimen by 200% (σ_{200}) were used as the results applicable for comparison. These force related variables were additionally compared to Shore A hardness (ΔSh) calculated before and after storage and/or service.

1.3.3.1.1 Results

The results of the stress, strain and hardness analyses from (Kataoka, et al., 2003) are shown in Figure 1.3 and Figure 1.4. These results are consistent with the forms and trends evident in Figure 1.2 and Figure 1.1 of swelling and oil component content. As one can see in Figure 1.3 and Figure 1.4, the stress required to elongate the rubber specimens by 200% and the Shore A hardness linearly increase when stored and are slightly accelerated when in service. This correlates well with the oil component content since the decrease in the oil component content of the rubber “brings about a greater extent of physical interaction” (Kataoka, et al., 2003) between the rubbers. The decrease in ϵ_{break} and σ_{break} are representative of an increased brittleness of the rubber and can additionally be related to the corresponding decreases in percentage swelling and oil component content.

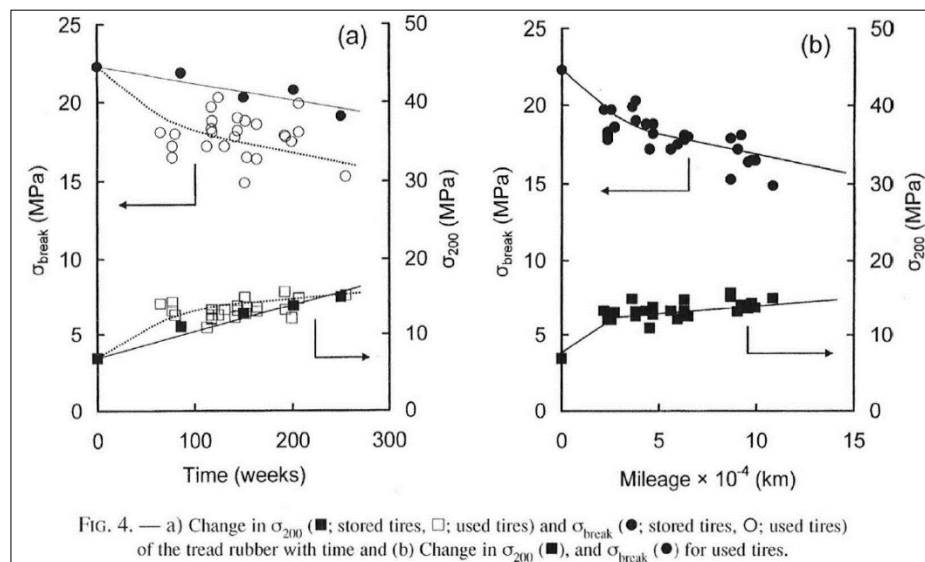


Figure 1.3 - Specimen stress values as a function of time and mileage (Kataoka, et al., 2003)

Of greater significance, is that the values discussed above (σ_{200} , σ_{break} , ϵ_{break} and ΔSh) for tyres stored for just less than 5 years are equivalent to tyres in service for approximately 100 000km.

INTRODUCTION AND LITERATURE REVIEW

This highlights the fact that the effects of stored tyres on performance cannot be neglected since most tyres are replaced after approximately half of this mileage. It additionally suggests that the Shore A hardness measurement (a non-destructive measurement method) can be used to estimate the age of the tyre.

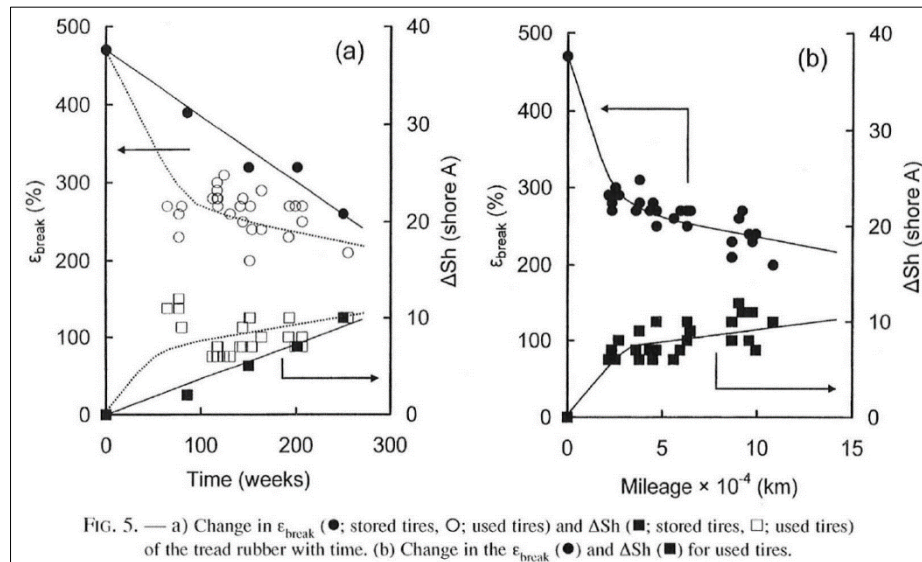


Figure 1.4 - Specimen strain and Shore A hardness as a function of time and mileage (Kataoka, et al., 2003)

1.4 ACCELERATED AGING OF TYRES

Baldwin et al. (2003, 2005, 2006, 2008), Bauer (2005) and Ellwood (2004) have published several articles on the artificial aging of tyres using static oven aging. Their research effort is significant and includes the testing of a large number of tyres aged in the field from different regions and in different climates. Several methods were researched and used to evaluate the condition of each tyre. This research was captured in Baldwin et al. (2005, 2006) and included one other related papers not referenced here. Thereafter, in an additional two papers Baldwin et al. (2005, 2005) describing methods of artificially aging tyres were investigated using the same evaluation method compared to the field aged tyres. As a result, a comprehensive method for accelerating the age of a tyre in order to obtain equivalent conditions as those aged in the field was found.

Figure 1.5 shows the typical construction of a passenger car tyre. The rubber property measurements of Baldwin et al. (2006) are focused around the steel belts and the strength of the rubber around them.

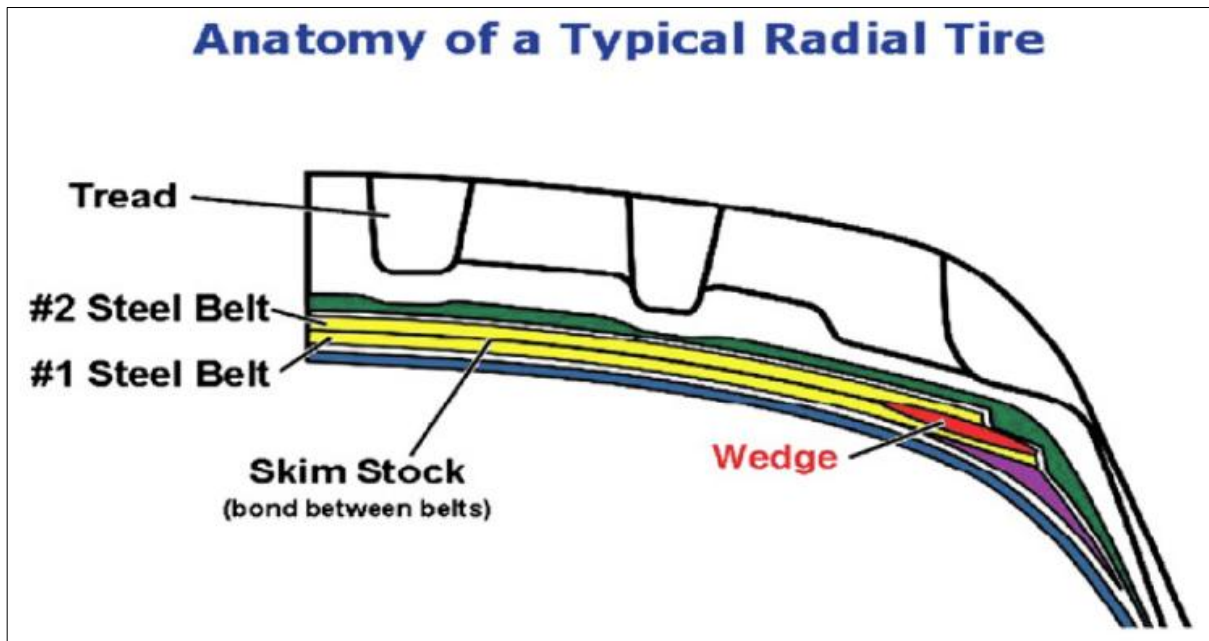


Figure 1.5 - Typical construction of passenger car tyre (Baldwin, et al., 2006)

1.4.1 Oven Based Aging

The first published paper (Baldwin, 2003) of this series involved the oven aging of tyres at various temperatures inflated with either air or a 50:50 mix of N_2 and O_2 . The purpose of which was to investigate if the same rubber properties can be acquired in comparison with tyres aged whilst in service. These rubber properties are discussed below.

1.4.1.1 Property Measurements

The measurements used to quantify the age of the tyres are repeated through this series of papers so as to remain as fair a test as possible. The tests are focused around the strength between the steel belts and rubber surrounding them as can be seen in Figure 1.5.

1.4.1.1.1 Tensile and Elongation

Belt wedge samples as seen in Figure 1.5 were removed, buffed and cut to a specific sample size. Thereafter the specimens were clamped and tested via elongation to acquire the modulus at 25, 50, and 100% elongation and further stretched to acquire the tensile strength.

1.4.1.1.2 Peel Strength

Radial samples of the steel belt were removed in this case and by initiating the peel between the two belts to allow sufficient clamping area the two steel belt layers were peeled apart, thereby measuring the strength of the skim stock rubber by allowing the belts to separate.

INTRODUCTION AND LITERATURE REVIEW

1.4.1.1.3 Crosslink Density

Five specimens per tyre were swollen in a solution of toluene for 24 hours. The crosslink density was thereafter determined using the Flory-Rehner equation Baldwin et al. (2003). This is a relevant test given the anticipated increase in crosslink density due to aging as mentioned previously.

1.4.1.2 *Test Setup*

The setup involved inflating each tyre to a specific pressure and then mounting the tyres in an oven set at temperatures ranging from 50 to 100°C for between 2 to 8 weeks. In the case of the 50:50 mix of N₂ and O₂ the air naturally inside the tyre was not purged therefore resulting in an actual mixture of approximately 42% O₂.

In order to achieve equivalent rubber properties to tyres aged in the field it is important that the same aging mechanism is achieved. In Baldwin (2003), the predominant aging mechanism is oxidation, thus it is important that the oven-based aging accelerate the aging of the tyre in the same manner. This was ensured by plotting the results of the rubber tests and comparing them to an empirical solution for oxidised natural rubber (Baldwin, 2003).

1.4.1.3 *Results*

1.4.1.3.1 Oxidation Aging Mechanism

As mentioned in Section 1.4.1.2, the oven-based aging needed to illustrate oxidation as the dominant aging mechanism. In Figure 1.6 (Baldwin, 2003) the results of tensile measurements on the wedge rubber of a tyre is shown where the tyre was aged at various temperatures. The 70°C aging temperature is the only temperature illustrating oxidation as an aging mechanism. The higher temperatures all illustrate either aerobic or anaerobic aging which is undesirable when compared with tyres aged in the field. Furthermore it was shown that the same trend is clear when aging using a 50:50 mix of oxygen and nitrogen.

1.4.1.3.2 Advantage of N₂/O₂ Inflation Media

Figure 1.7 shows the percentage change in the crosslink density of the wedge rubber as a function of aging time compared between the two different inflation media. The addition of enriched oxygen increases the change in crosslink density by 25% in Tyre 1 and 18% in Tyre 2.

The same trend was observed with the change in the strain ratio at break where with Tyre 1 an increase of 30% was seen and 18% with Tyre 2.

INTRODUCTION AND LITERATURE REVIEW

1.4.1.3.3 Effect of Temperature

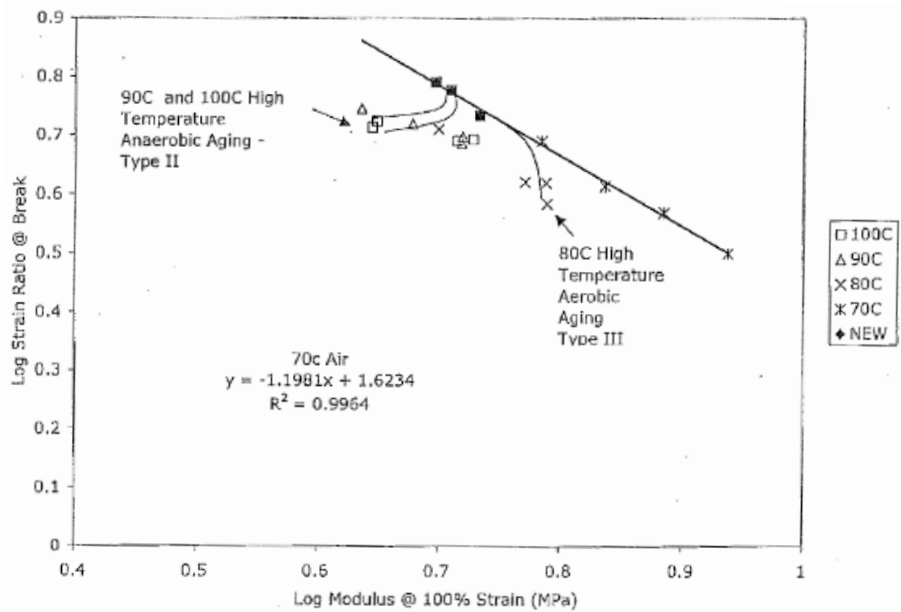


Figure 1.6 - Tyre wedge strain data for aging at various temperatures (Baldwin, 2003)

In the second paper (Baldwin, et al., 2005) based on the accelerated aging of tyres, further investigation is completed on the range of oven temperatures and which aging mechanisms are achieved. Figure 1.8 shows the time shift factor (refer to Section 1.4.2.1 for further explanation on this factor) for aging as a function of oven temperature. Clearly evident is the change in mechanism above 70°C where Diffusion Limited Oxidation (DLO) and/or anaerobic aging starts taking place. All temperatures leading up to 70°C only increase the rate at which the tyre ages aerobically as desired.

INTRODUCTION AND LITERATURE REVIEW

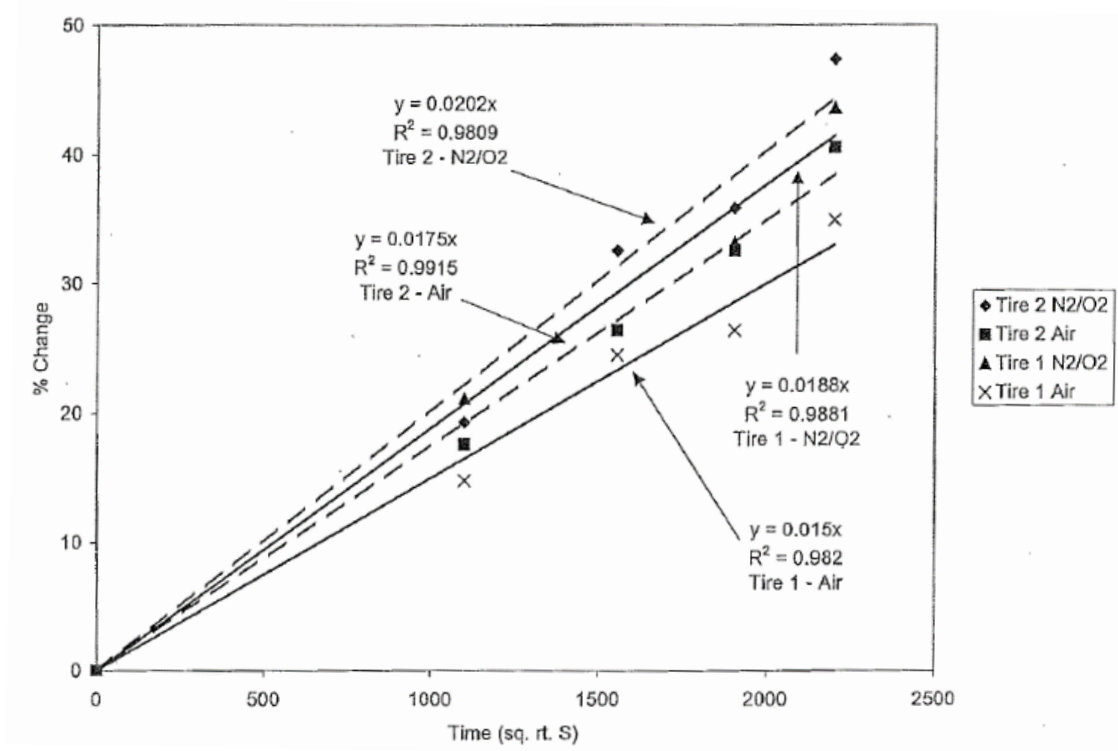


Figure 1.7 - Percentage change in crosslink density between air and N₂/O₂ inflation media (Baldwin, 2003)

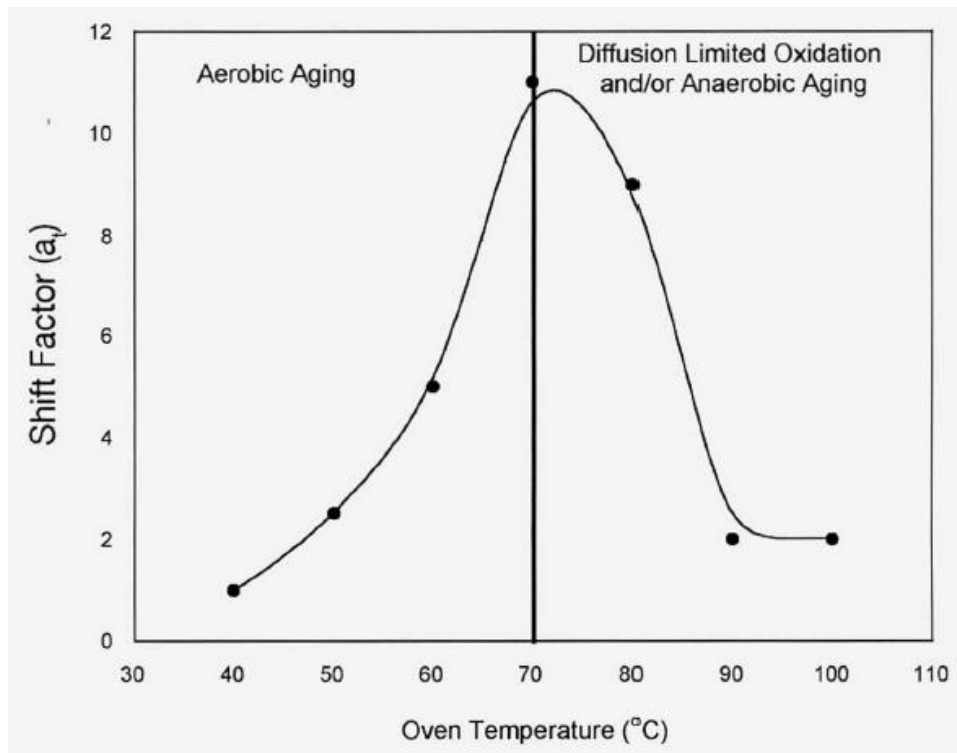


Figure 1.8 - Aging rate as a function of oven temperature (Baldwin, et al., 2005)

INTRODUCTION AND LITERATURE REVIEW

1.4.2 Field Based

In the first of the field based published papers (Baldwin, et al., 2006) over 1500 tyres in total were collected from four different locations in the USA based on their different ambient temperatures. The tyre range included those used for six different vehicle types and three different brands. They additionally ranged in age from 2 weeks to 6 years and were a combination of in-service and spare tyres. Changes in the rubber properties of tyres were shown to be as a result of oxidation as shown in Section 1.4.1.3.1 and thus in this paper each tyre's steel belt package was tested in line with the tests conducted on the oven-aged tyres.

1.4.2.1 Results

The tyres aged in different locations were anticipated to oxidise at different rates due to the different ambient temperatures at the different locations. As a result this paper shows the capability of modelling the aging of the field tyres despite their different locations or aging rates. The method initially employs a classic time-temperature superposition approach to account for the different aging rates and thereafter all the data can be fitted to the empirical equation line.

Using the results obtained in (Baldwin, 2003), it was expected that the crosslink density and modulus of the skim and wedge rubber would increase. Shown in graph on the left in Figure 1.9 it can be seen that the tyre's wedge rubber moduli increase at a near linear rate and are expressed in (Baldwin, et al., 2006) as in Equation (2):

$$A(t) = A(0)(1 + \alpha t), \quad (2)$$

where α is the oxidation rate for crosslink density and modulus of the rubber sample. With respect to the peel strength and elongation-to-break properties which were expected to decrease with age, they were shown to behave as depicted in the graph on the right in Figure 1.9 and described as in Equation (3):

$$B(t) = \frac{B(0)}{1 + \beta t}, \quad (3)$$

where β is equal to the oxidation rate.

The shifted time factors of Detroit and Hartford are due to their lower ambient temperatures compared to Phoenix. As a result the aging process is noticeably slower. However, using superposition the correlation to the empirical formulas of Equations (2) and (3) are still apparent once they are shifted.

INTRODUCTION AND LITERATURE REVIEW

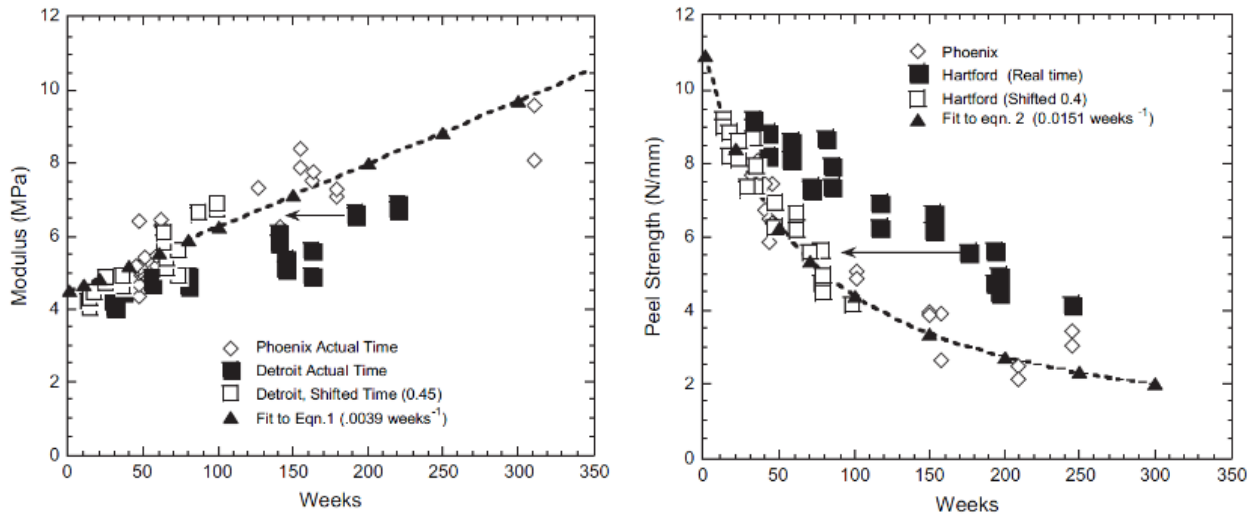


Figure 1.9 – Modulus of the wedge of rubber and peel strength of the skim rubber results for field tyres (Baldwin, et al., 2006)

The paper continues in more detail to consider the remaining rubber properties such as elongation-to-break and crosslink density in the different tyres and the different cities. The aging rates of which have been summarised for the tyres from Phoenix in Table 1.5:

Table 1.5 – Field Aging Rates (weeks^{-1}) (Baldwin, et al., 2006)

Vehicle Type – Brand	Tyre Size	Elongation-to- break	Peel Strength centre	Peel Strength belt edge
SUV/Minivan – A	215/70R15	0.0075	0.0096	0.0120
SUV/Minivan – B	235/75R16	0.0026	0.0057	0.0055
SUV/Minivan – C	215/65R16	0.0045	0.0043	0.0047
Large Car – C	225/60R16	0.0026	0.0026	0.0022
Small Car – BFG	195/65R15	0.0030	0.0046	0.0044

Table 1.5 shows a definite change in aging rates depending on the tyre and the test. Comparison of these results were then made to the oven-based aged tyres in a subsequent paper and will be discussed later in the Chapter.

Despite providing a positive correlation, it was stated that a large variability in the aging results of the tyres was noticed. This was the motivation behind testing a wide range of tyres. This variability is likely due to the variation in initial property values and aging rates.

1.4.3 Correlation of Oven-Aged and Field Tyres

As covered by Bauer et al. (2005) a final validation of oven-aged tyres is conducted via direct comparison of rubber properties to field-aged tyres. As in Section 1.4.2.1, where the method of

INTRODUCTION AND LITERATURE REVIEW

shifted time factors was used to compare aging trends in regions of the USA where the aging rate was different, the time shift factor was used in the case of validating the oven-aged tyres as well.

Figure 1.10 shows the elongation-to-break and peel strength of tyres aged in an oven at 40, 50, 60 and 70°C. As mentioned above, the time shift factor gives a good indication of the rate of aging at each temperature where aging at 70°C ages at a rate 11.7 times faster than at 40°C. These values are directly compared to those obtained in the field for a similar tyre in Table 1.6.

Table 1.6 - Comparison of aging rates (weeks⁻¹) of oven aging to field aging in Phoenix (Bauer, et al., 2005)

Property	Rate at 70°C	Rate in Phoenix	Acceleration Factor
Skin Crosslink Density	0.059	0.00175	34
Wedge Modulus	0.061	0.0166	37
Wedge Elongation-to-break	0.168	0.0042	40
Skin Peel Strength	0.216	0.0084	26
Average			34±6

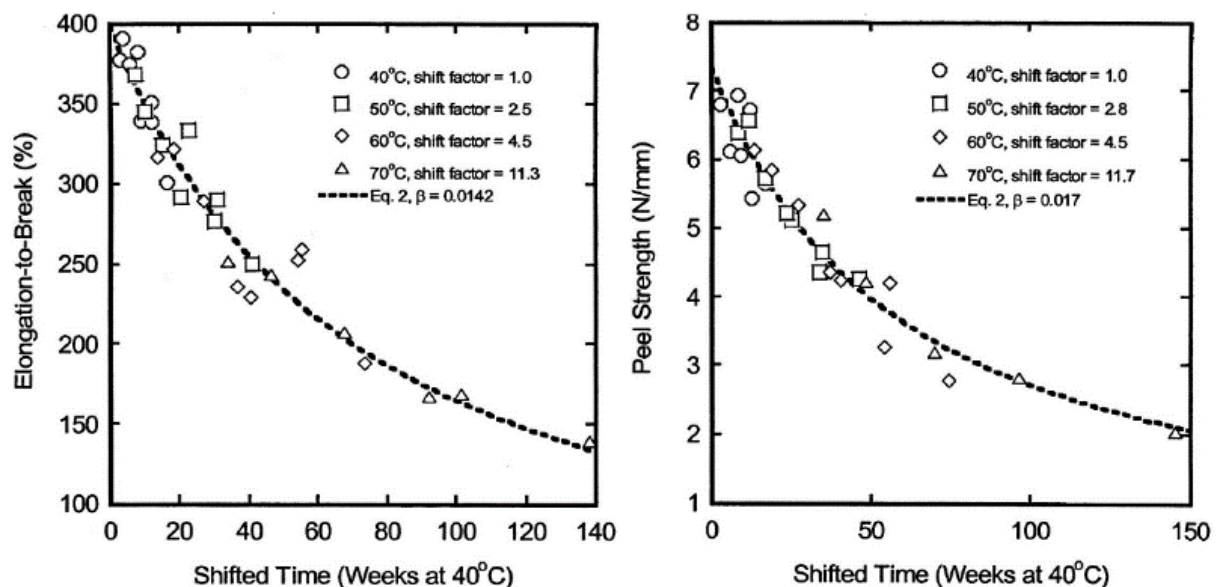


Figure 1.10 - Elongation-to-break and peel strength of oven aged tyres at various aging temperatures (Bauer, et al., 2005)

Although the exact same tyre couldn't be compared between field and oven-aged conditions, the results in Table 1.6 are for two tyres similar in overall dimensions. These results demonstrate a surprisingly good correlation as a relatively consistent acceleration factor is obtained between the different tests conducted on the tyres. Albeit with a deviation of approximately 17% from the mean, Figure 1.11 shows how drastically the aging of a tyre depends on the tyre itself. The 'Tire

INTRODUCTION AND LITERATURE REVIEW

Type and Brand' vary as per the sizes listed in Table 1.5. This implies that there is no specific dependency on the size of the tyre causing neither a quicker nor slower aging rate, nor the brand/or use of the tyre. Knowing this highlights the impressiveness of the results shown in Table 1.6.

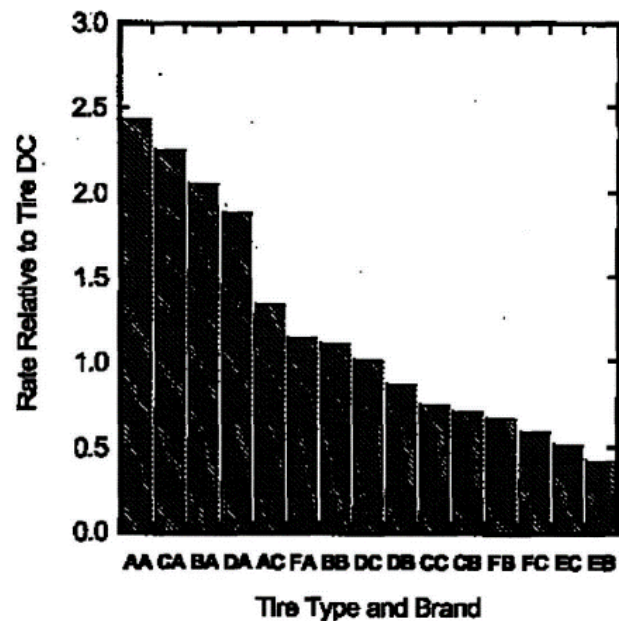


Figure 1.11 - Dependency of aging rate as a function of different tyres (Bauer, et al., 2005)

Further correlation is depicted in Figure 1.12 where a line of best fit has been plotted for the shift factors of the oven aging as a function of aging temperature and then extrapolated to include the low shift factors of the field tyres.

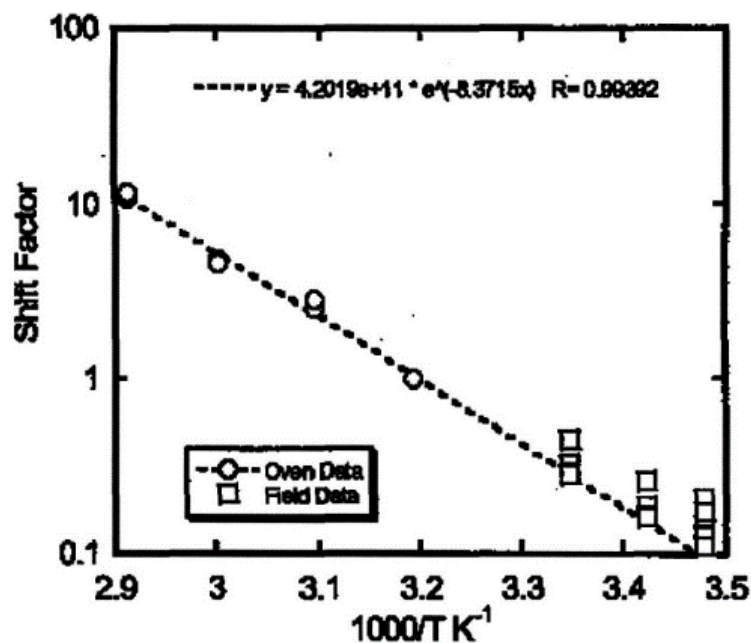


Figure 1.12 - Shift factor obtained from oven aging and field aging (Bauer, et al., 2005)

INTRODUCTION AND LITERATURE REVIEW

Once again the correlation is good except for a few points from the field tyres which were predicted and accounted for by the fact that the tyre in the field doesn't only experience the ambient temperature of the region but also heating from usage, direct sunlight and reflected heat from the road.

Returning to the values tabulated in Table 1.6, if the mean acceleration value of 34 is used it implies that by aging a tyre in an oven set at 70°C for 6 to 7 weeks an approximately 4 year old tyre in Phoenix, USA will be obtained. It must be understood that this is a rough estimate and will vary significantly depending on the brand and type of tyre and the geographical location of the tyre.

1.5 WEARING OF TYRES

It is common knowledge that the rate of the wear of a tyre is generally accepted to be the determining factor for the life of the tyre (Yong, et al., 2011). This being said literature on potential changes in the stiffness characteristics of a tyre as it is worn is rare. In this section factors influencing tyre wear are briefly discussed as they give an indication of the potential impact tyre wear has on these factors. Thereafter the effects of tyre wear on rolling resistance are also discussed.

1.5.1 Factors Affecting Tyre Wear

Yong et al. (2011) conducts an extensive investigation into the extent that temperature and dynamic characteristics of a vehicle have on the tyre wear. This was completed with the use of a theoretical, physics based model. Figure 1.13 shows both the list of most influential factors as well as the extent of their influence on the tyre wear. Topical to this dissertation is the tread and sidewall's respective stiffness and damping. Figure 1.13 indicates that these factors have negligible influence on the tyre wear. This does not necessarily translate to these factors not being influenced by tread wear itself, however, it gives an indication that the extent of that influence may be relatively small.

INTRODUCTION AND LITERATURE REVIEW

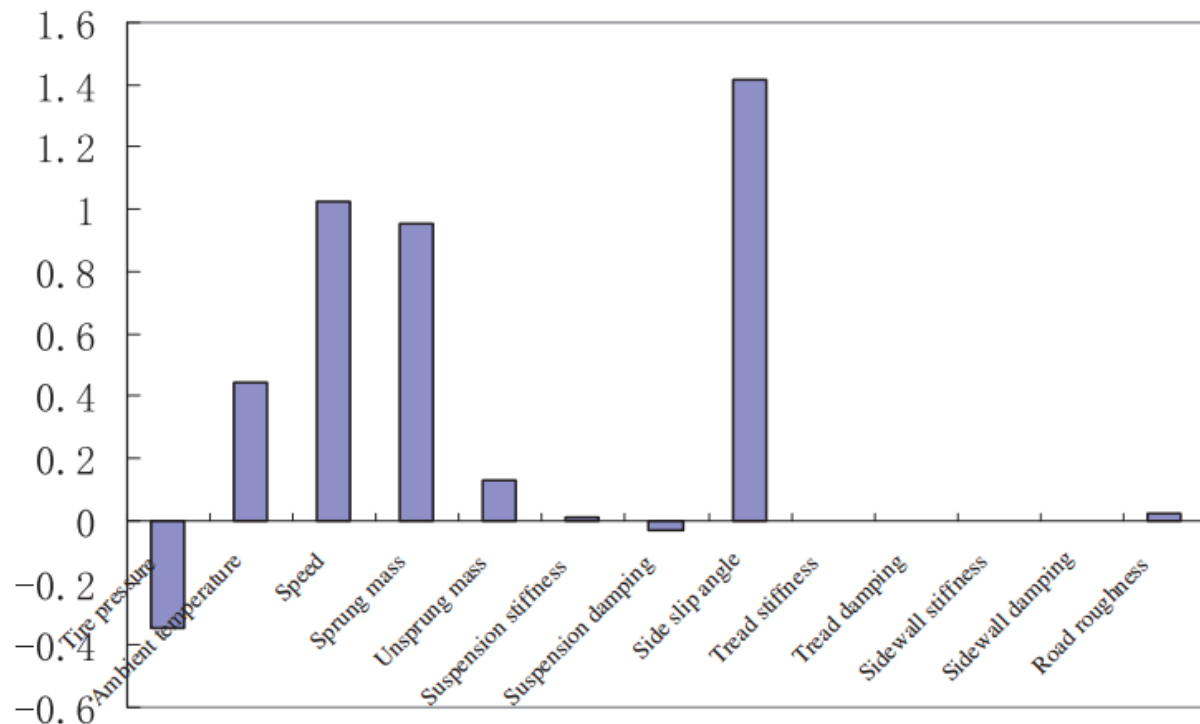


Figure 1.13 - Comparative histogram of the sensitivity of the parameters influencing tyre wear (Yong, et al., 2011)

1.5.2 Effect of Tyre Wear on Rolling Resistance

Sandberg et al. (2008) presented results on the effect of artificially worn tyres on their respective rolling resistances. Five different passenger car tyres' rolling resistance were experimentally acquired on a drum test rig in accordance with IS 14777 (Indian Standard, 2010) and the direct force measurement described therein. The tyres are worn on an abrasive drum setup which accelerates the rate at which the tyres are worn by running the tyres at approximately 90km/h and at each tyre's load index. Each tyre's rolling resistance was measured after 2mm of tread was removed until only 2mm of tread was left. Interestingly each test tyre was run-in over a distance of 300km at 140km/h at an unspecified load. A summary graph is depicted in Figure 1.14 of the five different tyres that were worn and tested.

Figure 1.14 shows the results of the rolling resistance test conducted on a plain steel drum. It evaluates the change in rolling resistance due to the wear of the tyres to be an average decrease of 20%. More detailed results also revealed that the relationship between rolling resistance and tyre wear was linear with a slightly larger decrease in rolling resistance between tread depths of 4 and 2mm. Sandberg et al. (2008) also showed that the decrease in rolling resistance was slightly less at 17% on a rough surface. These are significant decreases in what is arguably a small component of the forces generated by the tyre in general.

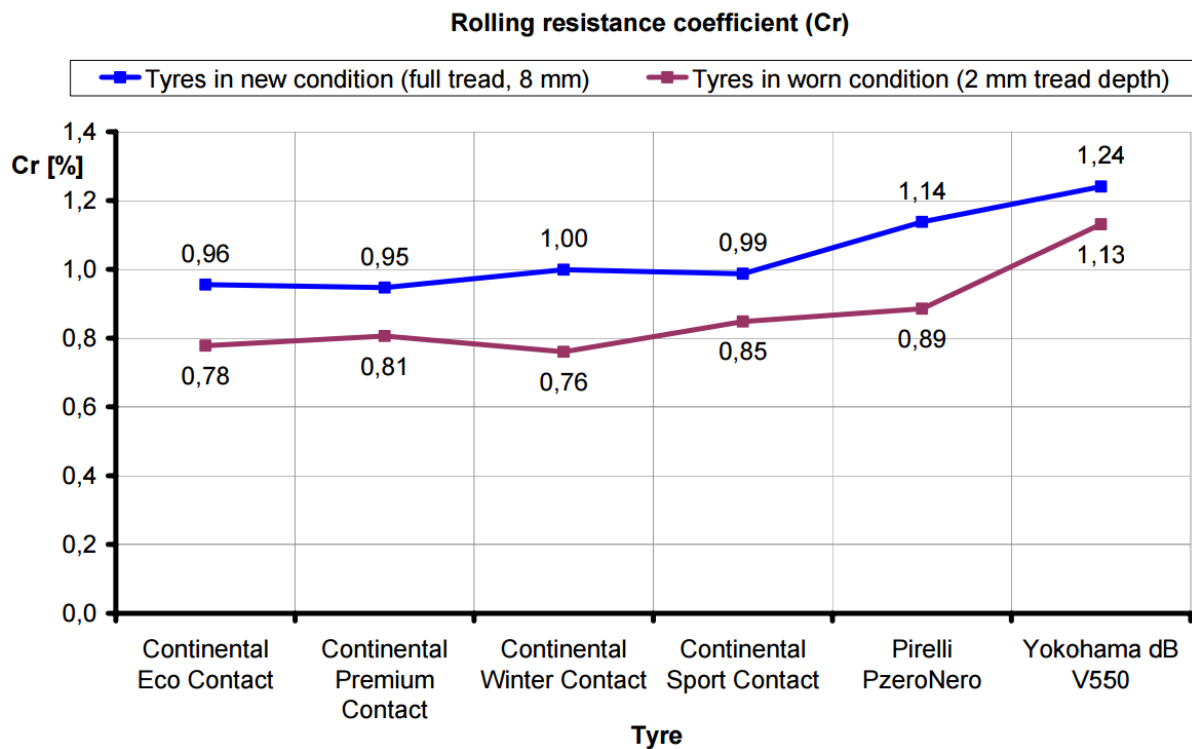


Figure 1.14 - Change in rolling resistance between new and fully worn tyre (Sandberg, 2008)

1.6 METHOD OF COMPARING STIFFNESSES

The testing sensitivity, aging and wear analyses to be discussed produced a significant amount of tyre stiffness curves. An easily interpretable method needed to be used to quantify the change in these stiffnesses. Of utmost importance to this method was that it should be relevant and understandable in the context of a tyre and its operating conditions.

As a result it was decided that the change in the deflection of the tyre required to reach 50% of the tyre's load index would be used in the current study. This method gives the user of the captured data a quantifiable value which is easily interpreted as it is a physical dimension and is easily visualised. Furthermore it uses a load which is close to the normal operating load experienced by the tyre.

1.7 SUBJECT TYRE

The subject tyre used to capture all the test data for the current study was a Pirelli Scorpion Verde 235/55 R19 all-season tyre with a nominal inflation pressure of 2.5Bar. The tyre is directional as it has an asymmetric tread pattern. The tyre mass was 13.625kg and together with the rim

INTRODUCTION AND LITERATURE REVIEW

weighed 23.8kg . Finally the load index of the tyre was 9.1kN . Indicating that the 50% of the LI referred to in Section 1.6 would equate to 4.55kN .

1.8 CONCLUDING REMARKS

The literature discussed in this chapter showed that age and wear have an influence on certain characteristics of the tyre behaviour. These include physical properties such as the Shore A hardness and crosslink density of the rubber itself in terms of age whilst rolling resistance was shown to be influenced by tyre wear. Little evidence, however, could be found on the effect these two factors of a tyre have specifically on the various stiffnesses of the tyre. These stiffnesses are used directly in the modelling of the tyre and are consequently of interest.

The potential of easily updating the FTire model was also demonstrated. Through simple tests such as the Shore A hardness of the tread and the geometry in terms of the tread depth some evidence suggests that the model could be updated. The simplicity and relevance to the tyre model would determine whether or not they are suitable methods for updating the model.

Given the desire for more accurate tyre models, the effects of age and wear would need to be further investigated. This would involve two separate processes in which individual tyres would be aged and worn. The aging process followed could be authenticated by the in-depth literature survey of an accelerated aging process which was well-researched by Baldwin (2003). Thereafter simplified methods of quantifying the age of the tyre would be investigated such that the tyre model could easily be updated.

To replicate the wear of the tyre various abrasive handling manoeuvres would be used on a dynamic test trailer. This would avoid the traditional buffing of a tyre commonly used to remove the tread which does not subject the tyre to the forces it experiences when in service.

1.9 PROBLEM STATEMENT

The clear shortage in literature pertaining to the specific influences of the aging and wear of a tyre on its stiffness characteristics provides the basis for an investigation into these influences. Due to the anticipated small variations in these stiffness characteristics, it is also necessary to investigate the sensitivity of acquiring the stiffness characteristics of a tyre.

Importantly, the ability to easily update a tyre model based on the changes endured due to either age or wear should be explored.

INTRODUCTION AND LITERATURE REVIEW

1.10 HYPOTHESIS

Some evidence suggests there are influences to the parameters of a tyre due to aging and wear. These influences will thus be confirmed and quantified by testing the tyre. Finally, methods of accounting for these changes in a tyre model will be investigated.

1.11 PROJECT OVERVIEW

This dissertation therefore involved several processes where a large quantity of test data was acquired. A total of four subject tyres were used to capture the necessary data. One tyre would represent the control whereby aging was minimised by storing it, deflated in a closed room at ambient temperature. Another tyre would be artificially aged and periodically tested on a static test rig during this aging process. Finally two other tyres would be worn using abrasive longitudinal and lateral actions on a dynamic test rig, they too would be tested on the static test rig during this process.

These two processes, namely the aging and wearing processes would be carried out simultaneously and all the potential parameters which could be later used to update the tyre model would also be captured.

Taking advantage of the variety in test equipment and tyres, several sensitivity and repeatability tests would also be conducted.

A baseline FTire model would also be parameterised to represent the new tyre using data acquired on a static and dynamic test rig. Parameters would thereafter be investigated into their influence on updating the tyre model. These updates will then be validated against real test data of the aged and/or worn tyre.

1.12 DISSERTATION SUMMARY

The dissertation consists of 8 chapters, the introduction of the problem statement based on literature reviewed is covered in Chapter 1.

Chapter 2 describes the test equipment built and used to acquire all the data used in the dissertation. The intricacies of these test rigs are important to the sensitivity data later discussed as well as the eventual accuracy of the tyre model to be developed.

Chapter 3 deals with these sensitivities in detail. It covers test repeatability as well as the sensitivity between the different tyres. Further detail is added such as the potential influence of ambient temperature and the contact surface.

INTRODUCTION AND LITERATURE REVIEW

Chapter 4 describes the FTire parameterisation process followed and the validated baseline tyre model that was developed. It also discusses potential pitfalls due to data not acquired.

Chapter 5 is focussed on the aging aspect of the tyre. These include influences to the tyre due to the accelerated aging process. This is followed by the validation of the updated tyre model where the Shore A hardness was used to update the model.

Chapter 6 similarly engages with the wear component of the dissertation. Some additional factors such as the runin period of a tyre are also considered here. Thereafter a validation of the updated tyre model is conducted where the mass and new outer geometry of the tyre are used to update the model.

Finally chapter 7 provides a summary of the dissertation with recommendations for further investigations of the problem. Chapter 8 provides all the references used in the dissertation.

2 TEST SETUP

2.1 INTRODUCTION

In order to obtain the tyre data required to parameterize FTire, as well as investigate the effects of aging and wear on tyre characteristics, extensive experimental work was performed. Required test data included contact area, static stiffness in different directions as well as quasi-static side force vs. slip angle and longitudinal force vs. slip characteristics.

Three different experimental setups were used to acquire data for this dissertation. The first two were used for static laboratory tyre tests whilst the third was used for on-road tests with rolling tyres. An additional feature was adapted to one of the rigs to accurately measure the tread profile as well.

Initial static tests were performed on an improvised test rig whilst a dedicated static tyre test rig was commissioned and used for subsequent tests. Test data on a rolling tyre was also needed, thus a dynamic tyre test trailer was included in the scope of equipment used.

2.2 STATIC TYRE TEST RIG

The Static Tyre Test Rig (STTR) was used to test a tyre in its static position with locked wheel rotation. The principles and tests conducted on this test setup were simple however ensuring the accuracy of the data acquired complicated the process. This section covers the tests to be completed on the STTR and a full list and explanation of all the equipment used. Note that the orientations referred to are always with respect to the tyre in its normal operating orientation as per the TYDEX C-axis system (Unrau, et al., 1997).

2.2.1 Tests to be completed

As described in Table 1.3, tests completed on the STTR include all vertical, lateral, longitudinal and footprint tests as well as the overall geometry of the tyre and the tread profile.

2.2.2 Equipment

2.2.2.1 STTR Operation

The STTR is depicted in Figure 2.1 and Figure 2.2 in its position suitable for the vertical and longitudinal stiffness tests and finally in its position suitable for the lateral stiffness test in Figure 2.3 and Figure 2.4.

Figure 2.2 illustrates how the STTR operates when testing the vertical and longitudinal stiffnesses of the tyre. The green arrow indicates the direction of travel when only testing the vertical

TEST SETUP

stiffness. The associated green dots indicate all the components of the STTR that move in the vertical direction of the tyre including those labelled with blue dots.

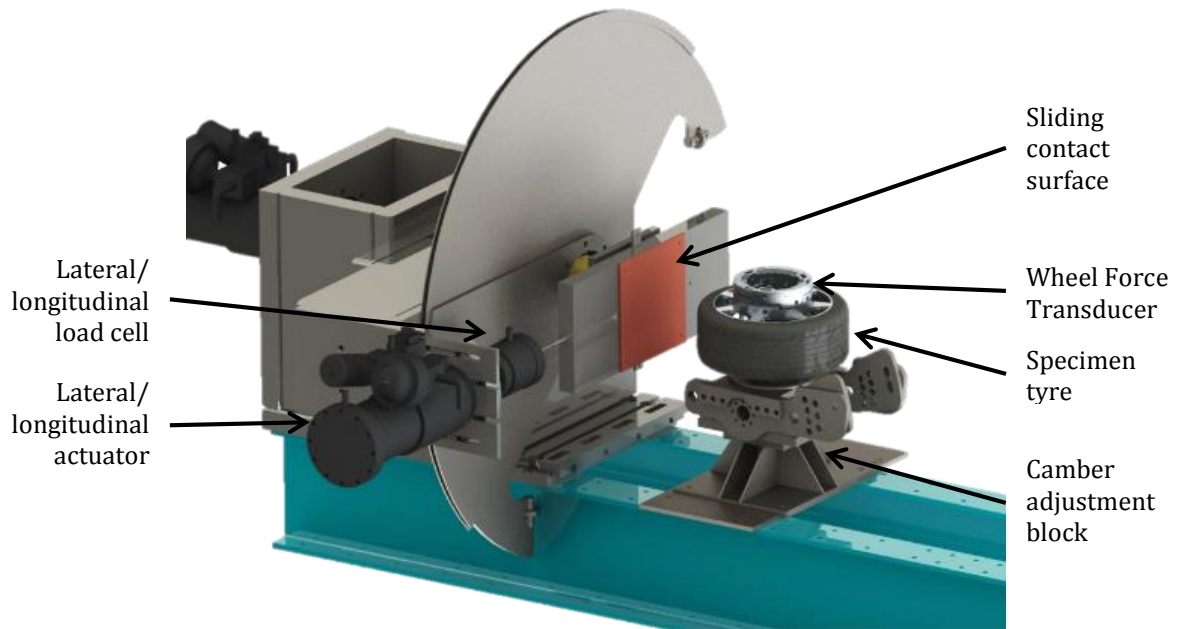


Figure 2.1 - Isometric view of STTR in position for vertical and longitudinal stiffness test

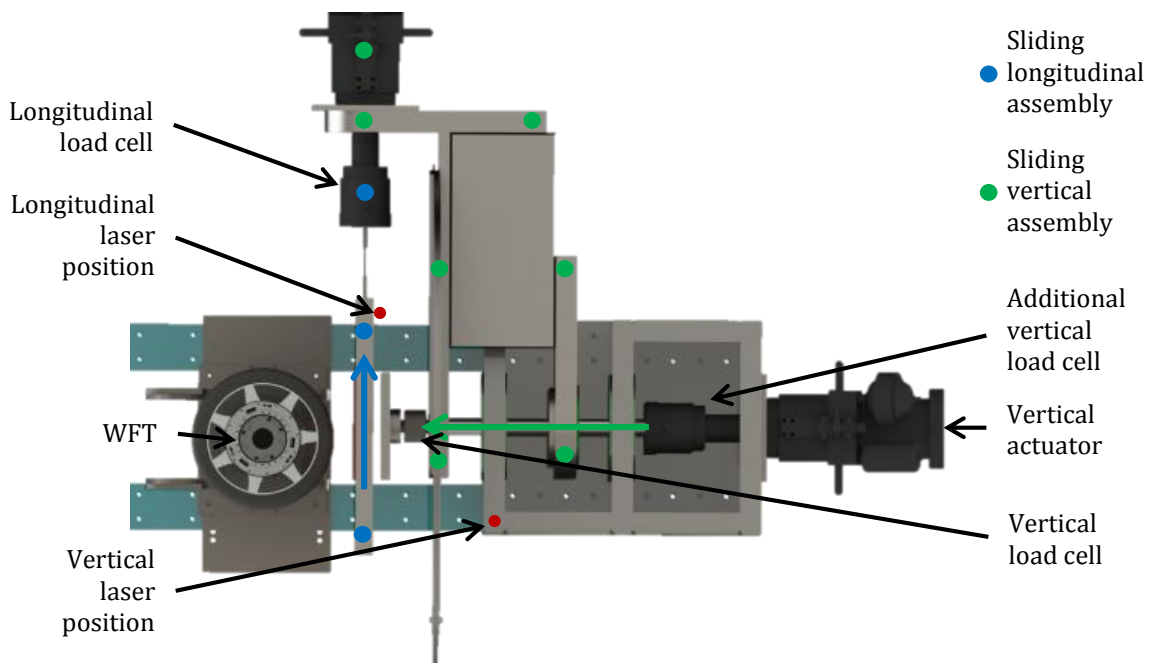


Figure 2.2 - Plan view of STTR in position for vertical and longitudinal stiffness test

TEST SETUP

When testing the longitudinal stiffness, the tyre is vertically loaded and then held at a specific load whilst the sliding longitudinal assembly, indicated by all those components connected with the blue dots, moves in the direction of the blue arrow. The displacement laser transducer positions are indicated by red dots and remained in the same position for all three test setups.

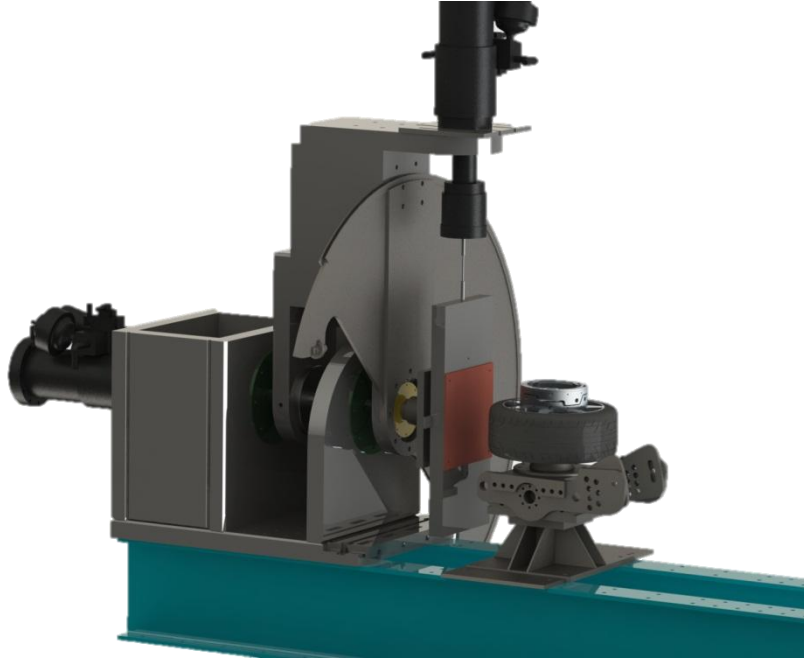


Figure 2.3 - Isometric view of the STTR in position for the lateral stiffness test

Figure 2.4 depicts the STTR for the lateral stiffness test as an isometric view whilst Figure 2.4 shows the side view of this setup. Once again the green arrow and associated green dots show the vertical travel of the setup. The blue arrow and blue dots indicate the components and their direction of travel when acquiring the lateral stiffness of the tyre.

TEST SETUP

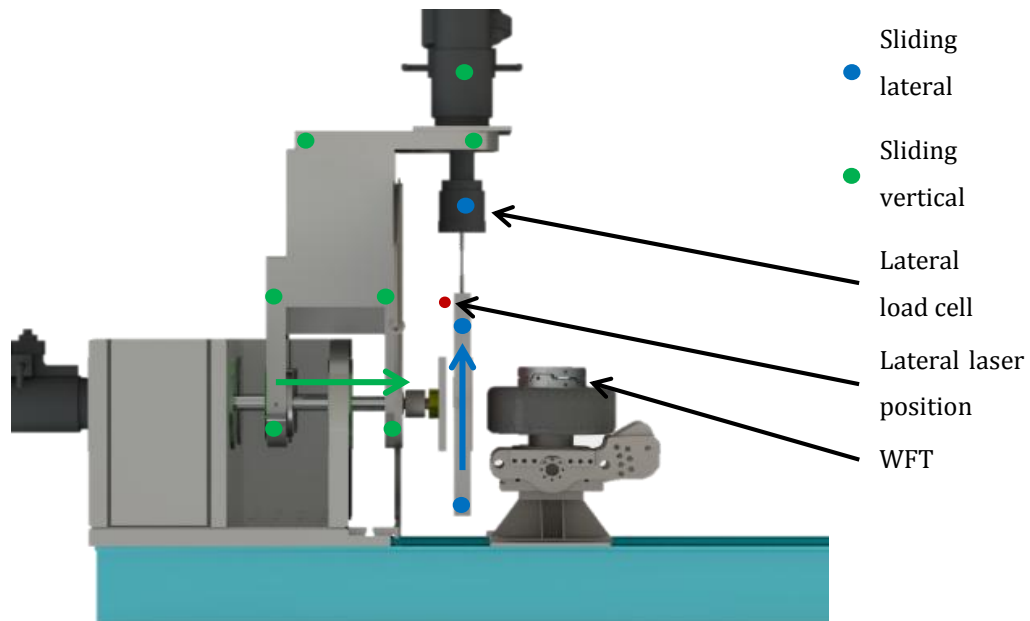


Figure 2.4 - Side view of STTR in position for lateral stiffness test

2.2.2.2 STTR Operating Equipment

The STTR makes use of two hydraulic actuators, namely a 100kN actuator for actuating in the vertical direction and a 40kN actuator for actuating in the lateral or longitudinal direction depending on the orientation.

Each actuator is fitted with a Linear Variable Differential Transformer (LVDT) displacement transducer and coupled with a Universal Low Profile (ULP) load cell (labelled as the vertical and lateral/longitudinal load cell in Figure 2.1 and Figure 2.2) of equivalent force range to that of the actuator are used as control inputs for each actuator. These together with a Moog solenoid valve are connected to a Zwick Roell controller which is used to operate each actuator. Each of these measuring devices was calibrated with a vernier and a calibration load cell respectively.

2.2.2.3 Miscellaneous Testing Equipment

The remaining test equipment includes that used to acquire the forces at the centre of the wheel, the actual displacements in the vertical, lateral and longitudinal direction, the tyre pressure and finally the data acquisition system.

2.2.2.3.1 Wheel Force Transducer

The Wheel Force Transducer (WFT) measures the forces and moments between the tyre contact patch and the wheel hub. This is achieved through the use of six load cells which use strain gauges in a Wheatstone bridge configuration to determine the axial force in each load cell. The device is ring shaped whereby three load cells are mounted in the axial direction and three in the tangential direction around the ring.

TEST SETUP



Figure 2.5 - Wheel Force Transducer (WFT) mounted onto the sample tyre rim

By measuring the angle of the WFT, the vertical, longitudinal and lateral forces in each load cell can be summed to attain the overall vertical, longitudinal and lateral force as well as all three moments generated by the tyre. Figure 2.5 shows the WFT mounted onto the rim of the tyre to be tested. From this figure, the lower side of the WFT is fixed through bolt connections to the rim. Thereafter the upper ring is connected using a hub adapter connected through the centre of the WFT to the hub of vehicle or in this case the hub mounted on the camber adjustment block shown in Figure 2.1.

Each of the six load cells are calibrated to the design load of 5000kg thereby acquiring a millivolt per volt sensitivity or calibration value of approximately 1.6 mV/V for each load cell which is used to determine the force experienced by each load cell. The resolution of each load cell is approximately 0.2mV/N .

2.2.2.3.2 Road-Profiling Lasers

As indicated by the red dots in Figure 2.2 and Figure 2.4, the road-profiling laser displacement transducers are used to capture the actual displacement of the contact surface in both the vertical and longitudinal or lateral direction depending on the test rig orientation (Acuity, 2016). They are extremely accurate displacement transducers with a resolution of 0.01mm across the span of 200mm . It was important to ensure the lasers were orthogonal to the surface they were measuring the displacement of. Furthermore, despite having a prescribed calibration value of 20.32mm/V the displacement outputs of these lasers were thoroughly checked.

2.2.2.3.3 Pressure Transducer

A Kyowa 1MPa PGL-A pressure transducer was used to measure the inflation pressure of the tyre, it has a sensitivity of $0.5275\text{kPa}/\mu\text{V/V}$.

TEST SETUP

2.2.2.3.4 Data Acquisition

An in-house data acquisition unit was used to capture all the necessary data at 1000Hz sampling frequency. Table 2.1 shows a list of all the channels captured on this unit.

Table 2.1 - List of data acquisition channels

Device	No. of Channels	Measurement	Units (post calibration)	Description
WFT	6	Force	N	3 lateral and 3 tangential load cells
Lasers	2	Displacement	mm	Vertical and lateral or longitudinal
Actuators Output 1	2	Force	N	Vertical and lateral or longitudinal
Actuators Output 2	2	Displacement	mm	Vertical and lateral or longitudinal
Pressure Transducer	1	Pressure	kPa	Tyre inflation pressure
Total	13			

2.2.3 Tread Profile Measurement

The tread profile of the tyre was measured using an improvised setup adapted to the STTR. The setup included a road profiling laser as well as a string displacement transducer. The two devices were coupled with the road profiling laser radially measuring the tread profile whilst moving along a guide constrained to the lateral direction of the tyre. Meanwhile, the string displacement transducer measured the laser's travel along this guide. Therefore by plotting the results of both devices the lateral tread profile could be obtained.

This test was conducted at five different locations around the tyre and the average profile was used to determine the overall dimensions of the tyre as well as the average tread wear for the wear analysis of this dissertation.

2.3 DYNAMIC TYRE TEST TRAILER

The Dynamic Tyre Test Trailer (DTTT) is used to test the tyre while it is rotating. This is the main difference between the two test setups. This setup is only used for acquiring data to parameterise the FTire model as well as wear down the tyres for the wear analysis.

TEST SETUP

2.3.1 Tests to be completed

Two tests are completed on this setup: the longitudinal force against the longitudinal slip (also known as the traction test) and the lateral force against the lateral slip angle (also known as the side force slip angle test).

2.3.1.1 *Traction Test*

The traction test involves measuring the longitudinal force generated by the tyre as the longitudinal slip of the tyre is steadily increased. This is achieved by slowly increasing the brake pressure on a tyre until it reaches lock up. Important here is a constant velocity and an accurate means of measuring the longitudinal slip.

2.3.1.2 *Side Force Slip Angle Test*

The side force slip angle test is a measurement of the lateral force generated by the tyre whilst the lateral slip angle is steadily increased. Here the tyre must be freely rotating and ideally swept through both positive and negative lateral slip angles. However, the latter is only necessary on an asymmetric tyre.

2.3.2 Data Not Acquired

Despite the large number of tests conducted, the set of data used to identify the rubber damping properties of the tyre was not performed. This data is usually acquired with the dynamic cleat test. This test is commonly conducted on a rotating drum and the resultant oscillatory deflection of the tyre as it continues rolling after overcoming the cleat is used to determine the damping properties of the tyre. The test is repeated at camber, different loads as well as cleats in an oblique orientation at 45° to the direction of travel.

These tests are very difficult to emulate on the dynamic tyre test trailer (DTTT) as it is nearly impossible to isolate the tyre's deflection due to damping of the tyre over the dynamics and suspension of the trailer itself. An estimate for the tyre damping, based on values for similar tyres were used in the model.

2.3.3 Equipment

2.3.3.1 *DTTT Operation*

The above mentioned tests are completed by controlling the brake pressure and slip angle of the tyre respectively. An isometric view of the DTTT is depicted in Figure 2.6, the various components of the general operation of the rig are also labelled in the figure. For the traction test, the trailer makes use of pneumatic brakes whose pressure is slowly ramped until the wheel locks up.

TEST SETUP

With regards to the side force slip angle test, two electric actuators are mounted to the slip angle arms shown in Figure 2.6 and used to apply a positive toe angle on the tyres. This ranges from -1° to 16° and is then swept back to -1° .

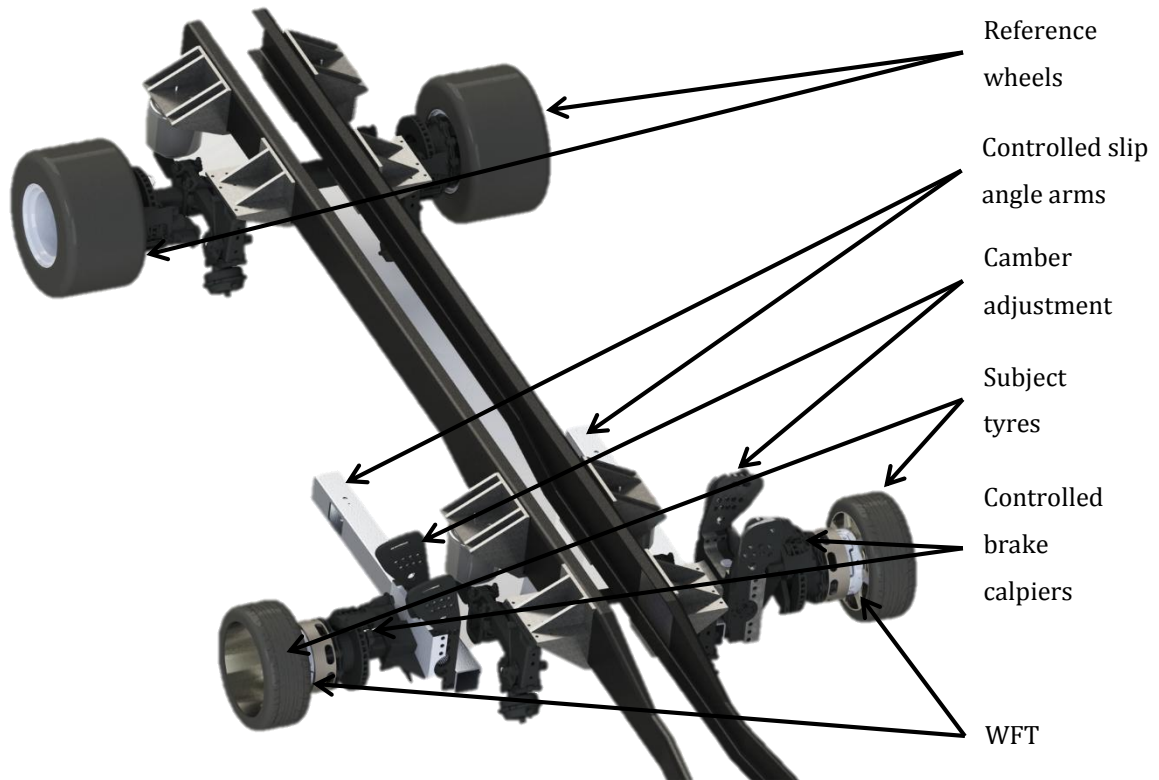


Figure 2.6 - Isometric view of the Dynamic Tyre Test Trailer

2.3.3.2 Measurement Equipment

The trailer makes use of the same instrumentation and data acquisition equipment as that used on the STTR. Therefore two WFT's measure the force at each of the sample wheels whilst road-profiling lasers are used to measure the displacement between the centre of the wheel and the road.

Proximity sensors are used to measure the angular velocity of each wheel as well as the reference wheel (free rolling) which are assumed to have a constant rolling radius. From this data the longitudinal slip can be calculated. However, digital image correlation (Botha, et al., 2014) is also used to measure the longitudinal and lateral slip at the tyre contact patch with the use of two cameras videoing the tyre-road contact patch.

Finally, angle encoders are used to measure the slip angle of the wheel. It is assumed here that the slip angle is equal to the steer angle of the wheel. All of these channels as well as the two

TEST SETUP

sample tyre's inflation pressures are acquired on a similar data acquisition unit as that used on the STTR also sampling at 1000Hz.

2.3.4 Wheel Slip Calculation

The measurement of the wheel's longitudinal slip is briefly covered here as it forms an important role in the parameterisation of the FTire tyre model, thus its accuracy needed to be validated. There are two methods for acquiring this feature of the tyre, one is based on a theoretical formula for calculating the effective rolling radius of the tyre from the road-profiling lasers. It then makes use of the proximity sensors on the reference wheel and the sample tyre to finally calculate the percentage slip based on the assumption that the reference tyre does not slip. The second method makes use of digital image correlation (Botha, et al., 2014) as previously mentioned and is a direct measurement of the slip as it compares the velocity of the road (representing the velocity of the centre of the wheel) to the actual velocity of the tyre sidewall at the contact patch.

2.3.4.1 Theoretical Method

From Blundell, et al. (2004) the effective rolling radius of a tyre is said to be equal to that shown in Equation (4):

$$R_e = R_l + \frac{2\delta_z}{3}, \quad (4)$$

where R_e is the effective rolling radius, R_l is the loaded radius measured by the road-profiling laser and δ_z is the change in the radii between the loaded and unloaded radius of the tyre. Using Equation (4), the theoretical longitudinal velocity of the sample tyre is acquired from Equation (5) (Gillespie, 1992):

$$V_l = R_e \times \omega, \quad (5)$$

where V_l is the theoretical longitudinal velocity of the tyre and ω is the angular velocity of the tyre acquired from the proximity sensor measurement. Using Equation (5), the effective rolling radius of the reference tyre can also be calculated using its measured angular velocity and the longitudinal velocity of the sample tyre taken at the beginning of the test run when it is still free rolling. This is done due to the fact that the loaded radius of the reference tyre is not known.

Finally, using the effective rolling radius of the reference tyre which is assumed to be constant, the longitudinal velocity of the reference tyre is calculated for each sampled data point. This value is compared to that of the theoretical longitudinal velocity of the sample tyre in Equation (6):

$$\Phi = \frac{V_{ref} - V_l}{V_{ref}}, \quad (6)$$

TEST SETUP

where Φ is the longitudinal slip of the sample tyre, V_{ref} is the longitudinal velocity of the reference tyre and V_l is the theoretical longitudinal velocity of the sample tyre.

The above formulation was used to determine the longitudinal slip because the reference tyre and the sample tyre had different rolling radii because they were different tyre sizes.

2.3.4.2 *Correlation*

The two methods were compared and whilst the data was spread with noise, the correlation was assuring. This indicated that the assumptions made were fair and that either method could be used to capture the longitudinal slip of the tyre.

2.4 CONCLUDING REMARKS

Two test setups were described and detailed in this chapter. The STTR is used to capture the large majority of the test data used to compile this dissertation. Therefore an explanation of its operation and the equipment used to capture data was given in detail.

This was followed by a brief explanation of the operation of the DTTT which was only used to capture the data necessary to parameterise the FTire tyre model. Some further detail was provided regarding the theoretical calculation of longitudinal slip as there was some uncertainty surrounding this data collection. Nevertheless, assuring correlation was found using two independent methods thereby validating the data for use in the parameterisation of the tyre model.

3 TESTING METHOD SENSITIVITY

3.1 INTRODUCTION

Due to the uncertainties surrounding the effects of aging and wear on the stiffness properties of a tyre as well as the fact that the changes are not expected to be large, general sensitivities regarding the test setup, testing method and the repeatability of the tests needed to be scrutinised. These sensitivities mainly include how the vertical stiffnesses of the tyre are acquired.

The investigation involves examination of the effects of a multiple cyclic loading, the loading velocity, the loading and unloading waveform, the contact surface and small temperature variations. These analyses are presented in the form of graphs and are scrutinised using the variations in the percentile deflection at specific loads as explained in Chapter 1. More details concerning the actual tyres are studied through tests on four of the same tyre as well as tests on the two different test setups.

Ultimately, the testing sensitivity was determined by defined accuracy boundaries. These boundaries will be used in the wear and age investigation presented later in this dissertation as the threshold for any changes to be solely attributed to either aging or wear.

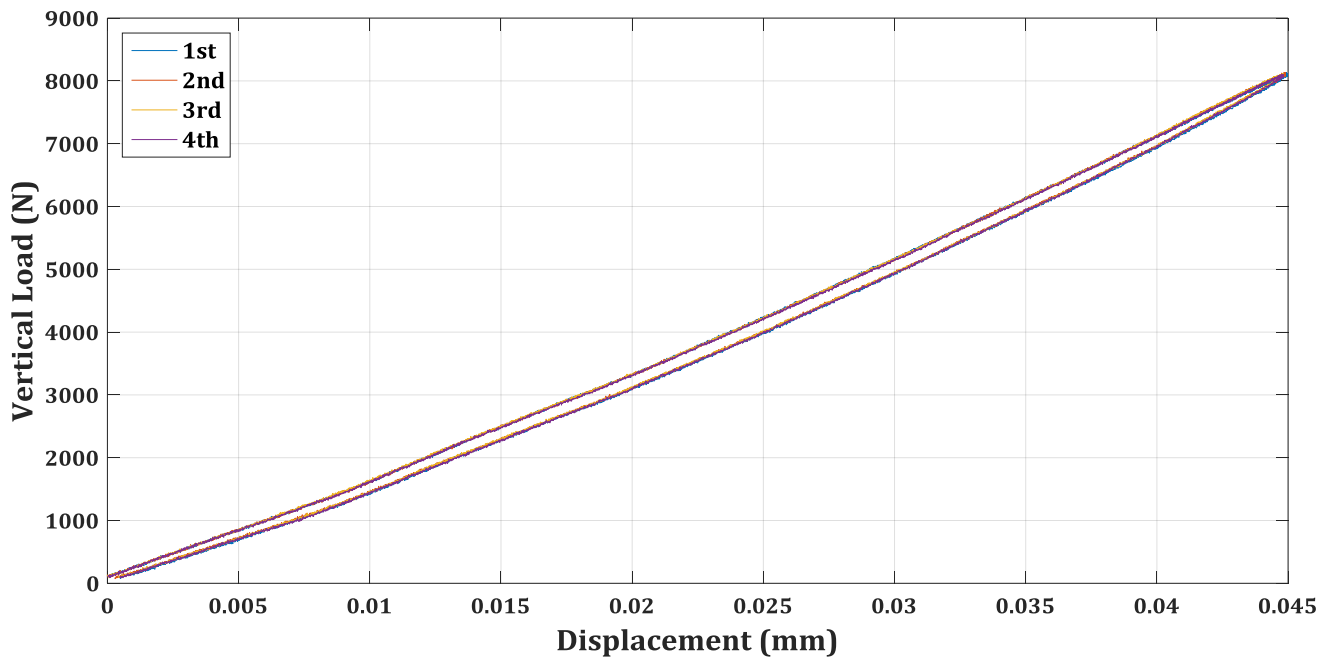


Figure 3.1 - Comparison of four consecutive cycles at 0.1 Hz with vertical stiffness

TESTING METHOD SENSITIVITY

3.2 CYCLE SENSITIVITY

The first analysed sensitivity is that of consecutive cycles. It was to be determined whether a dependency existed on the number of consecutive cycles applied to the tyre. Figure 3.1 shows the results using a sinusoid and triangular waveform with a frequency of 0.1Hz and an amplitude of approximately 22.5mm with four consecutive cycles applied to the tyre.

It is evident from this figure that the force-displacement characteristic of the tyre is independent of the number of cycles applied to the tyre. This implies that when selecting a specific loading cycle or singling out one loading line, the potential error from the actual stiffness is negligible. This is confirmed as a maximum percentile change in deflection at 50% of the LI was 0.2%.

3.3 INPUT WAVEFORM

Two different input waveforms were tested, namely a sinusoidal input and a triangular input. The effect of the waveform in the form of the vertical stiffnesses on a flat surface is shown in Figure 3.2.

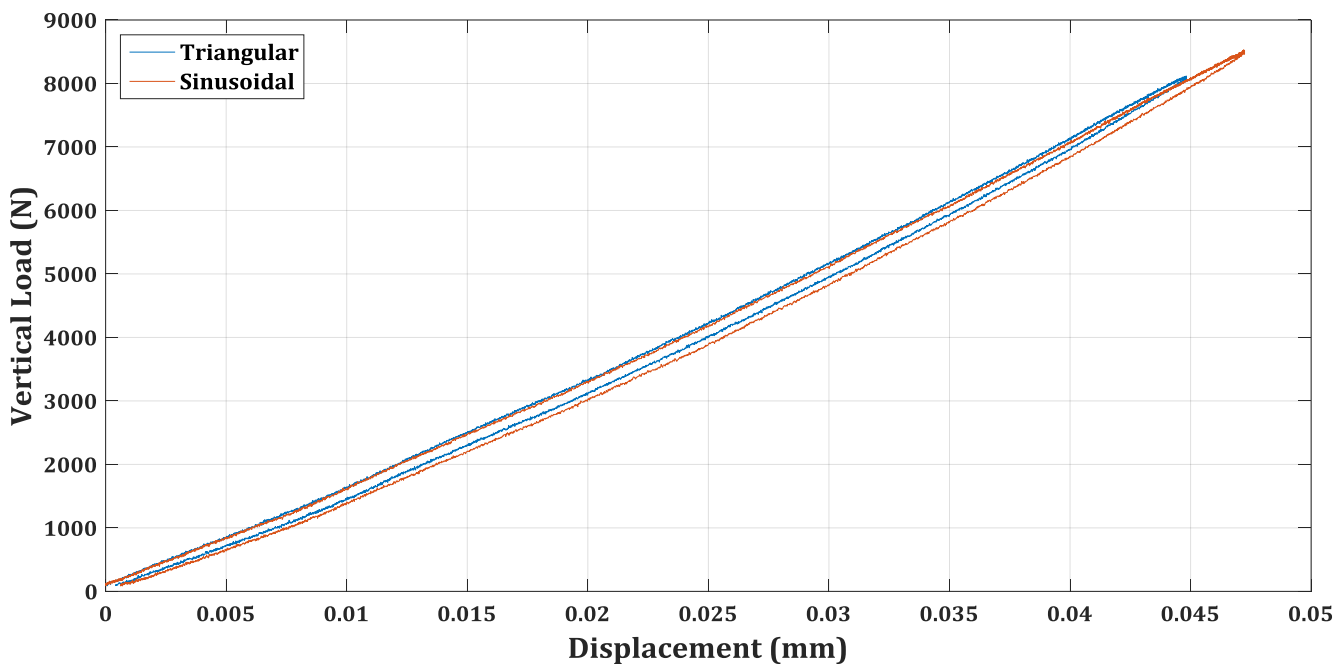


Figure 3.2 - Comparison of input waveform at 0.5 Hz loading velocity with vertical stiffness

Here, a slight dependency does appear such that the percentile deflection at 50% of the LI is 0.7%. Although still very small, this change is more visible. It indicates that the same loading waveform should be used for all tests.

TESTING METHOD SENSITIVITY

3.4 LOADING VELOCITY SENSITIVITY

The loading velocity was hypothesised to have one of the larger influences on the resultant vertical stiffness of the tyre. This is simply due to the scrubbing effect at the tyre contact patch and its dependency on the damping of the tyre which is well known as being dependent on velocity. The results of loading the tyre at 0.1, 0.2 and 0.5 Hz are shown in Figure 3.3.

Figure 3.3 indicates that significantly different maximum loads are achieved by each velocity

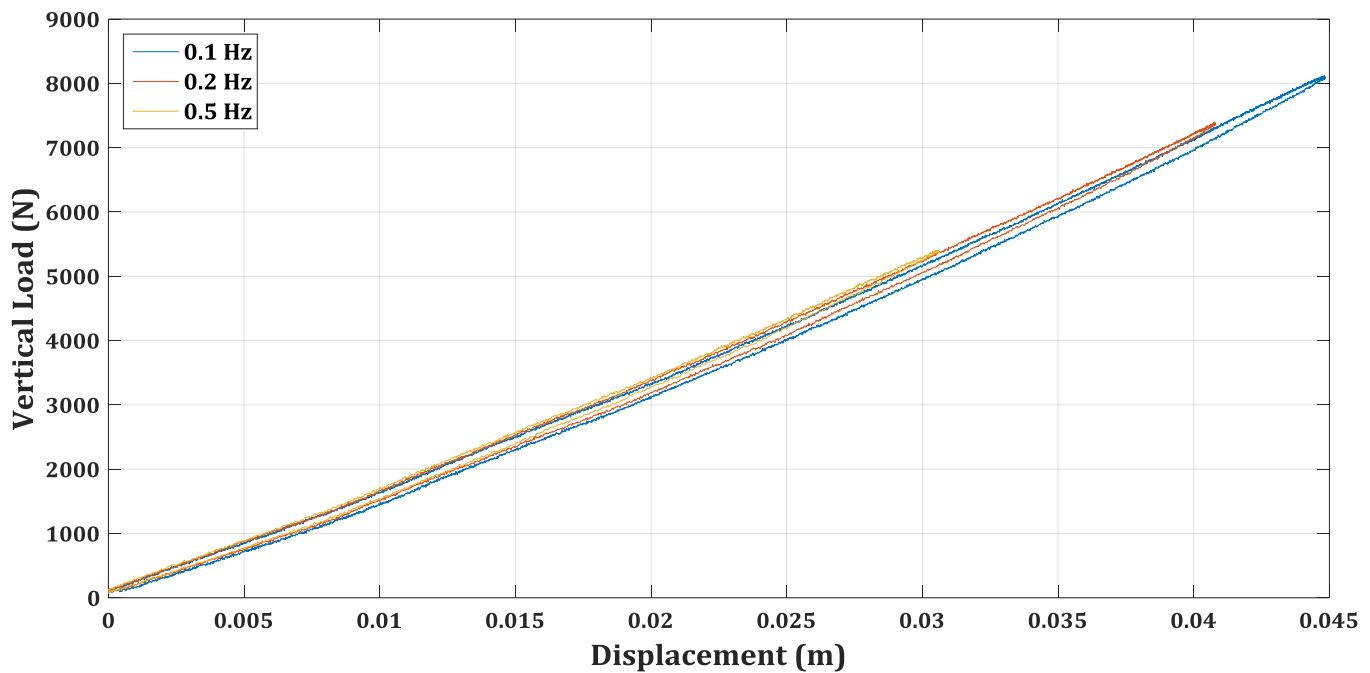


Figure 3.3 - Comparison of input waveform velocity with vertical stiffness

stiffness line. This occurs due to an equipment limitation where the actuator is not able to follow the required displacement vs. time as the velocity is increased. Furthermore, the actual velocities obtained were 8.8, 15.4 and 25.4 mm/s for the 0.1, 0.2 and 0.5 Hz cycles respectively and the velocities were not completely constant as one would expect with a triangular waveform. Nevertheless, the velocity dependency is clear from this figure and relates to a percentile deflection change of 1.9% between the fastest and slowest loading velocities at 50% of the LI.

3.5 DIFFERENT TEST SETUP

As discussed in Section 2.2, initial tests were performed on an improvised test setup whilst additional tests were conducted on the dedicated tyre test rig (STTR) described in detail in Section 2.2. This section seeks to compare the STTR results to the initial results. The results of the vertical stiffness are presented in Figure 3.4.

In the initial phase of this stiffness, below the 50% of the LI, the correlation is excellent with a percentile deflection difference of approximately 0.4%. At higher loads, a discrepancy clearly

TESTING METHOD SENSITIVITY

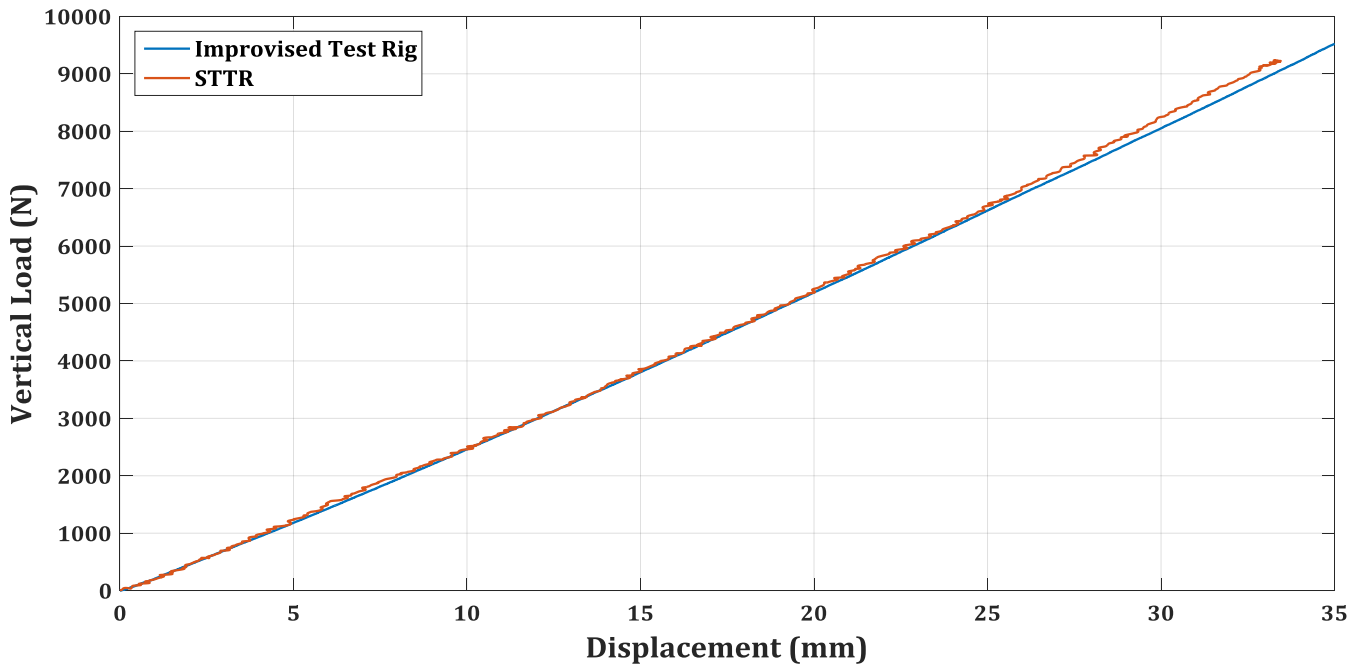


Figure 3.4 - Comparison of vertical stiffness measured on two different test rigs

exists up to the LI of the tyre where the change in deflection is as much as 2%. This could be due to a different contact surface as well as the fact that the improvised setup allowed the wheel to freely rotate whereas the STTR setup locks the rotation. Furthermore the STTR provided better stiffness than the improvised setup: These will be discussed later in the chapter.

3.6 DIFFERENT TYRES

Four of the same tyres were tested in this section, with the only difference between one of the tyres being its respective date of manufacture differing by 3 weeks. This is important as it positions this tyre (tyre 1) in a different batch from the other three (tyres 2, 3 and 4) which are most likely from the same batch. The results of the tests at 0° and -4° camber are depicted in Figure 3.5.

In this figure it is clear that there is a distinction between tyre 1 and the remaining three. It results in a percentile change in deflection at 50% of the LI of 1.6% from the other three tyres, which at the same load only vary by $\pm 0.2\%$. The case of the vertical stiffness at camber appears to depict an even larger discrepancy; however a very similar percentile change in deflection of 1.5% indicates otherwise.

TESTING METHOD SENSITIVITY

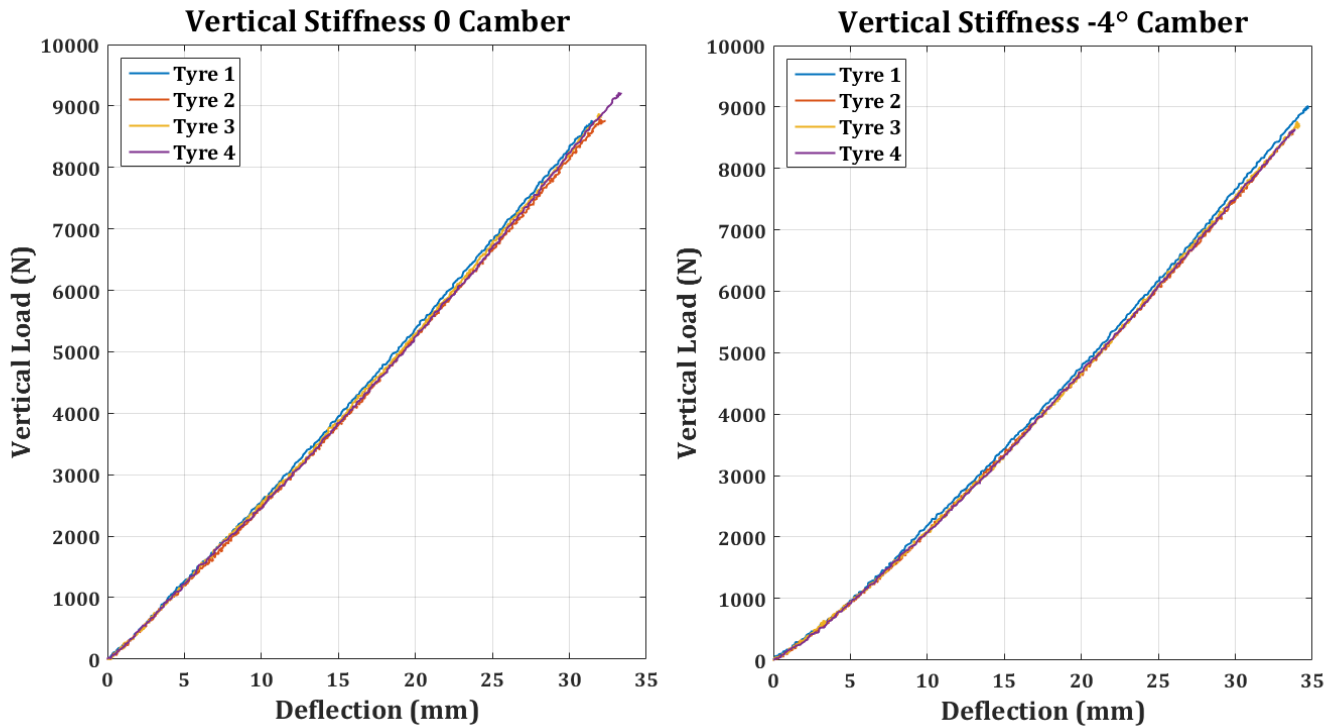


Figure 3.5 - Comparison of 4 of the same tyre with the vertical stiffness on a transverse cleat at 0 and 4° camber

3.7 SMALL TEMPERATURE VARIATIONS

This sensitivity analysis involves checking the effect of a small variation in the ambient temperature, thus a change in temperature of the tyre. The change in temperature was 6°C, with the original test taking place with a tyre temperature of 26°C measured on the tyre. The results are presented in Figure 3.6 and demonstrate a negligible dependency on this temperature variation for the full load of the tyre with a variation of 0.5% on the deflection at 50% of the LI. This sensitivity could have potentially more dependence with larger variations in temperature.

3.8 CONTACT SURFACE

Two largely differing contact surfaces were used to check the vertical stiffness dependency on the friction coefficient of the contact surface. The first contact surface, also being the surface used for the remainder of the tests in this dissertation, was a sheet of P80 corundum sand paper as frequently used for tyre tests. This was compared to a very smooth Perspex sheet coated with a liquid soap to reduce the friction coefficient further. Figure 3.7 illustrates the results of these tests and includes the hysteresis loop to reveal potential effects of damping. The results, at an inflation pressure of 1.5Bar, are also depicted.

TESTING METHOD SENSITIVITY

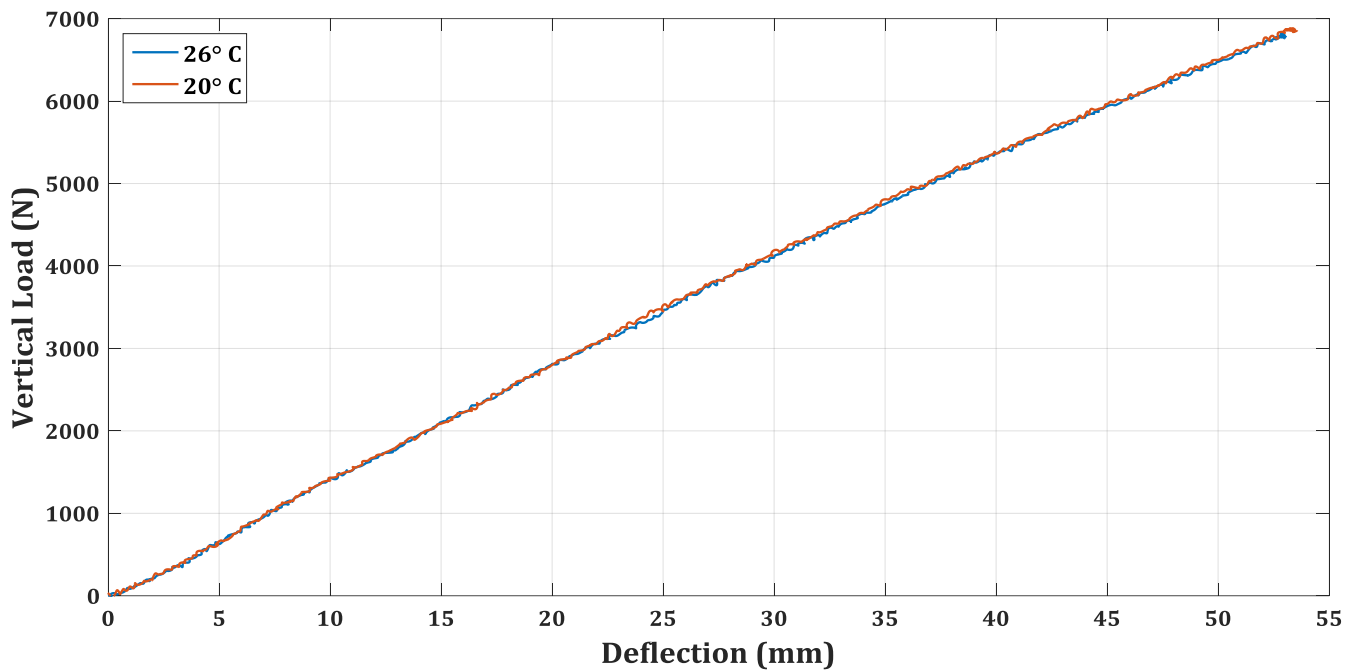


Figure 3.6 - Comparison of minor changes in the tyre temperature with the vertical stiffness on a transverse cleat at -4° camber

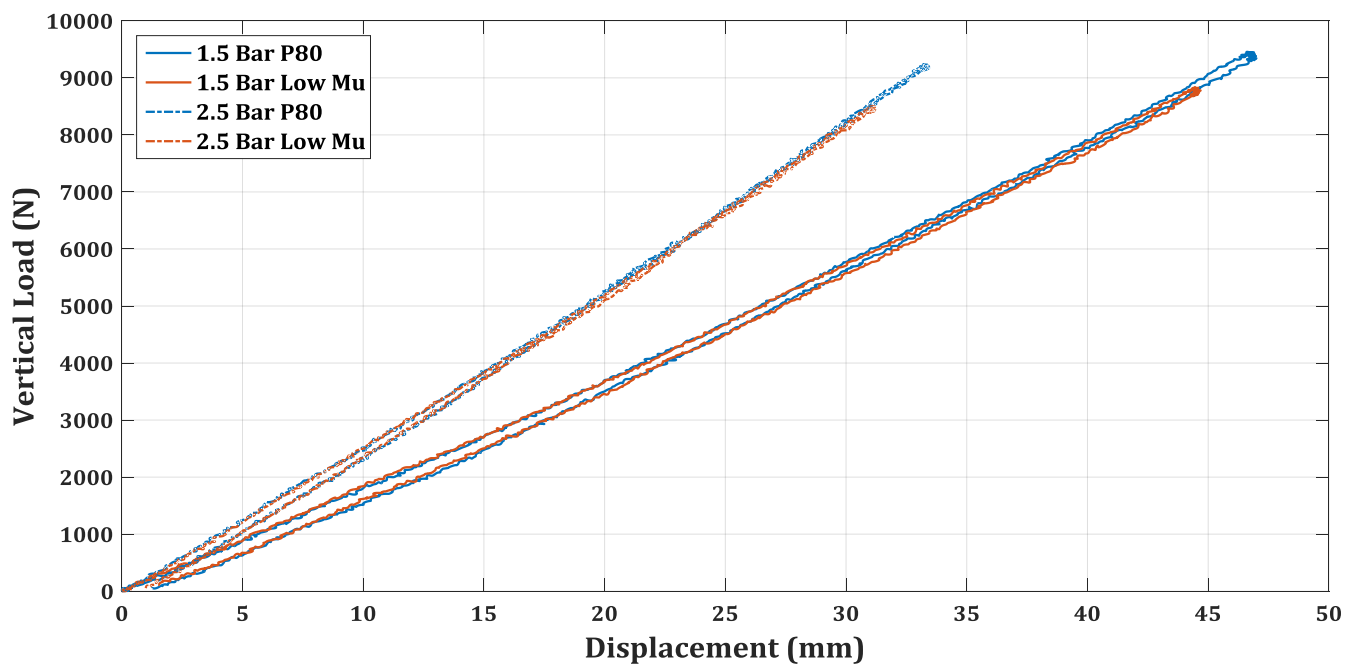


Figure 3.7 - Comparison of two different contact surface friction coefficients at 1.5 and 2.5 Bar inflation pressure with the vertical stiffness

From Figure 3.7 it appears that the dependency on the friction coefficient of the actuating surface has negligible effect on the vertical stiffness of the tyre. The variations observed in the lower inflation pressure, despite being small, are slightly more visible. They relate to 0.9% where the

TESTING METHOD SENSITIVITY

2.5Bar variations relate to 0.5% at 50% of the LI. Furthermore, there also appears to be very little effect to the hysteresis loop which holds a similar width for both pressure cases and both surfaces.

3.9 CONCLUDING REMARKS

The sensitivity analysis presented demonstrated a wide variety of testing parameters which can lead to uncertainties in the results produced and presented in the remainder of this dissertation.

Negligible changes were observed as those which produced changes in the percentile deflection at 50% of the LI of less than 1%. These include the selection of a loading cycle in between multiple cycles (0.2%), the loading waveform whose minor variations (0.7%) can be accounted for due to the variation in velocity of the sinusoid waveform, a tyre temperature variation of less than 6 °C (0.5%) and a change of contact friction coefficient (maximum of 0.9% at 1.5 Bar inflation pressure).

Some more noticeable dependencies were observed in the loading velocity (1.9%), the different test setups (2%) and the different tyres (1.6%). The variations are relatively significant however they are smaller when recalling that the error in measuring the vertical stiffness of a tyre has boundaries of $\pm 1\%$.

The most noticeable change occurs in the comparison between the two test setups. Whilst it was initially anticipated that the contact surface could account for this discrepancy, it was found to only have an absolute maximum influence of 0.9%. The remaining +1.1% can be argued to be caused by the locking of wheel rotation in the new setup or the increased rigidity of the new setup, however, further investigation would be required to confirm this. Nevertheless for the remainder of this dissertation the loading velocity was held constant whilst the same test setup was always used. Therefore the direct influence of these variations does not influence the relative results of this dissertation.

That being said, however, it can be concluded that any vertical tyre stiffness acquired from this test rig and testing procedure will have error margins of $\pm 1\%$ change in the vertical deflection around 50% of the LI of the tyre. As a result of this, in order for a change in percentile deflection presented hereafter to have any bearing on being a characteristic of the tyre it should show a change of at least greater than $\pm 1\%$.

4 FTIRE PARAMETERISATION

The process of parameterising an FTire model is discussed in this chapter as well as the validation of the tyre model acquired. It follows the process discussed in Section 1.2 and reflects on the accuracy and usability of the developed model.

4.1 CHECKING-IN OF DATA

To parameterise the tyre model, the relevant data is 'checked-in' to the FTire/fit environment. Thereafter validation and identification of the tyre parameters commences.

use reference tire for:

car, SUV, or van tire

truck tire

motorcycle front tire

motorcycle rear tire

aircraft tire

create tire with size / rating:

sect. width	asp. ratio		rim diam.	LI	speed sym.
235	/	55	R 19	105	V
235	/	55	ZR 19	105	V
mm or in	%		in		

and basic data:

tire manufacturer	pirelli	pirelli
tire type	passenger	passenger
rim width	9.1	9.1 in
nominal inflation pressure	2.5	2.5 bar
second inflation pressure		bar
tire mass	13.6	13.6 kg
deflection at LI load	32.400	32.400 mm

leave fields blank if value unknown; blue value: reference tire

customize estimation formulae ..

prefer this kind of data:

same as in reference tire

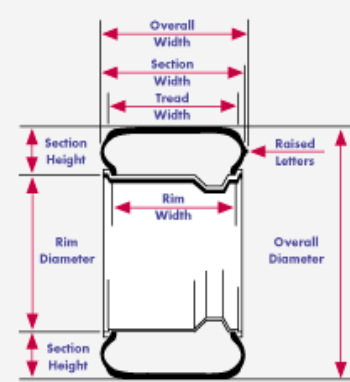
direct

static

handling (standard)

handling (motorcycle)

modal



unit converter:

1	mm =	0.039	in
1	bar =	14.504	psi
1	N =	0.225	lbf
1	kg =	2.205	lbs
1	km/h =	0.621	mph
1	MPa =	32.278	Shore A

(formula as used in FTire)

show load index table

show speed symbol table

external link: tire/rim sizes

Figure 4.1 - FTire/fit tyre estimate and geometrical data

FTIRE PARAMETERISATION

4.1.1 Tyre Geometrical Data

The selection of a tyre model estimate is important in the FTire parameterising process. The greater the similarity between this estimate and the tyre being modelled, the easier and more efficient the parameterisation process. Depicted in Figure 4.1 is the first step in generating a tyre model. The ‘car, SUV, or van tire’ is selected as the reference tyre. Thereafter the relevant geometrical data based on actual measurements are added.

Figure 4.2 illustrates the tread and carcass profile generated from the data captured of the tread profile and interpolated in MATLAB. These geometrical specifications are crucial to the accuracy of the footprints of the tyre model.

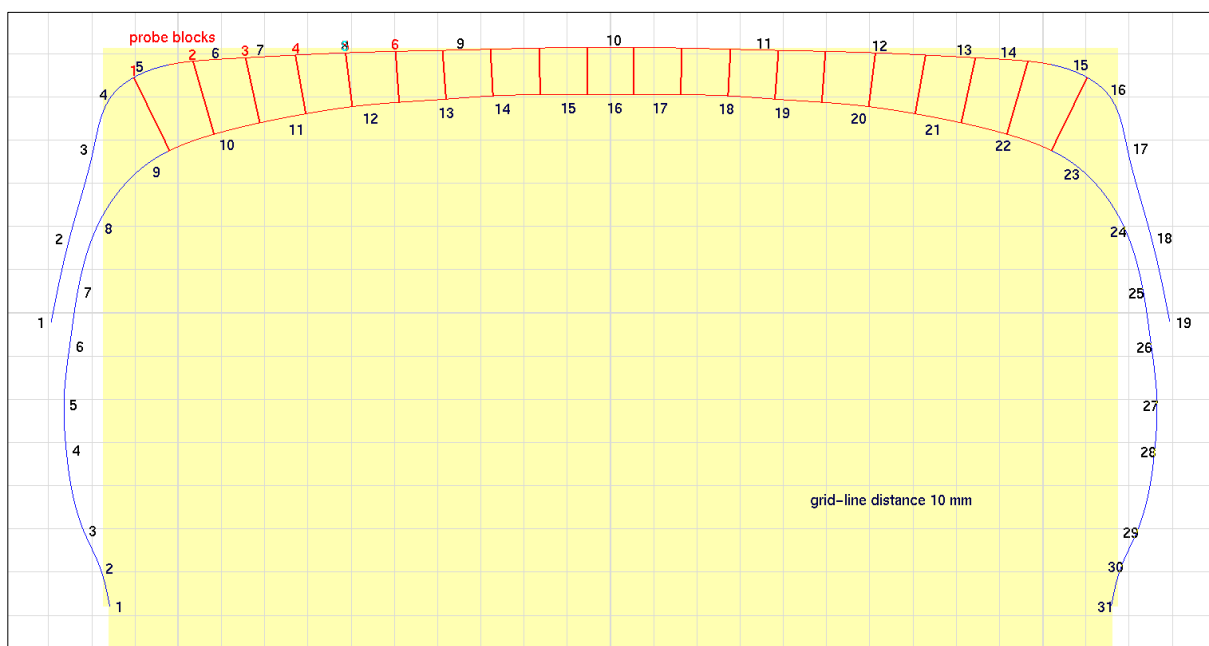


Figure 4.2 - FTire/tools tread and carcass cross-section

4.1.2 Tyre Footprints

The tyre footprints were measured at two camber angles: 0° and -4° at 50 and 100% of the load index (LI).

4.1.2.1 Footprint Capture

The footprints were generated by placing a 4mm thick white plastic sheet painted with non-drying paint, or dye (Ardrox HF-P High Sensitivity red dye penetrant – usually used for Non-Destructive Testing) as per Els et al. (2016). The tyre is loaded to the desired vertical load and then unloaded. The marked sheet is photographed in a fixed, calibrated camera setup where the camera height and angle were kept constant for all the footprint measurements. The camera used to capture the footprints was calibrated using a ‘chequered’ black and white board (Figure 4.3) which was later used in MATLAB to determine the actual length of each pixel in the captured

FTIRE PARAMETERISATION

footprint. An example of one of these calibration photos is shown in Figure 4.3. Figure 4.4 is an example of the raw footprint image taken at 100% of the LI and at -4° camber.

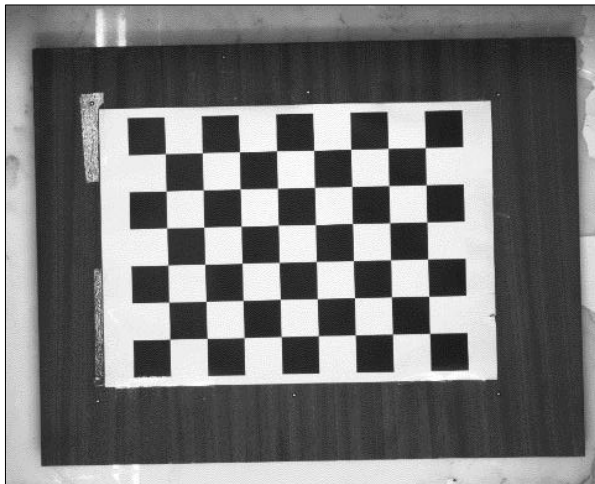


Figure 4.3 - Calibration board

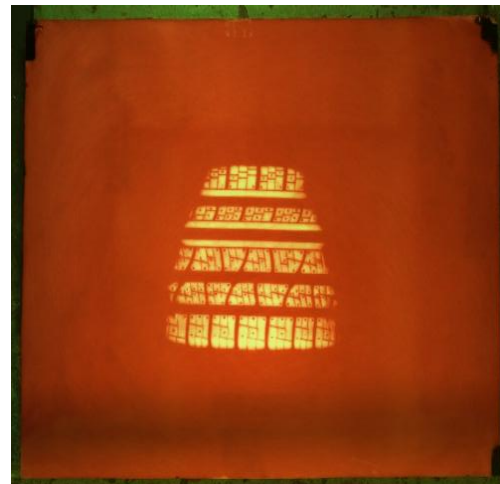


Figure 4.4 - Footprint at 100% of the LI and -4 degrees camber

4.1.2.2 *Footprint Post-Processing*

To ensure that the footprints captured were accurately represented in FTire/fit, the camera lens distortion was accounted for and thereafter a calibration factor was implemented. All footprints were initially rectified removing any curvature that may be present due to the lens being used as completed in Els et al. (2016). Thereafter a MATLAB script is used to interpret the known dimensions of the calibration board to acquire a calibration value for the camera setup. This is then used to scale the footprint images and convert them to bitmaps. Furthermore FTire/fit requires a red line of known dimension in each bitmap which it uses to interpret each footprint.

Finally, the colour images are converted to black and white and a scaling factor is used to single out the footprint from the surrounding untouched paint. The final footprint bitmap of Figure 4.4 is shown in Figure 4.5. This process results in a very detailed, well-defined and accurate footprint.

4.1.2.3 *Footprint and Tread Pattern check-in*

The footprints were checked into the FTire/fit environment in the form of a black and white bitmap. As mentioned in Table 1.3, these footprints are used to identify the belt torsion and twist stiffnesses (footprints at camber) and the belt lateral and in-plane stiffnesses (footprints at 0° camber).



Figure 4.5 - Final scaled black and white footprint bitmap

For the dynamic test data validation and identification, the tread pattern of the tyre was checked-in despite only being recommended for the modelling of tyres with large tread blocks and/or grooves (Gipser, 2005). It was anticipated that a better model of the contact patch friction would be achieved by including this data.

The tread pattern is cropped from the bitmap of the footprint at 100% of the LI at 0° camber as FTire/fit requires the most repeatable tread pattern strip. This option was activated for the validation and identification of the dynamic data and was otherwise deactivated.

4.1.3 Tyre Static and Dynamic Data

As per Table 1.3 and Table 1.4, the static test data includes a variety of tests for the vertical, longitudinal and lateral stiffnesses of the tyre. The dynamic data comprises mainly of longitudinal and lateral slip of the tyre. As is for this dynamic test data, TYDEX (.tdx) is the standard file format recognised by FTire/fit for all test data. Conversion to this format was completed in MATLAB. The format is text based and therefore simple to compile in this environment.

4.1.3.1 Data Manipulation

In order to lessen the load on the optimisation process in FTire/fit, all test data was sub-sampled in order to reduce the file size. Whilst original data was sampled at 1000Hz in both cases (static and dynamic), the data was filtered and subsampled to 100Hz. Figure 4.6 and Figure 4.7 illustrate this process for a static and dynamic test respectively.

Evident in Figure 4.6 is a small shift in the displacement of the graphs. This is done intentionally to ensure all TYDEX stiffness files start from the same value.

FTIRE PARAMETERISATION

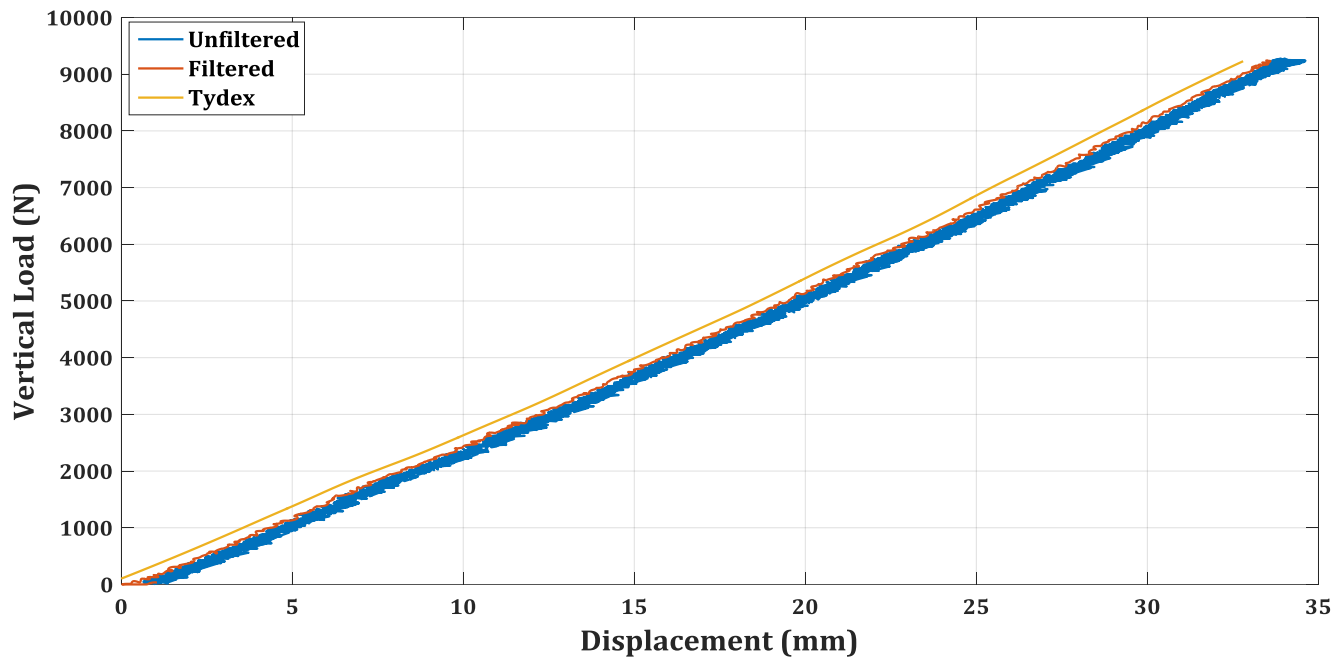


Figure 4.6 - Vertical stiffness data filtering and sub-sampling

Figure 4.7 illustrates a more drastic change from the original data to the TYDEX format. High frequency excitation from the road as well as the dynamic response of the tyre is filtered out at 40Hz and also subsampled such that only the quasi-static response remains. However, an additional smoothing function is used to attain the final lateral stiffness line. Due to the fact that FTire/fit makes use of the trend of the data given to it, the 'line-of-best-fit' shown in Figure 4.7 was accepted as sufficient to represent the behaviour of the tyre.

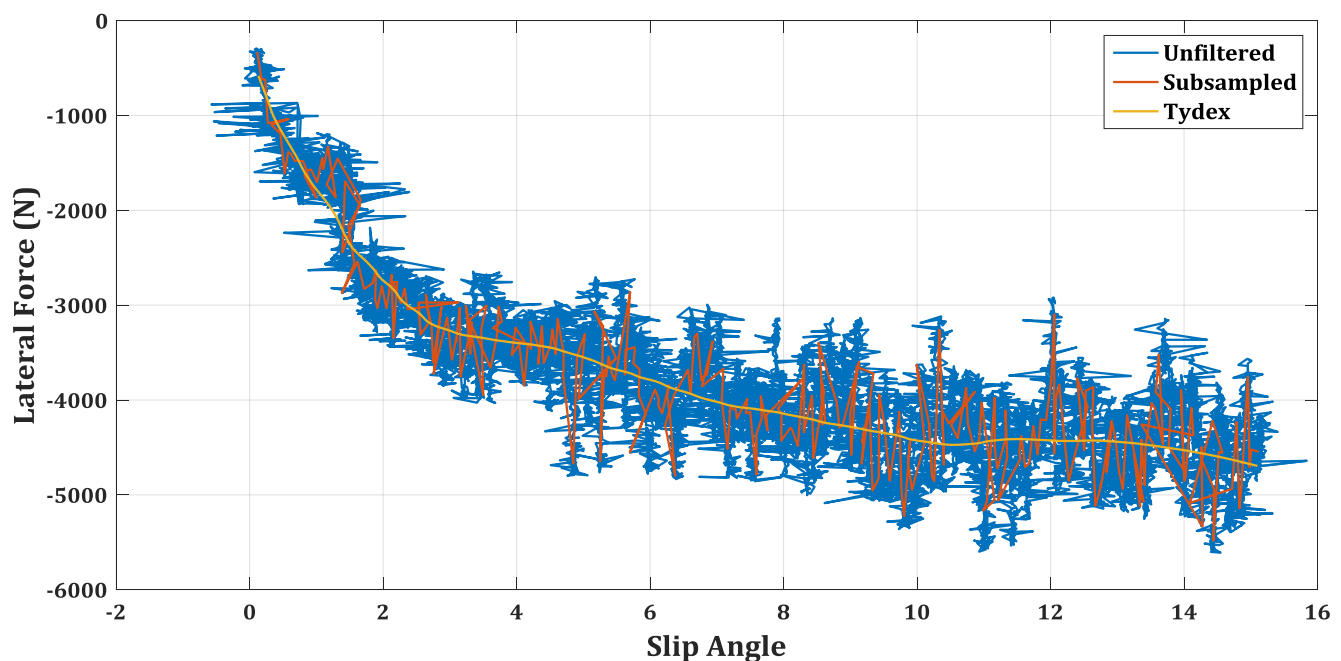


Figure 4.7 - Side force vs slip angle data filtering and sub-sampling

FTIRE PARAMETERISATION

4.2 INITIAL VALIDATION

Having imported all the captured data, the section below shows the first validation of the footprints of the default tyre model. This simply illustrates the ‘gap’ that needs to be filled by the parameterisation process. As with most models, the user must start off with an initial estimate. The closer this estimate is to the final product the greater the possibility of finding a good representation of the real tyre.

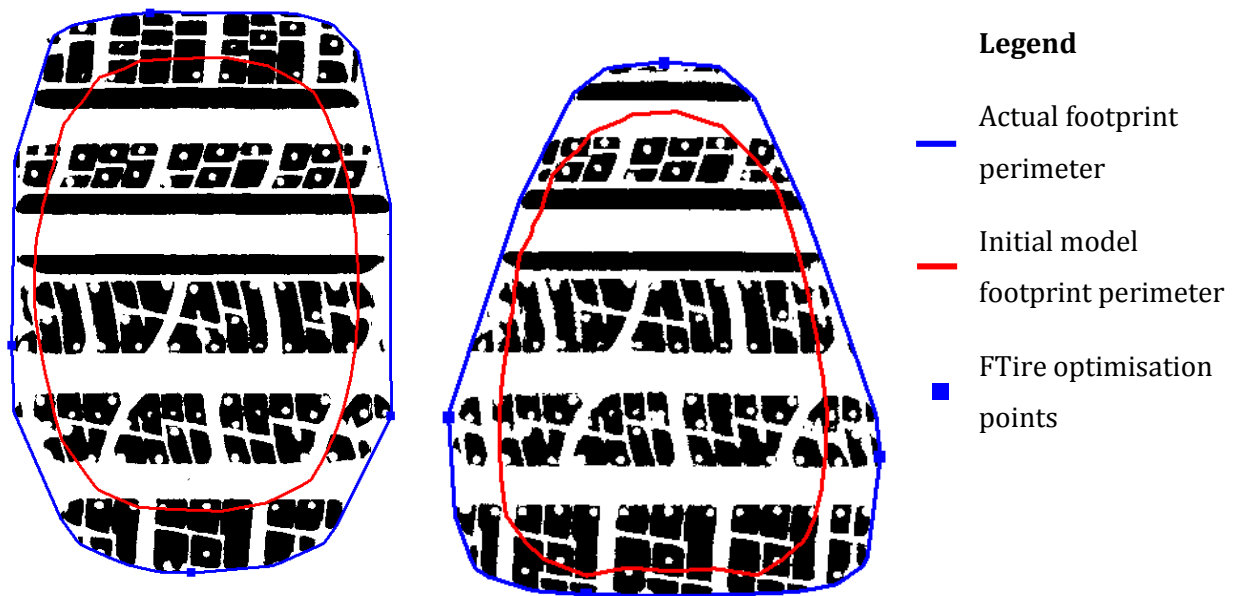


Figure 4.8 - Initial validation of footprints at 50% of the LI: 0° camber (Left), -4° camber (Right)

Figure 4.8 shows the first validation of the footprint area with that of the FTire tyre model. Clearly evident is the large discrepancy between the measured footprint and the tyre model. According to the FTire/fit software the error for both footprints is in the region of 30%. In essence, FTire/fit will only use the four square dots around the periphery of the measured footprint to determine this error and optimise the necessary parameters to reduce this error. Through the identification of the parameters governing these footprints and the remaining parameters, the error will be minimised in the sections to follow.

4.3 IDENTIFICATION AND FINAL VALIDATION

The identification process is in general very simple. The parameter or parameters of the tyre model being identified in each test are adjusted by a percentage value specified by the user. The resultant tyre model is simulated under the same conditions as that of the measurement data and subsequently compared to this measurement data resulting in a certain error. This error is then used in three major steps for each identification process.

FTIRE PARAMETERISATION

4.3.1 Process

The process of identifying the parameters involved by first identifying the steady-state tests. Thereafter the footprints were identified. Each parameter is identified individually, where possible, otherwise the FTire/fit solver will be under-constrained and won't solve. This can be a tedious process, as the optimisation of one parameter can lead to the divergence of another. Thus it can become somewhat of a compromising process between parameters.

4.3.2 Steady-State Test Identification

4.3.2.1 Vertical Stiffness Tests

4.3.2.1.1 Vertical Stiffness on a Flat Surface

The first test identified was the vertical stiffness on a flat surface at 0° camber. Table 4.1 indicates the changes in the percentage error of the displacements at 50 and 100% of the LI from before and after the identification.

Table 4.1 - Change in vertical stiffness error at 50 and 100 % of the LI

Load (% of the LI)	Initial Error (%)	Final Error (%)
50	-1.5	-0.21
100	-3.3	-1.7

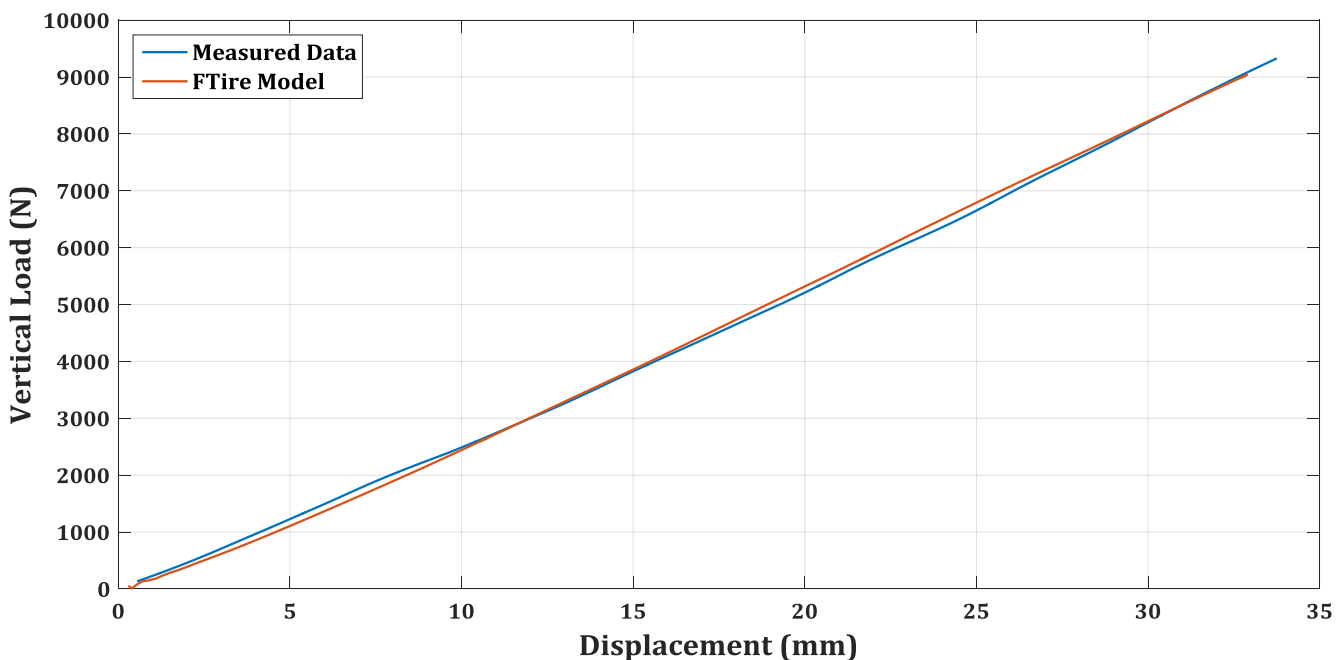


Figure 4.9 – Final FTire Validation - Vertical stiffness at 0° camber

FTIRE PARAMETERISATION

Evident in Figure 4.9 are the two parameters identified in this test. These are the first and second deflection points and are shown by the locations on the graph where the model's stiffness line crosses that of the test data.

4.3.2.1.2 Vertical Stiffness with a Cleat

The transverse cleat is placed parallel to the lateral direction of the tyre and was ensured to be in the middle of the tyre. The validation of the model is depicted in Figure 4.10: the results of which are promising. There is a slight discrepancy in the slope at the low loads of the graph, however, accuracy drastically improves as the load is increased. This discrepancy could not be avoided as a change in the in-plane bending stiffness (which is too low in this case) would negatively affect the footprint validation at 0° camber.

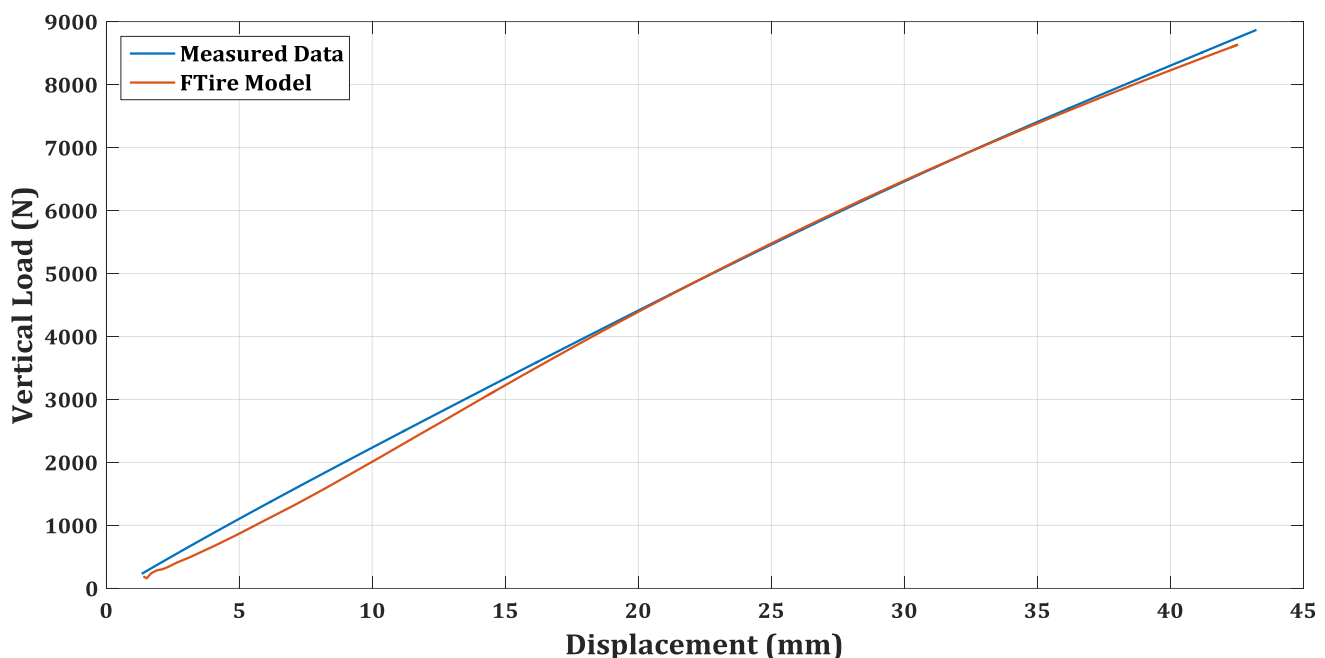


Figure 4.10 - Final FTire validation - vertical stiffness on transverse cleat at 0° camber

The final vertical stiffness upon which a parameter can be identified is that with the longitudinal cleat. In this case, as can be seen in Figure 4.11, the correlation is not ideal. Firstly evident in the test data is the distinct change in slope at the higher loads of the stiffness. This occurs due to the tyre making contact with the surface upon which the cleat is mounted.

In FTire/tools it is possible to manipulate the deflection at which this change occurs in the model however this only improves the accuracy of the stiffness line at the higher loads and worsens it at the lower loads. Despite this, the actual gradient after this change has occurred in both data sets shows a positive correlation. Nevertheless, there appears to be information missing in the

FTIRE PARAMETERISATION

test data or in the checking-in process as FTire is not able to capture this behaviour in the same way it has been tested.

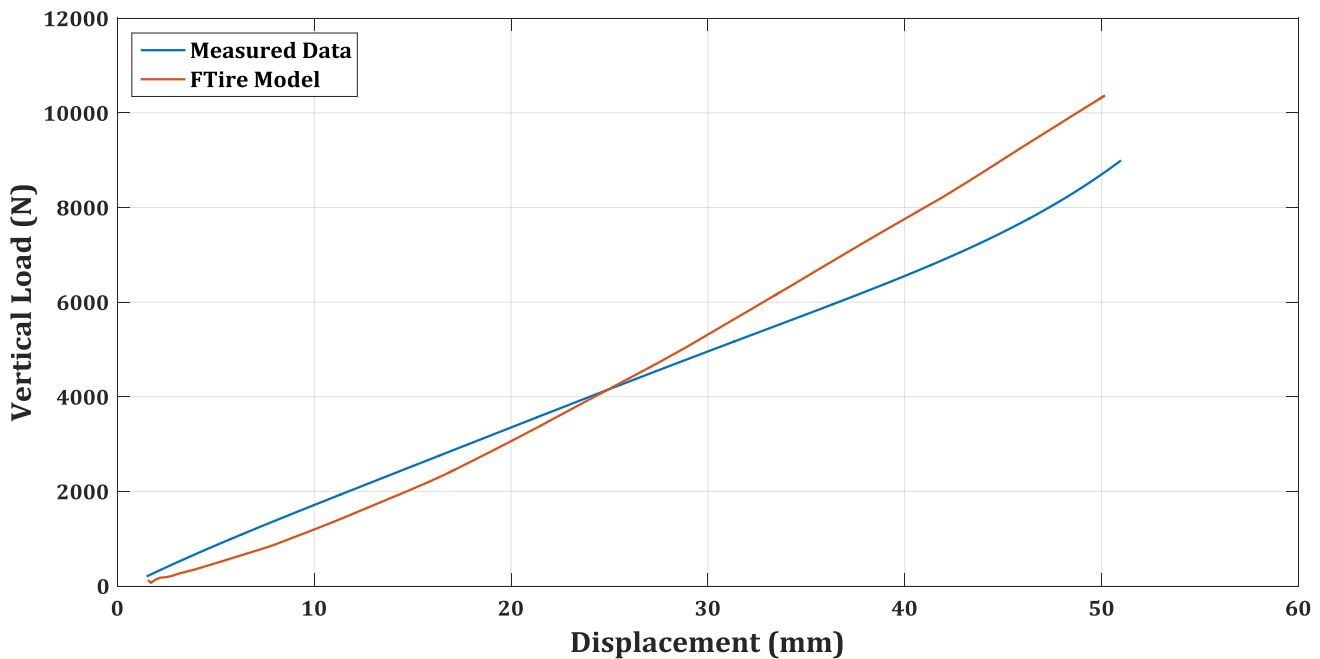


Figure 4.11 - Final FTire Validation - vertical stiffness with longitudinal cleat at 0° camber

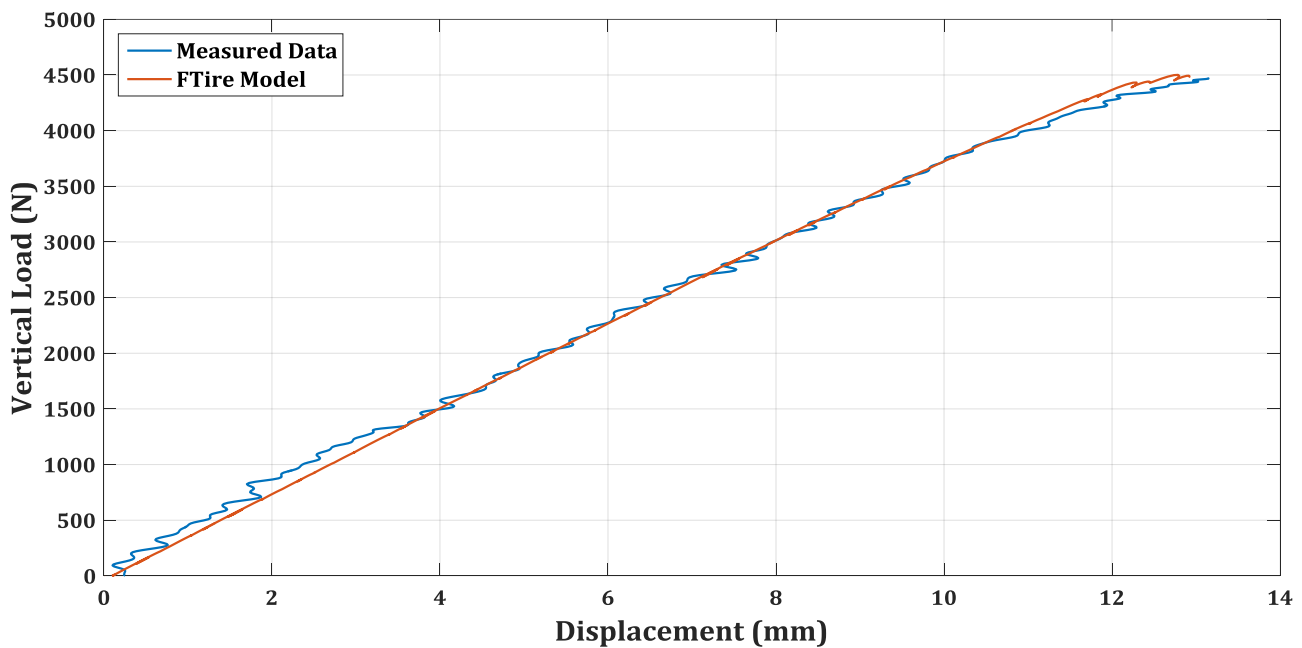


Figure 4.12 - Final FTire Validation - longitudinal stiffness

4.3.2.2 Longitudinal Stiffness Test

The validation of the longitudinal stiffness test is shown in Figure 4.12. Excellent correlation is evident here, illustrating that the longitudinal stiffness parameter has been accurately captured

FTIRE PARAMETERISATION

in the model. It is important to note that this is only the longitudinal stiffness prior to any slip occurring.

4.3.2.3 Lateral Stiffness Test

The identification of this test was only completed with the measured data from the WFT, however, the ULP load cell provides an additional form of validation in Figure 4.13. The unusual nature of the WFT data could be characteristic of the tyre due to its asymmetric tread pattern, however, further investigation is required to confirm this. As a result the tyre model was only identified to capture the stiffness at the lower lateral loads (less than 1500N). This assumption is fair because with the addition of the measured lateral load from the ULP the same gradient is matched in the tyre model. Evident, however, in Figure 4.13 is that the measured lateral load from the ULP load cell is slightly higher than that of the measured data from the WFT. This makes sense as the WFT will isolate forces into their respective three directions, whereas the measured data from the ULP load cell will capture everything even if there is a slight change in the angle of the plate. Nevertheless it still provides an additional validation method confirming that the tyre model accurately represents the lateral stiffness of the tyre.

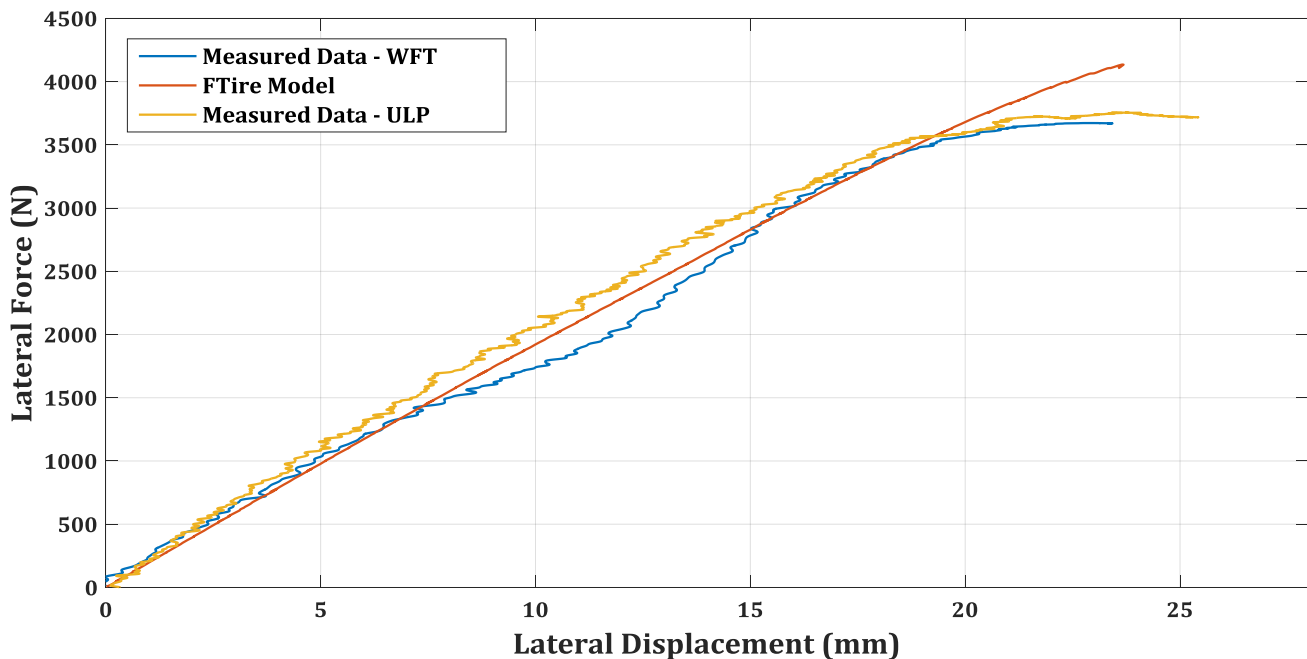


Figure 4.13 - Final FTire Validation - lateral stiffness

4.3.3 Dynamic Stiffness Tests

The validation of these tests was completed with the inclusion of the tread pattern.

FTIRE PARAMETERISATION

4.3.3.1 Calculation of Wheel Slip

The wheel slip was required for the validation of both the longitudinal and lateral force against slip test measurements. Detail regarding this calculation has been covered in Section 2.3.4. Evident from this discussion was the reliance on a theoretical formula and assuming the deflection of the tyre remains constant as the test is conducted. Due to the fact that this is a dynamic test there are several dynamic influences that are not specifically measurable and can greatly affect the accuracy of the longitudinal slip calculated. This should be kept in mind when using this test data to identify parameters of the tyre model.

4.3.3.2 Longitudinal Slip

The parameter which defines the longitudinal force against longitudinal slip is the stiffness of the tread rubber. In FTire/fit this is defined as the Shore A hardness of the tread which, as mentioned previously, was systematically measured at 5 locations on the tread around the tyre and repeated approximately 10 times to ensure a fair test was conducted. A summary of the results of the Shore A hardness measured before and after dynamic testing was completed is shown in Table 4.2. The anticipated change in Shore A hardness due to dynamic testing is clearly evident in the table where the hardness values all drop by approximately 6.

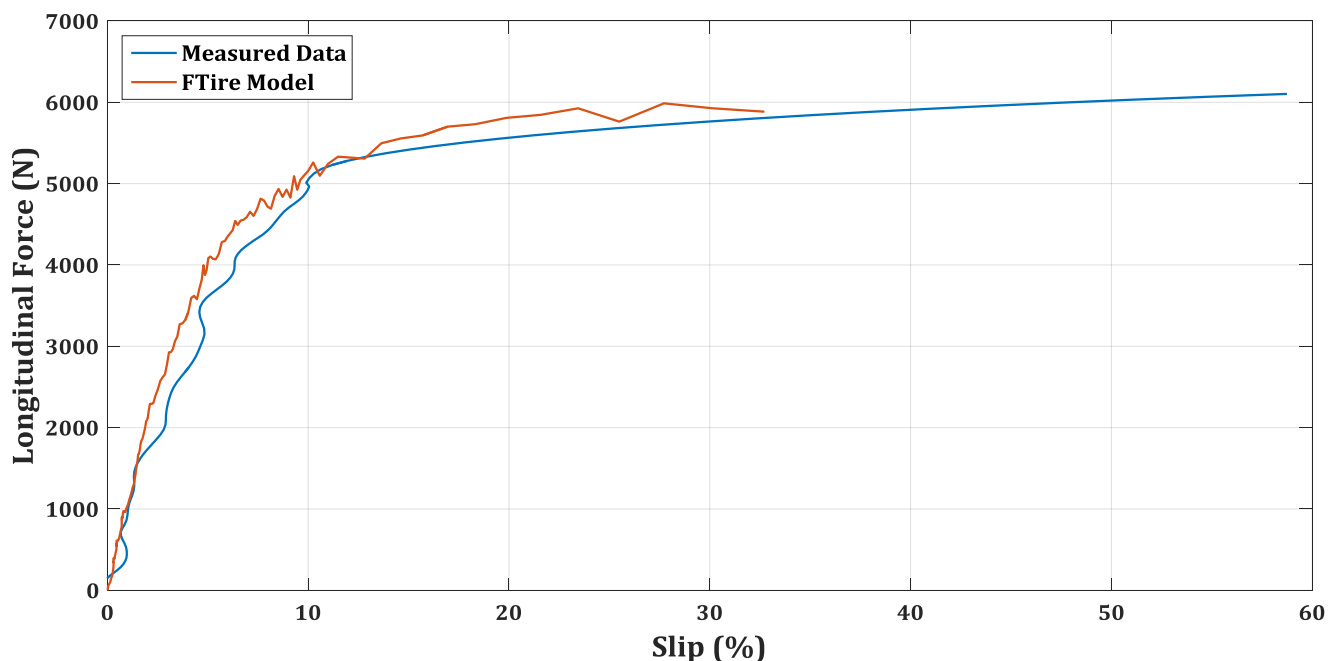


Figure 4.14 - Final FTire Validation - longitudinal force against longitudinal slip

The change is largely due to the abrasive wear that occurs during dynamic testing and the fact that the original hardness test was conducted on a brand new tyre. Table 4.2 thereby assists in providing a range within which the tread stiffness parameter can be adjusted to match the longitudinal slip graph. As a result the Shore A hardness value used to produce Figure 4.14 was

FTIRE PARAMETERISATION

70; this was decided to be the most reasonable estimate of the hardness at the time of the test. It would make more sense to trust the range of the hardness rather than allowing FTire/fit to change this tread stiffness drastically to match the test data which is less trustworthy compared to the Shore A hardness measurement due to the assumptions made in the longitudinal slip calculation.

Table 4.2 - Shore A Hardness of Tyre Tread Before and After Testing - Statistical Results

Shore A Hardness	Before Testing	After Testing
Average	71.64	65.5
Minimum	68.6	61.8
Maximum	75.1	69

Another positive result observed from Figure 4.14, is that the maximum longitudinal force correlates well between the tyre model and the test data. This indicates that the friction values for the tyre model are well aligned for the tyre being used on a concrete surface similar to that at the test facility.

4.3.3.3 *Lateral Slip*

The lateral slip test data was completed at 0° and -4° camber as well as at two different loads, however, only one parameter, the out of plane bending stiffness, is identified between all of these tests. Therefore the highest load at zero camber was used to identify the parameter and the remainder was used for validation purposes.

Figure 4.15 shows this test data validation after identification and despite some of the uncertainties with the test data the correlation is remarkable for the low slip angle section of the graph. Furthermore respectable correlation is observed with the maximum lateral force obtained implying that the friction values are well aligned.

FTIRE PARAMETERISATION

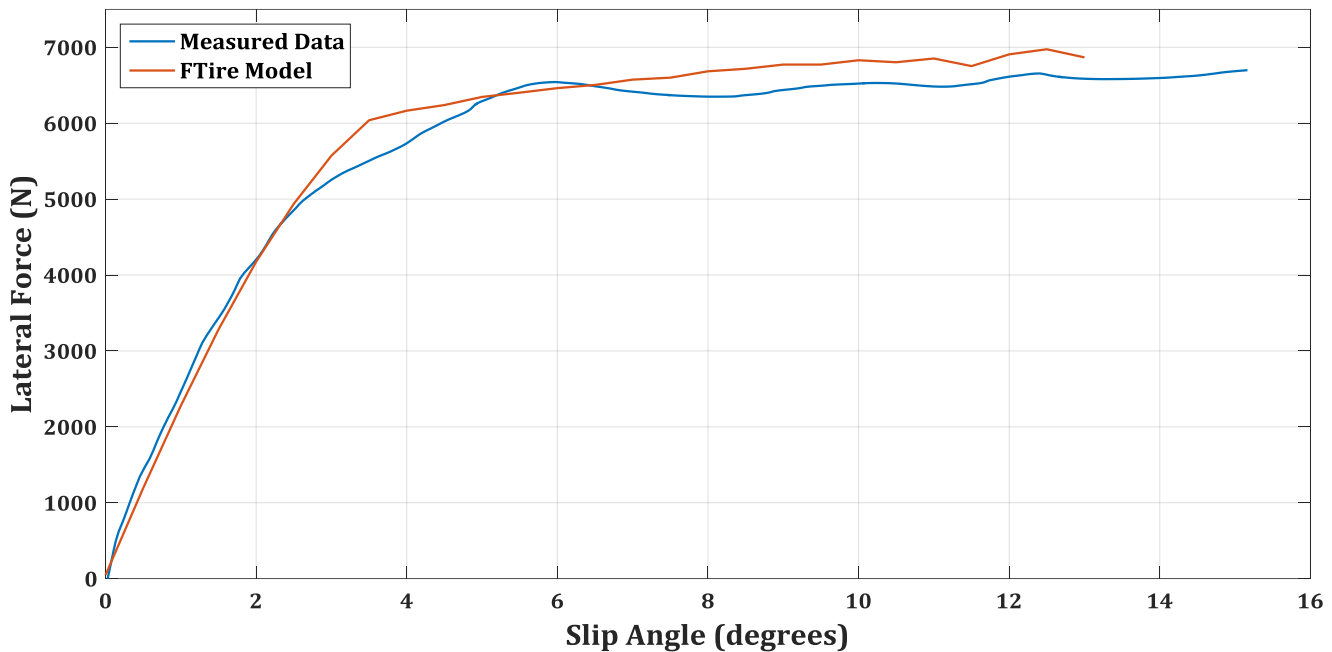


Figure 4.15 - Final FTire Validation - lateral force against lateral slip angle at 0° camber

Finally, the lateral force against lateral slip angle at -4° camber is used for further validation of the out of plane bending stiffness parameter. Poorer correlation was observed in this validation between the test data and the tyre model, however, identification of this parameter would directly affect the characteristic shown in Figure 4.15 of the lateral force at 0° camber. This is important as it is more likely that the tyre model will be used at 0° camber rather than -4° camber.

4.3.4 Footprints

Due to the high confidence in the footprint measurements, parameter identification was focused on ensuring the footprint validation was as accurate as possible. Arguably the most important part of the footprint correlation is that the correct tyre geometry has been given to FTire/fit. Thus having the tread profile measurements greatly assisted in ensuring the correct geometry was checked-in.

4.3.4.1 Flat Footprints

The footprints at 0° camber are produced by the lateral and in-plane bending stiffness parameters of the tyre model. Figure 4.16 shows the footprints 4.4kN (left) and 9kN (right). Clearly evident from this figure is exceptional correlation between the actual footprint and that of the tyre model. Whilst the error used in FTire/fit to produce an optimal result only takes into account the four blue squares around the footprints, the rest of the perimeter of the footprint is still well matched.

FTIRE PARAMETERISATION

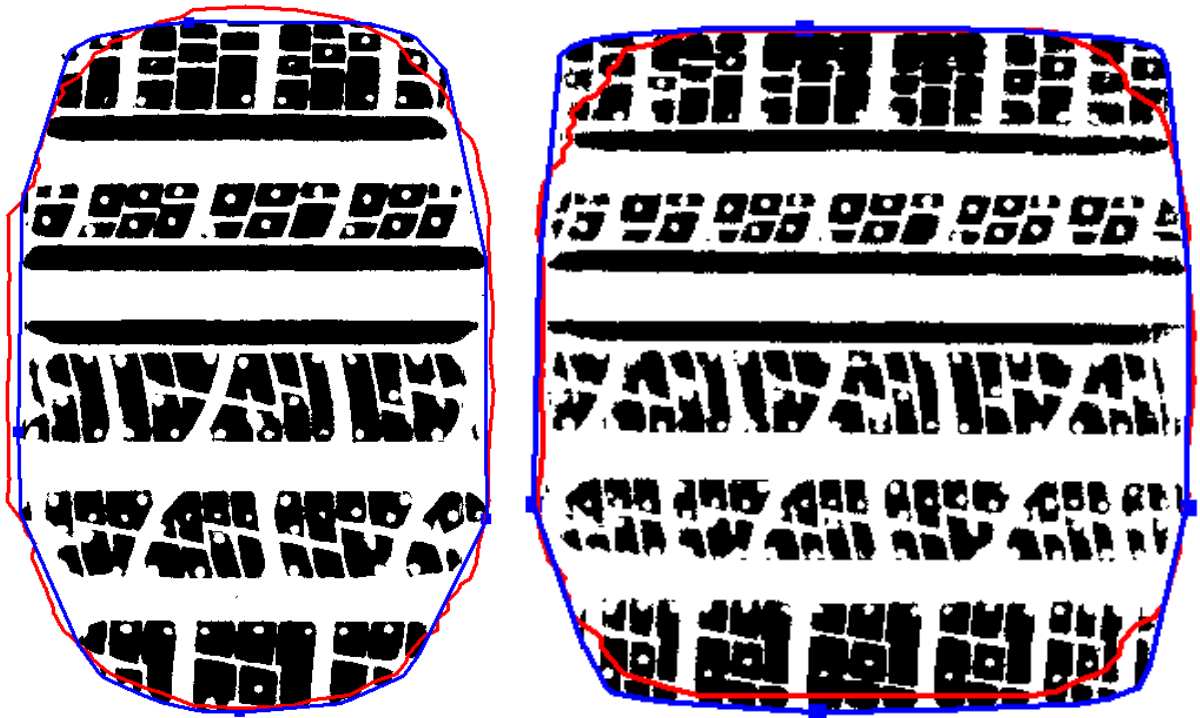


Figure 4.16 - Final FTire Validation - footprints at 0° camber

Legend

- Actual footprint perimeter
- Tyre model footprint perimeter
- FTire optimisation points

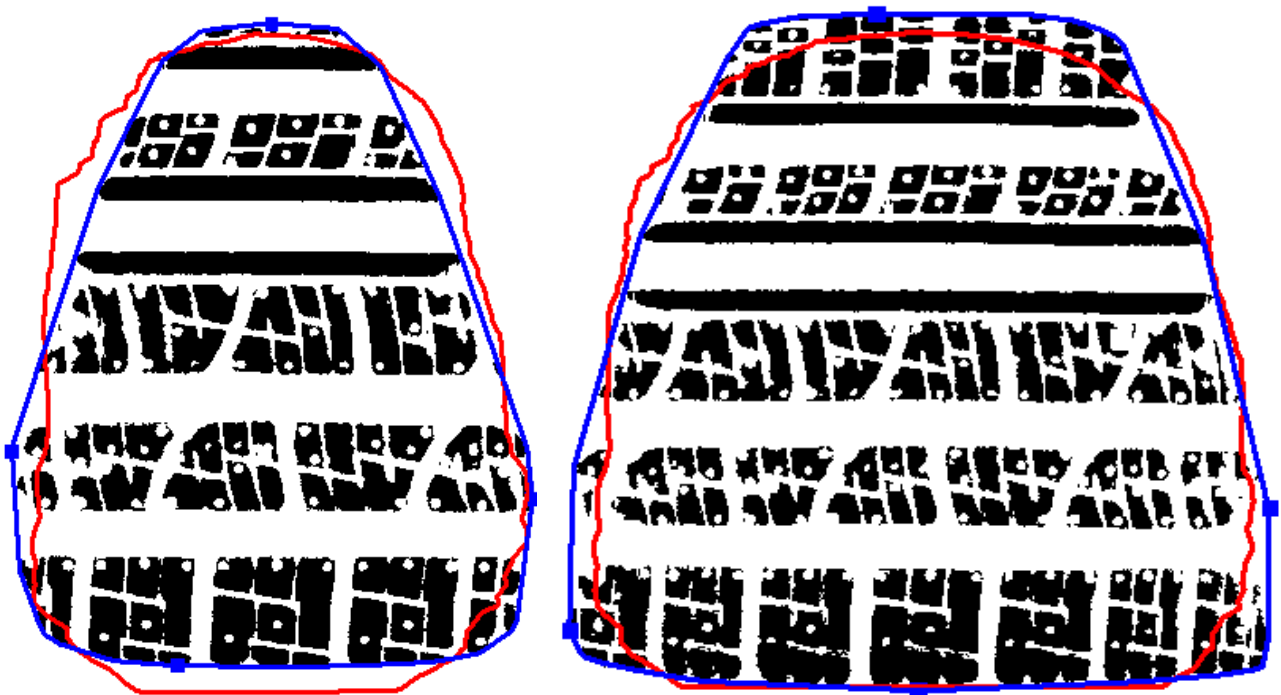


Figure 4.17 - Final FTire Validation - Footprints at -4 degrees camber

FTIRE PARAMETERISATION

4.3.4.2 *Footprints at Camber*

The footprints produced at -4° camber are identified with the longitudinal belt torsion and belt twist stiffnesses. They produce reasonable correlation with the tyre model as seen in Figure 4.17, but are not as accurate as the flat footprints. This is partly due to the sacrifice made to improve the vertical stiffness lines at camber and with a transverse cleat. Nevertheless the correlation is still outstanding.

4.3.5 Additional Validation Figures

Several validation figures of the remaining static and dynamic tests have been omitted from this illustration because they convey very similar correlation to the successful validation of Figure 4.9.

4.4 CONCLUDING REMARKS

The parameterisation of the FTire tyre model was an involved process. The above sections describe the systematic procedure in which the model was produced, identified and validated. Firstly, data was captured on both a static and dynamic test rig. Data included general geometric properties, the Shore A hardness of the tread rubber, the static footprints and the static and dynamic stiffnesses.

Subsequently, all data was prepared using the necessary standard formats accepted by FTire/fit and resultantly checked into the FTire/fit software environment. It was ensured that all test data was correctly recognised by the FTire/fit software. Finally the identification of all the possible tyre model parameters commenced followed by the validation of these parameters using the test data.

The result of this procedure is an FTire tyre model which accurately represents the vast majority of the tyre's behaviour under both static and dynamic conditions. Focus, however, was applied to the static test data as the parameters concerning these tests are the focus for the remainder of this dissertation.

5 AGING

5.1 INTRODUCTION

The effects of the age of a tyre on force-displacement properties are investigated and discussed in detail in this chapter. The foremost requirement is an artificial method of accelerating the aging process of a tyre. The intention is to replicate the rubber characteristics of a tyre aged from normal daily use as well as that of a spare tyre which may never be used until it has aged significantly. Fortunately, as covered in Section 1.4, literature provides detailed guidelines to specifically fulfil this intention.

The analysis that follows is of a tyre artificially aged in an oven at 65°C for approximately 8 weeks. This procedure ensured the tyre of concern would have approximately equivalent rubber properties to that of a 4 year old tyre used in the field in Phoenix, Arizona in the USA.

During the aging process the tyre was tested on the static tyre test rig. These tests included the vertical stiffness on a flat surface, a transverse and longitudinal cleat at 0° and -4° of camber as well as the longitudinal stiffness. The Shore A hardness was measured on the sidewall as well as the tread. The effects of the age of the tyre on these tyre characteristics are discussed in detail whilst taking into consideration the testing accuracy of the STTR. Thus, for any effects to be considered noteworthy the change in percentile deflection will need to exceed $\pm 1\%$ compared to the baseline.

The purpose of this investigation, should there have been any significant and noticeable effects due to aging, was to be able to replicate these effects in the FTire tyre model without repeating the full set of parameterising test data on the aged tyre. This is also discussed at the end of the chapter along with concluding remarks on the significance of the effects due to aging.

5.2 EXPERIMENTAL DETAILS AND ANALYSIS

5.2.1 Method of Comparing Stiffnesses

As covered in Section 1.6, the percentile change in the deflection relative to a new tyre will be used extensively in this chapter. The data captured in Baldwin et al. (2008) makes use of physical rubber properties to evaluate the effects of aging on the tyre. However, a method of correlating these rubber properties changes to the actual stiffnesses of the tyre is yet to be researched. Should there be any noticeable changes this method provides a means of quantifying the change in potentially the only way that would mean anything to the end user.

AGING

5.2.2 Tyre Age Calculation

Section 1.4 made use of an oven temperature of 70°C, however, for this dissertation an oven temperature of only 65°C was used. With the use of the data captured in Baldwin et al. (2008) and with reference to the discussion in Section 1.4.3, the actual representative age of the tyre needed to be calculated. From Figure 1.12, the empirical equation for calculating the shift factor due to the accelerated aging temperature can be calculated, as shown in Equation (7):

$$\varphi = (4.2019e + 11)e^{-8.3715\tau} \quad (7)$$

In Equation (7), τ represents $1000/T$ where T is the oven temperature in Kelvin and φ is the shift factor of the acceleration of the aging of the tyre. Substituting the 65°C used to age the tyre a shift factor of 7.44 is acquired. Seeing that data regarding aging rates are only provided for a 70°C oven temperature as per Table 1.6, the shift factor was also required for this new temperature. It equated to 10.67. The implication is that the aging rates and consequent acceleration rate when aging at 65°C are now shown in Table 5.1.

Table 5.1 - Aging rates (weeks⁻¹) and acceleration factor for aging at 65°C

Property	Rate at 70°C	Rate at 65°C	Rate in Phoenix	Acceleration Factor
Skim Crosslink Density	0.059	0.0411	0.00175	23.5
Wedge Modulus	0.061	0.0425	0.00166	25.66
Wedge Elongation-to-break	0.168	0.1171	0.0042	27.88
Skim Peel Strength	0.216	0.1506	0.0084	17.93
Average				23±5

The aging rates at 65°C are calculated based on the ratio of the shift factors calculated from Equation (7) between the 65 and 70°C oven temperatures. From this the same acceleration factor that was shown in Table 1.6 for 70°C oven temperature has been calculated and is observably much smaller. Nevertheless, in order to generate an equivalent tyre to the 4 year old Phoenix tyre previously mentioned, the number of weeks in 4 years is divided by this new acceleration factor and is calculated to be 8.76 weeks. Thus, to acquire an equivalently aged tyre whilst using an oven temperature of 65°C, the tyre should be left in the oven for 8 weeks, 5 days and 7 hours or 61.33 days. It's important to note that the tyre is more than likely to age differently to the tyre used to make this calculation. However, it gives an approximate value ensuring that the tyre is similarly aged to that of a 4 year old tyre used daily and this is all that is required for this investigation.

AGING

For the remainder of this analysis, however, the time spent in the oven will be used to quantify the age of the tyre. This is due to the fact that the acceleration factor is only based on one tyre's age after being used in the field. As was previously mentioned, the aging of individual tyres varies significantly and even more so when used in a different environment.

5.2.3 Tyre Aging Procedure

The tyre was aged according to the literature discussed in Section 1.4. As a result the tyre was inflated with a gaseous mixture of 50% Oxygen and 50% Nitrogen to 3.5Bar. This tyre was then placed in a convection oven set to a temperature of 65°C. After approximately 1 week the tyre was removed and allowed to cool before static testing commenced. Thereafter the tyre was deflated and inflated with more of the gaseous mixture to 3.5Bar. This procedure was followed for approximately 8 weeks where the tyre was tested a total of 5 times. It is important to note that this method of aging only performs accelerated aging from the inside of the tyre and ignores the less significant effect of the oxygen present around the outside of the tyre during normal operating conditions (Baldwin, 2003).

5.3 SHORE A HARDNESS EFFECTS

The Shore A hardness was anticipated to be a property of the tyre that would change with the aging of the tyre. This is based on results discussed in Section 1.3.3.1.1 from Figure 1.4 (Kataoka, et al., 2003) where the Shore A hardness of the tread rubber on a specific spare tyre was observed to increase by 10 Shore A hardness values over a period of approximately 250 weeks.

Ideally these potential changes in Shore A hardness can be used as an input into the FTire tyre model to account for any changes in tyre stiffness. This will be discussed later in the chapter.

5.3.1 Measurement Device and Method

The Shore A hardness was measured using a Bondetec BS-392A Shore A Hardness tester. Under ideal conditions the device requires a flat surface to accurately determine the hardness. This is difficult on a tyre as there are no flat surfaces larger than the area of the head of the hardness tester. As a result the hardness's measured were dependent on the user's experience and even this still produced varying results.

In an attempt to produce repeatable results, the hardness was measured at marked locations around the tyre. Five locations were marked around the tyre close to the rim on the sidewall of the tyre. An additional five locations were also marked around the tyre in the middle of the tread. With the repeatable tread pattern continuing circumferentially around the tyre, the same tread block was used each time around the tyre to measure the hardness.

AGING

At each of these locations the hardness was measured approximately 15 times. This was done to generate an acceptable average as the measurements were not consistent. At each location the standard deviation of the readings was approximately 1.5% on the sidewall measurements and 1.4% at the tread. These variations were checked each time the tyre hardness was measured to ensure that they remain the same. This would ensure that even if the variance in measurements exists, a trend, should there be one, would still be produced.

5.3.2 Results

The average value for the sidewall and tread measurements were used from each round of tests after the tyre had been in the oven for a certain period of time. The results of such measurements are shown in Figure 5.1.

Figure 5.1 illustrates a distinct difference in rubber hardness between the sidewall and the tread of the tyre. Where the sidewall gives clear indications of a change in hardness after the first round of aging, the tread hardness does not change by any noticeable amount until it is an equivalent of two years old.

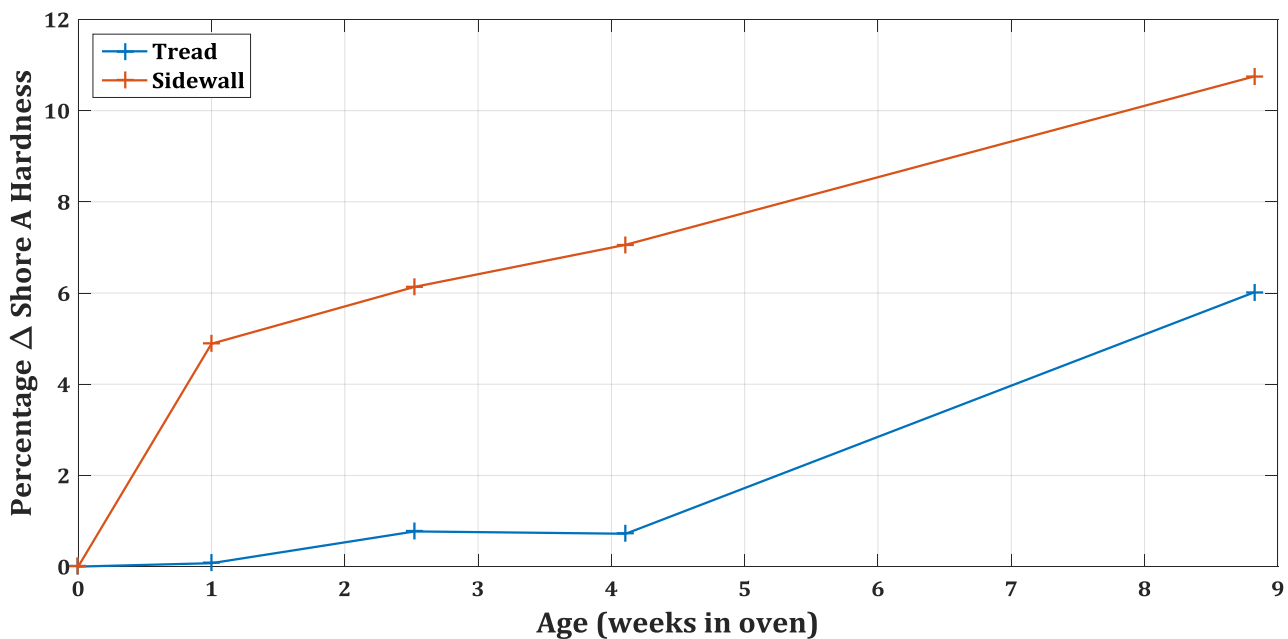


Figure 5.1 - Percentile change in Shore A hardness at the tread and sidewall whilst aging

5.3.3 Discussion of Results

Due to the fact that the aging mechanism being forced upon the tyre is oxidation, it can be assumed from this graph that the oxidation and subsequent hardening of the rubber occurs quicker at the sidewall than at the tread. This is potentially due to the lower thickness of the rubber at the sidewall compared to the tread.

AGING

Another point of interest is that once the tread does show indications of hardening, it does so at a similar rate to that of the sidewall. This indicates that the thickness of the rubber doesn't necessarily determine how quickly it hardens and subsequently ages.

Nevertheless, it is to be pointed out that the maximum change in Shore A hardness is only 10% of the original value. This in turn represents a change in Shore A hardness of approximately 6. Recalling from the discussion above, and Figure 1.4 from Section 1.3.3.1.1, the maximum change in Shore A hardness was 10 over 250 weeks which equates to just less than 5 years. These results can be substantiated by Figure 5.1, as it can be seen that if the trend shown was extrapolated, similar results would be obtained.

5.3.4 Application in FTire

The Shore A hardness measurement is usually determined in FTire/fit using the test data acquired for longitudinal force against longitudinal slip test. It is described as the tread stiffness parameter. Therefore with the changes due to aging evident above, this parameter could be updated and would at the very least have a direct influence on this parameter of the tyre. Whether this parameter influences the remaining stiffnesses of the tyre will be discussed at the end of this chapter.

5.4 THE INFLUENCE OF INFLATION PRESSURE

The overall vertical stiffness of a tyre is generated from a combination of the actual tyre stiffness and the compression of the air inside the tyre. Therefore in an attempt to amplify the potential effects on the stiffness of the actual tyre due to aging the tyres were additionally tested at 1.5 Bar which is approximately 1Bar lower than the nominal inflation pressure of the tyre. Whilst it would have been possible to test the tyre completely deflated, this would not have provided a relevant result because it is not recommended to drive a tyre when it is completely deflated. Therefore 1.5Bar was decided as the most appropriate compromise between remaining relevant to the operating range of a tyre and isolating the potential effects of aging on the stiffness of the tyre.

5.4.1 Results

Figure 5.2 demonstrates the influence the inflation pressure has on isolating the effect of aging on the vertical stiffness of the tyre. From this figure, a noticeable change in the vertical stiffness of the tyre is observed. This change is more visible for the 1.5Bar inflation pressure compared to 2.5Bar.

As a result, the remainder of this investigation will be presented for tyres tested at 1.5Bar. However, it is important to keep in mind that the effects of aging will be visibly reduced when

AGING

looking at a tyre inflated to its nominal pressure. This will be discussed in due course in the remainder of this chapter.

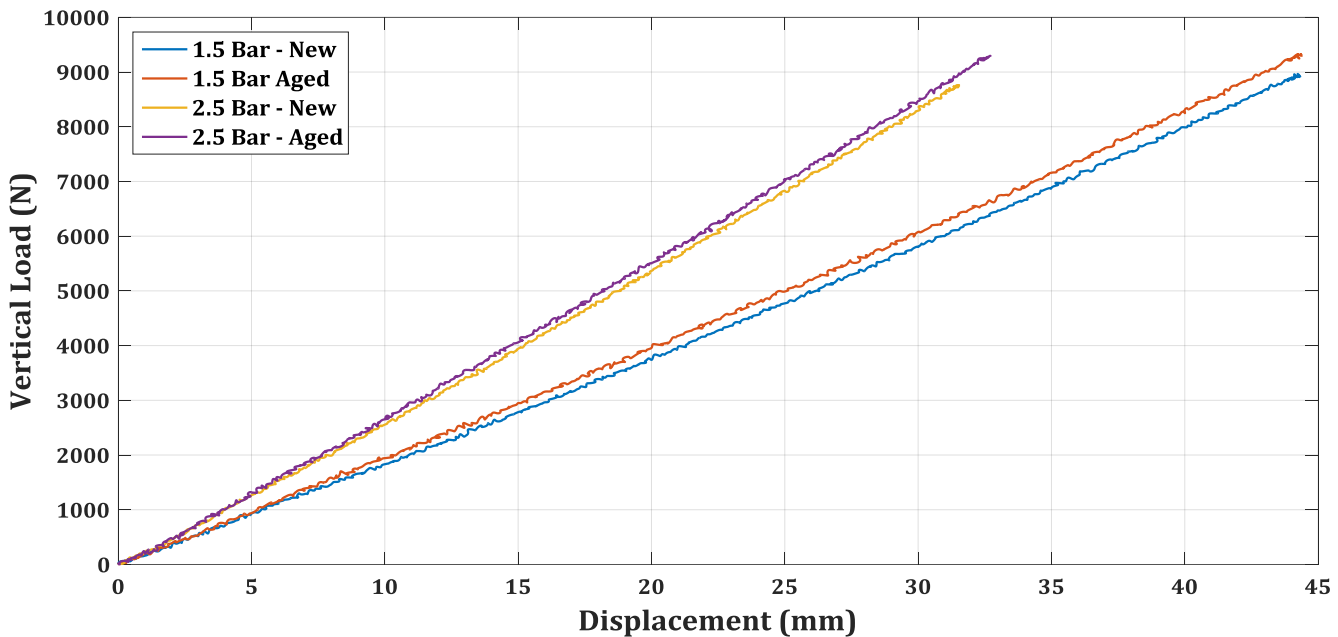


Figure 5.2 - Vertical stiffness comparison of inflation pressure

5.5 AGING STIFFNESS TEST RESULTS

A total of six tests were conducted each time the tyre was removed from the oven. They were the following:

- Vertical stiffness on a flat surface at 0° camber
- Vertical stiffness on a flat surface at -4° camber
- Vertical stiffness on a transverse cleat at 0° camber
- Vertical stiffness on a transverse cleat at -4° camber
- Vertical stiffness on a longitudinal cleat at 0° camber
- Longitudinal stiffness on a flat surface

In the sections that follow, the results of each of these tests are presented separately. For each test, the stiffnesses after each week are graphically shown; followed by a tabulated set of results of the percentile change in deflection at 50 and 100% of the LI which is only presented in full in Appendix A. These changes are, however, shown graphically and concluded by a discussion. In the case of the vertical stiffness tests on a flat surface the footprints are also presented.

The tyre was tested depending on the availability of equipment: As a result the time spent in the oven between tests was not constant. Nevertheless this is clearly depicted and does not affect the results of the investigation.

AGING

5.5.1 Vertical Stiffness on a Flat Surface

5.5.1.1 At 0° Camber

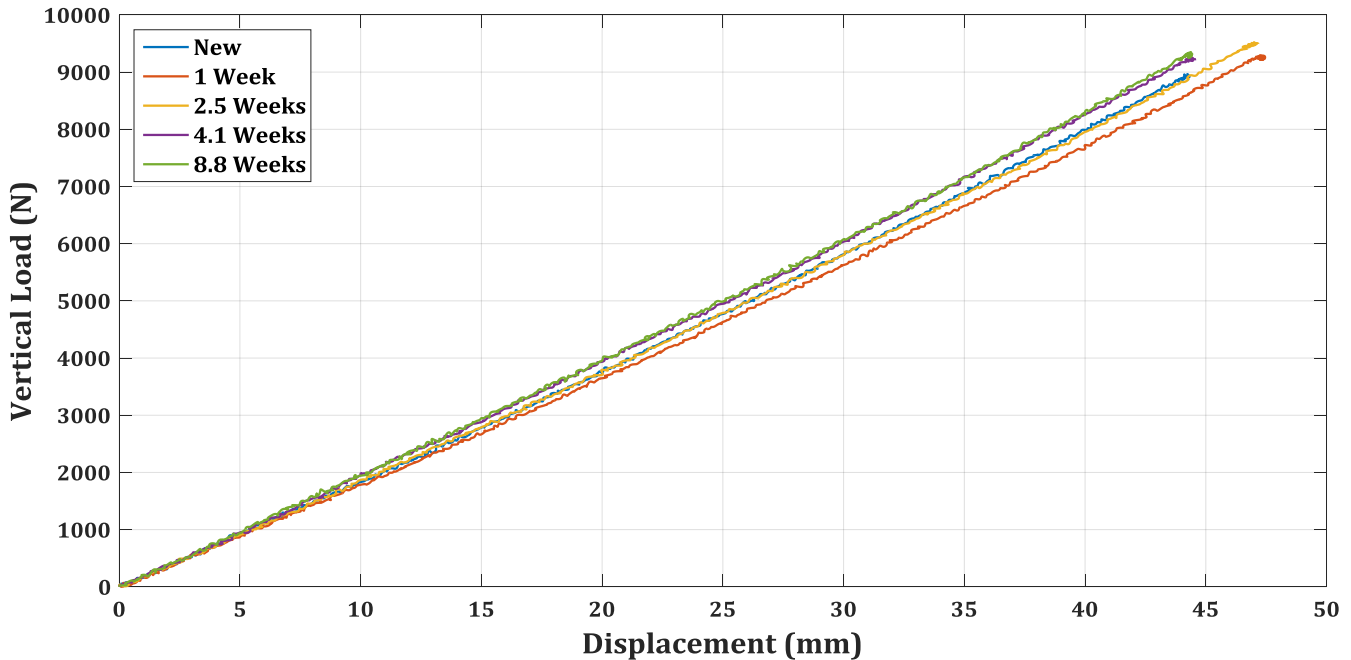


Figure 5.3 - Vertical stiffness changes on a flat surface as the tyre ages

Figure 5.3 shows the various vertical stiffnesses as the tyre was aged. Evidently the change in stiffness is not consistent because the tyre appears to get softer after the first week of aging before it starts getting stiffer over the weeks thereafter. Figure 5.4 shows the actual changes in deflection at 50 and 100% of the LI compared to the results of the tests of the new tyre.

Figure 5.4 indicates fairly small changes in deflection at the two load cases considered. Relative to the deflection required to reach the same load with the new tyre the percentage change is interestingly more significant at the lower load compared to the higher load. Despite the initial 'softening' of the tyre the stiffness appears to consistently increase for an additional three weeks of aging where the 1% threshold is seen to be exceeded after 4 weeks of artificial aging. Thereafter the rate drops significantly, almost as if it had stopped changing completely.

5.5.1.1.1 Footprint Comparison

The comparison between the footprints of the new tyre with that of the aged tyre must be compared with caution as the loads applied to produce each footprint aren't necessarily exactly the same. Nevertheless the shape of the footprints will be compared instead of to the actual area.

AGING

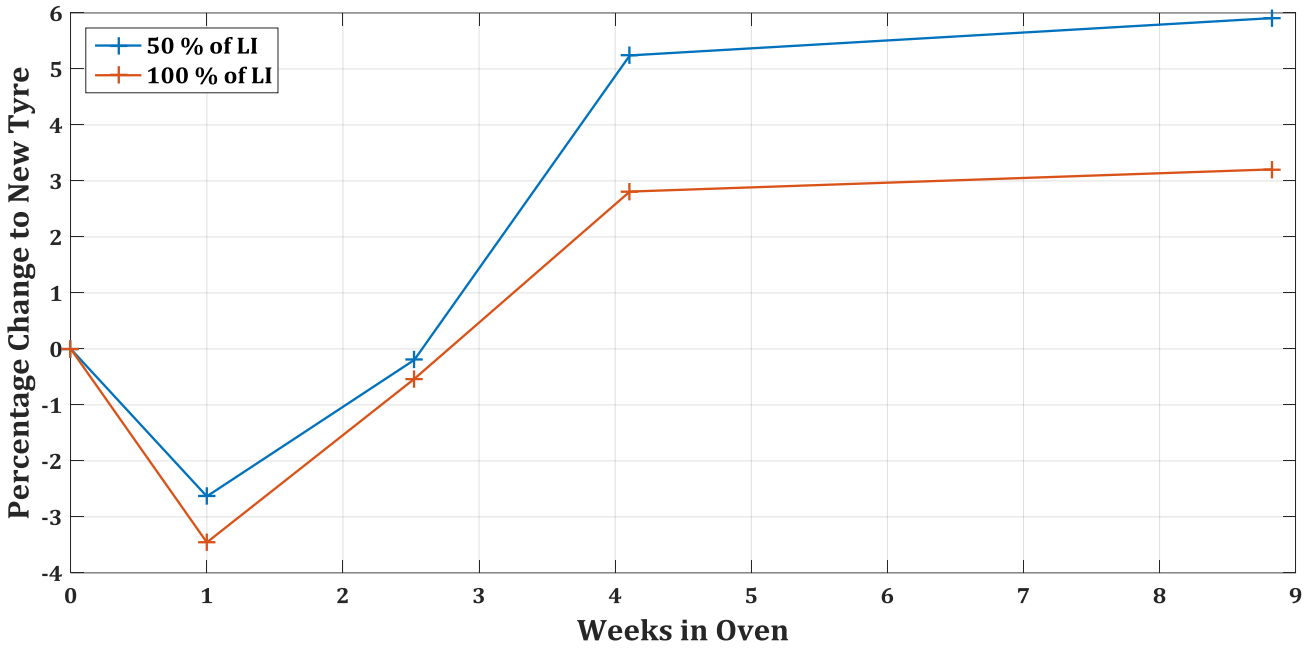


Figure 5.4 - Percentile change in deflection of aged tyre on a flat surface

Figure 5.5 shows the two footprints at the 100% of the LI. The left footprint is that of the new tyre and the right footprint is that of the aged tyre at the end of 8.8 weeks'. Largely apparent from these footprints is the change in shape of the footprint. The sidewalls appear much softer compared to the new tyre and the middle of the tread in the longitudinal direction is stiffer.



Figure 5.5 - Footprint comparison at 0° camber at 100% of the LI - New Tyre (Left), Aged Tyre (Right)

AGING

This change indicates a significant change in the deformation characteristics of the tyre despite the almost negligible changes observed in the stiffness tests. This indicates that the tests on the longitudinal cleat as well as the tests at camber should yield more apparent changes.

5.5.1.2 At 4° Camber

The first vertical stiffness test at camber was erroneously completed at 2° camber opposed to 4° camber. As a result only the stiffness data from the four sets of tests thereafter are shown in the discussion to follow.

Figure 5.6 shows the changes in this stiffness (at camber) of the tyre as it ages. This graph shows a clearer trend compared to the vertical stiffness tests at 0° camber. The change in deflection compared to the test data after 1 week of aging is plotted in Figure 5.7. Despite the actual changes in deflection increasing in this case and going beyond the 1% equipment threshold after at least 2.5 weeks of accelerated aging, the relative changes in the percentile value are very similar to those of the stiffness at 0° camber shown above. This is due to the fact that the overall stiffness of the sidewall is softer than that of the tyre on a flat surface. Nevertheless this is surprising given the drastic change in footprint shape observed previously.

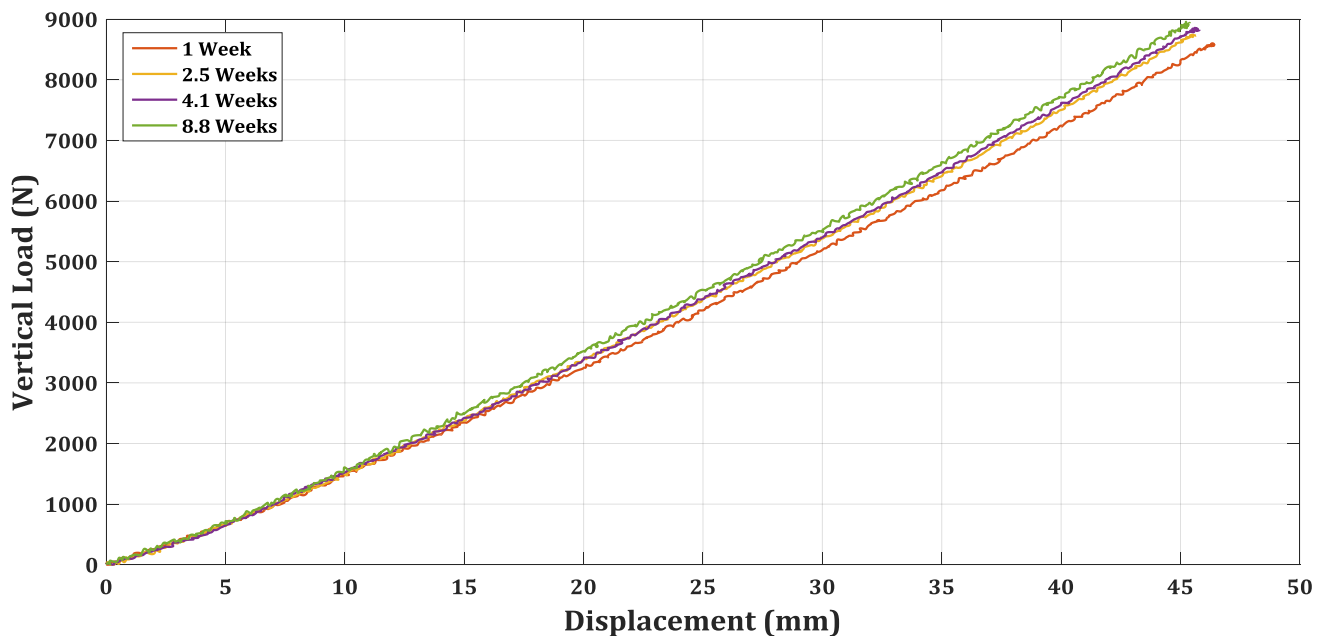


Figure 5.6 - Vertical stiffness changes on a flat surface at -4° camber as the tyre ages

Finally, Figure 5.7 indicates that the sidewall has continued stiffening and/or aging even after the 4 weeks of aging.

The comparison of the footprints once again illustrates a strange change in the shape of the footprint. However, instead of motivating a softer sidewall it can be seen here that it is the centre

AGING

of the tread, hence the belt of the tyre, that appears to play a more significant role in its increase in stiffness.

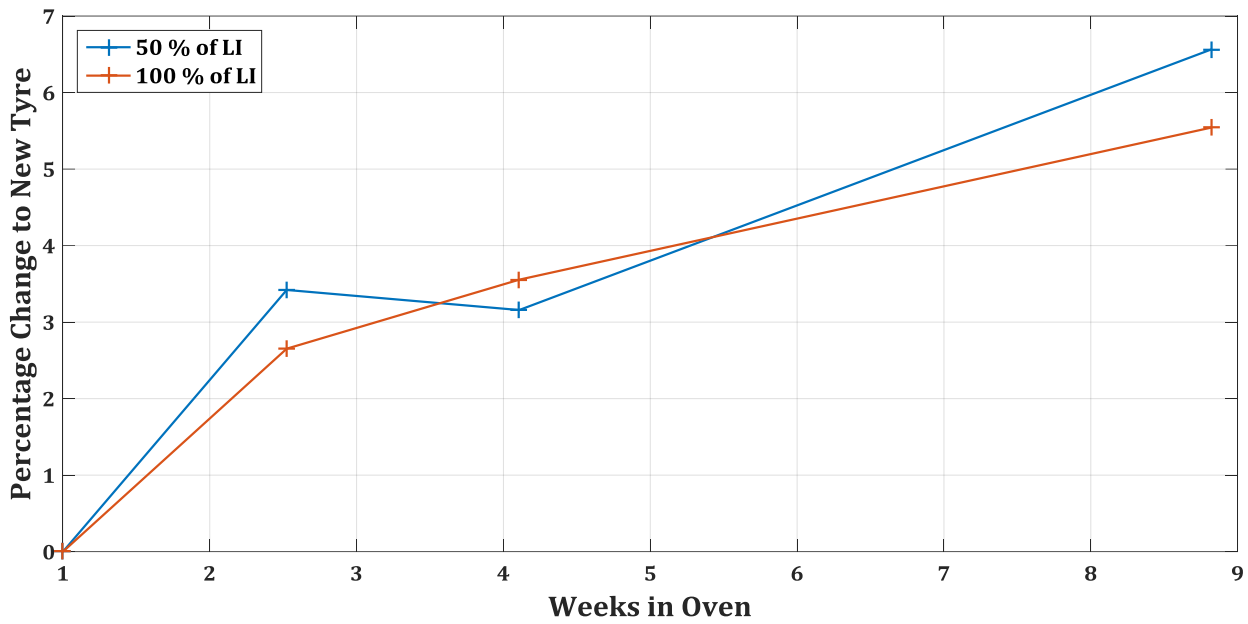


Figure 5.7 - Percentile change in deflection on a flat surface at -4° camber

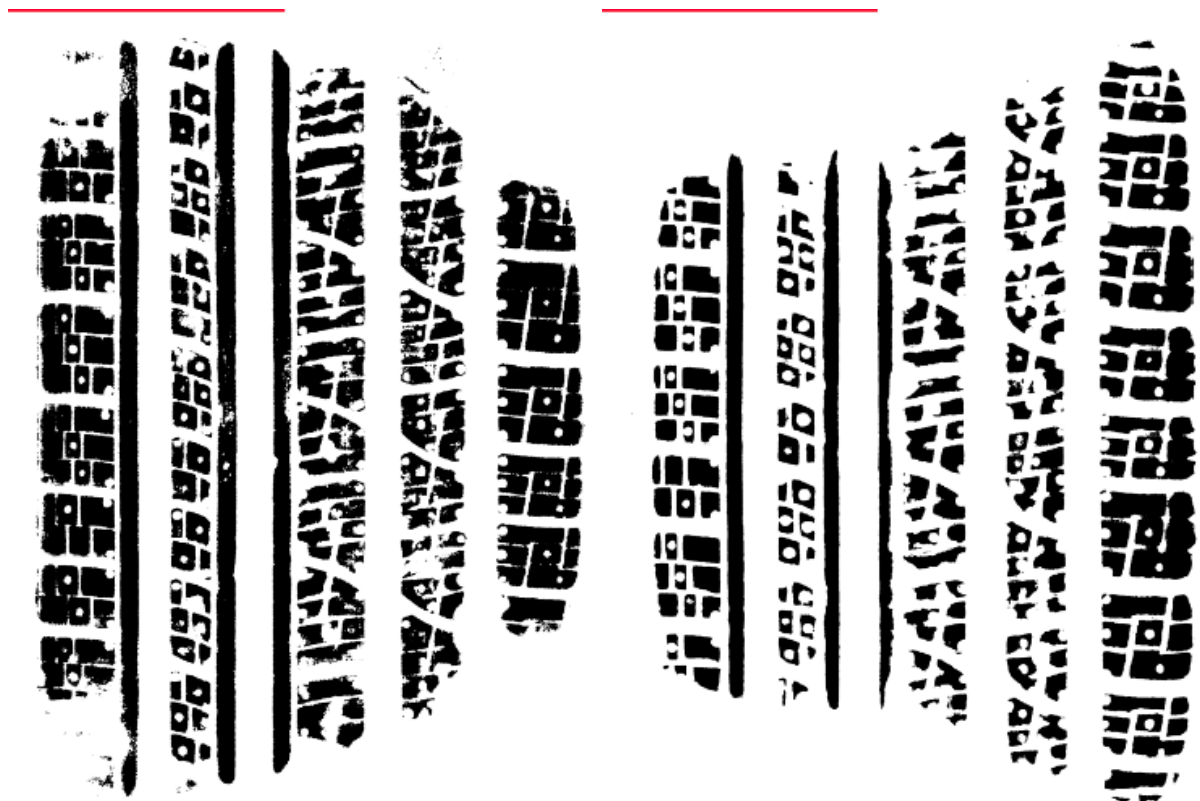


Figure 5.8 - Footprint comparison at 4° camber at 100% of the LI - New Tyre (Left) and Aged Tyre (Right)

AGING

Figure 5.8 shows the footprints at the LI for the 1.5Bar inflation pressure. It should be noted that the camber angle in the footprint of the new tyre was at positive 4° camber, however, that of the aged tyre was completed at -4° camber. This should have negligible effects on the footprint shape as the internal structure of the tyre is symmetrical.

To further illustrate this change in shape, the footprint at 2.5Bar inflation pressure at 50% of the LI has been shown in Figure 5.9. This demonstrates that this change in the tyre characteristic is still very relevant even at the nominal inflation pressure.



Figure 5.9 - Footprint comparison of 2.5 Bar Inflation at 4° camber at 50 % of the LI - New Tyre (Left) and Aged Tyre (Right)

Although not quantifiable, the changes in the shapes of the footprints at least give an indication that a certain change in stiffness, and thus tyre characteristic, has occurred due to aging. Furthermore it can be anticipated that the change in stiffness over the longitudinal cleat will be significant.

5.5.2 Vertical Stiffness with a Cleat

The vertical stiffness on a cleat includes three cleat setups, firstly the transverse cleat at 0 and 4 degrees camber and then the cleat in a longitudinal position only at 0° camber.

5.5.2.1 Transverse Cleat

Figure 5.10 shows the stiffnesses of the aging tyre at 0° camber on a transverse cleat. Unfortunately during the tests after 1 week of aging the tyre was only tested at 0° camber with the transverse cleat and not at any camber angle. The tests were still, however, completed for the remainder of the aging periods. These are shown in Figure 5.12.

AGING

5.5.2.1.1 At 0° Camber

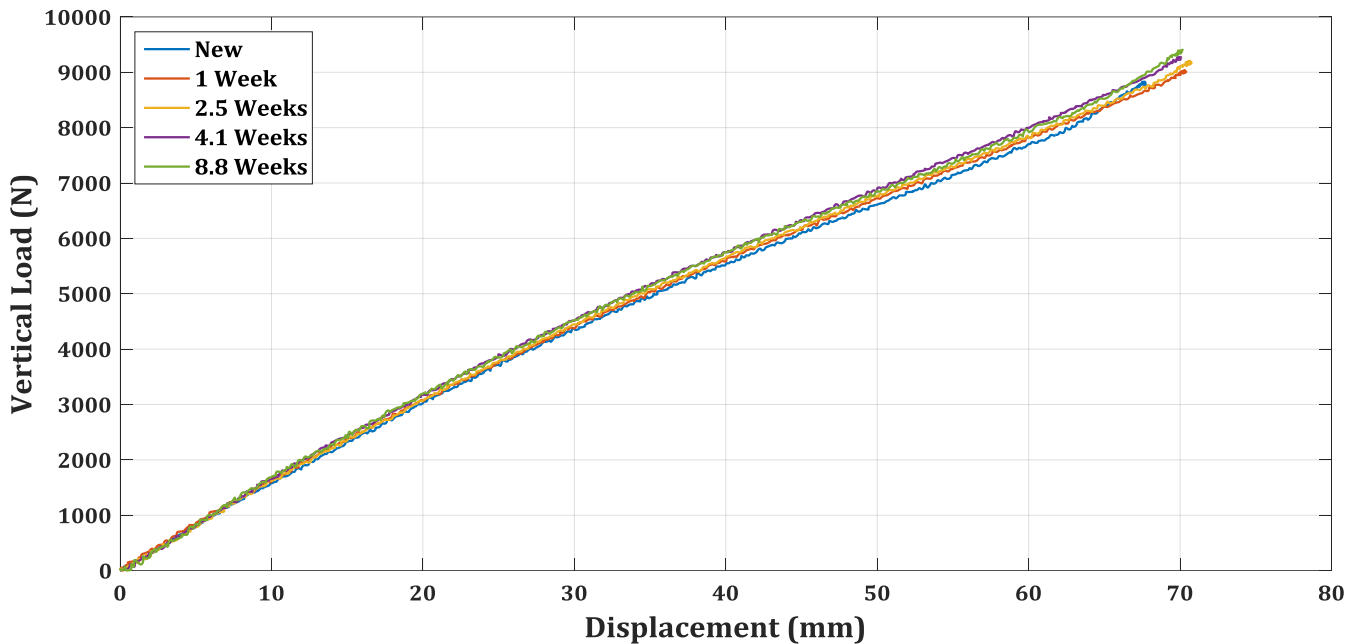


Figure 5.10 - Vertical stiffness changes on a transverse cleat at 0° camber as the tyre ages

From Figure 5.10, the apparent change in deflection over the cleat as the tyre ages appears to be negligible. The only distinguishable difference between the stiffnesses produced is the deflection at which there is a distinct change in gradient of the stiffness. This occurs when the tyre tread not in contact with the cleat makes contact with the surface upon which the cleat is mounted. The fact that this distinct change in gradient occurs after more deflection than the new tyre implies that the tyre is stiffer. However, this stiffness change is not as noticeable in the rest of graph. Figure 5.11, shows the actual changes in deflection at 50 and 85% of the LI this time so as to avoid the change in gradient point on the new tyre stiffness line.

Figure 5.11 demonstrates that the changes in deflection are even less significant than the results seen before in this investigation, however, the changes are still greater than the 1% threshold after 1 week of aging. Nonetheless, the trend is still very similar to results previously observed with a steep change in deflection over the first few weeks of aging and a drop off in this rate in the remaining 4 weeks of aging.

5.5.2.1.2 At 4° Camber

The results of the vertical stiffness test at 4° camber yield some interesting results. Despite the exclusion of the test after 1 week of aging there is still an observable trend in the remaining weeks of aging. It should also be noted that the LI previously reached during all tests was not possible due to test rig limitations with the transverse cleat at camber. Thus only a comparison at 50% of the LI was completed.

AGING

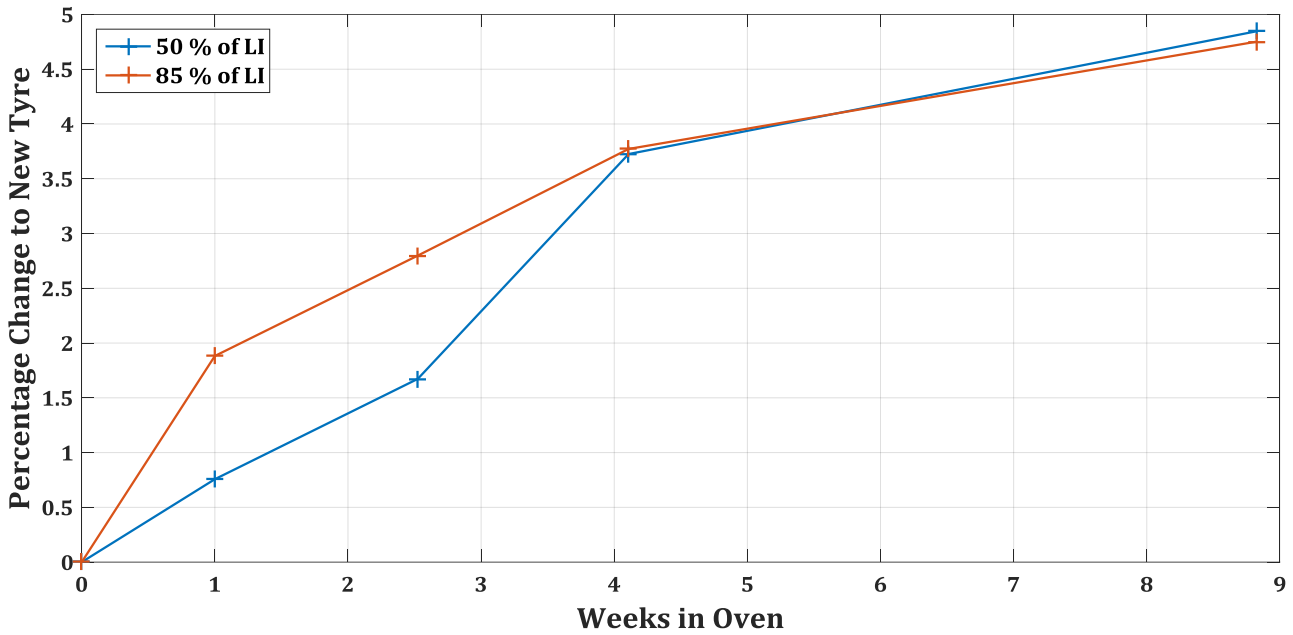


Figure 5.11 - Percentile change in deflection on a transverse cleat at 0° camber

In Figure 5.12, at approximately 5mm of deflection, the aged tyre results show a distinct change in gradient after being initially less stiff compared to the new tyre in the first 5mm of deflection. As a result of this initial lower stiffness, followed by the sudden change in stiffness also known as a nick point, the method used to compare the stiffnesses as demonstrated previously will produce a skewed result. Therefore the results of Figure 5.12 will be discussed only quantitatively.

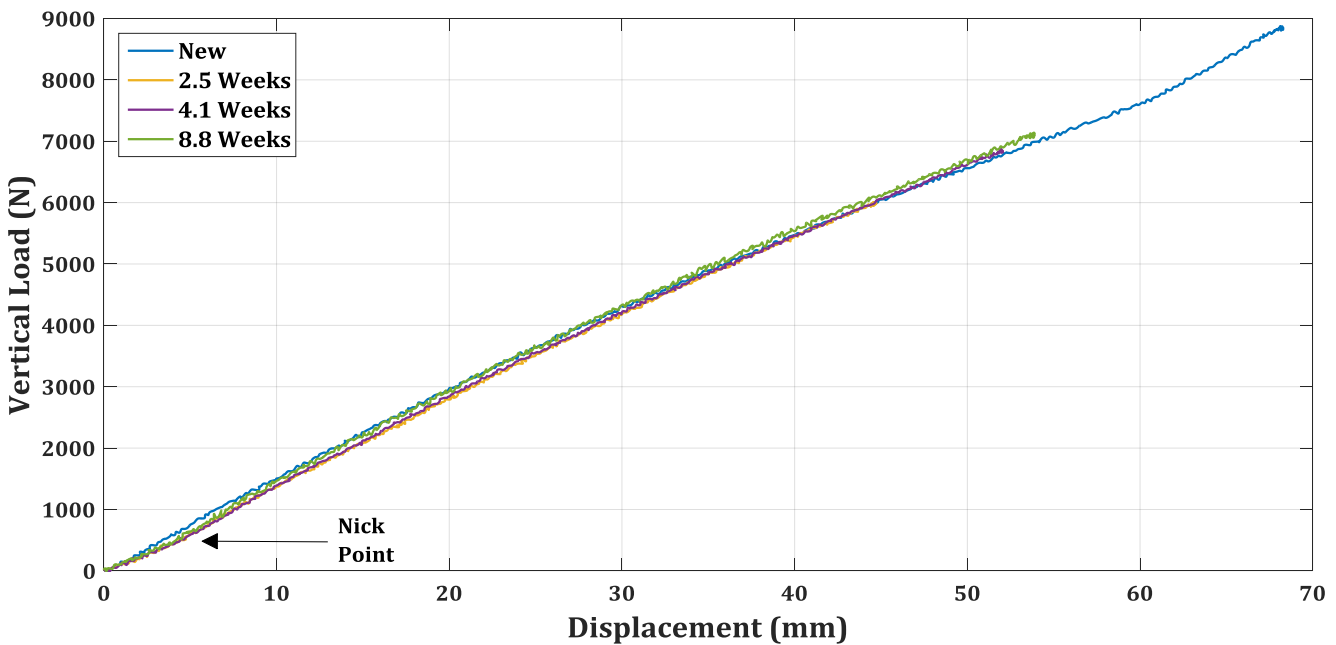


Figure 5.12 - Vertical stiffness changes on a transverse cleat at -4 degrees camber as the tyre ages

After the initial change in stiffness of the aged tyre results, it is clearly observed that a stiffer characteristic is followed by the aged tyre results over the new tyre. In an attempt to compare

AGING

these stiffnesses, a deflection of 1mm was added to the new tyre such that the deflection of all test data was equal at the nick point previously described. This resulted in a maximum percentile change in deflection at 50% of the LI of 3.6%.

The nick point in the aged tyre test data can be explained with reference to the footprints shown in Figure 5.8 and Figure 5.9. From these footprints it can clearly be seen that at camber the centre of the tread pattern provides less tread area to the contact patch and thus results in higher stiffness. However, this implies that initially, when only the side of the tread is in contact, the stiffness is lower. Therefore before the centre of the tread has made contact with the cleat, in the case of Figure 5.12, the stiffness appears lower.

5.5.2.2 Longitudinal Cleat

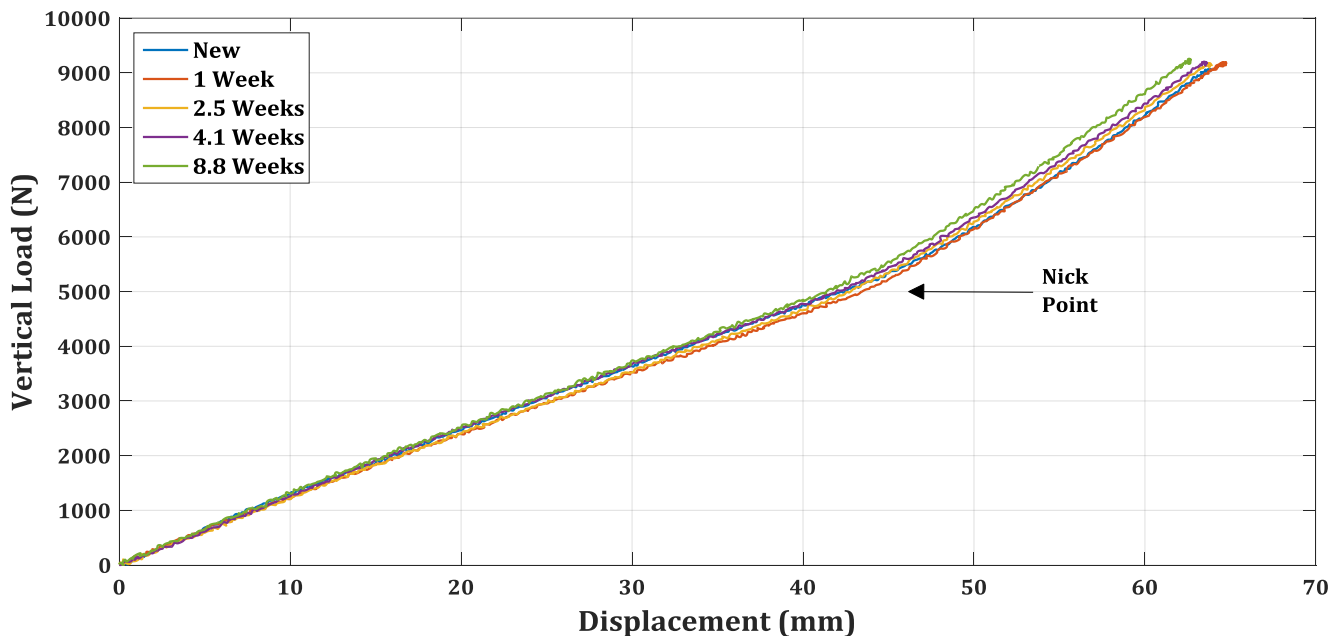


Figure 5.13 - Vertical stiffness changes on a longitudinal cleat as the tyre ages

The longitudinal cleat vertical stiffness test was anticipated to yield the largest deviations in deflection mainly due to the large changes in footprint shapes shown in the sections above. Although interesting results are produced, the changes are not significant. The nick point around 45mm of deflection, where the rest of the tyre makes contact with the mounting surface, is consistent for all test results. Figure 5.14 shows the changes in deflection at 50 and 100% of the LI and it should be noted that the deflections at 50% of the LI are before the nick point and the deflections at 100% of the LI are after this point.

The tyre does appear to be softer after the first 3 weeks of aging, however, it is a very small effect especially with regard to the 50% of the LI line which is well below the 1% equipment threshold. Interesting, after the nick point in Figure 5.13, the changes in deflection are more consistent. This

AGING

indicates that when one is not analysing the middle of the tread in isolation, the sidewalls or sides of the tread appear to be stiffer than the new tyre. Despite being almost negligible in magnitude, it does show that the hypothesis that the centre of the tread pattern was much higher in stiffness as indicated by the footprints, was not correct. Another possible explanation is that it is indeed stiffer but not sufficiently different to have a noticeable effect on the stiffness of the tyre as a whole.

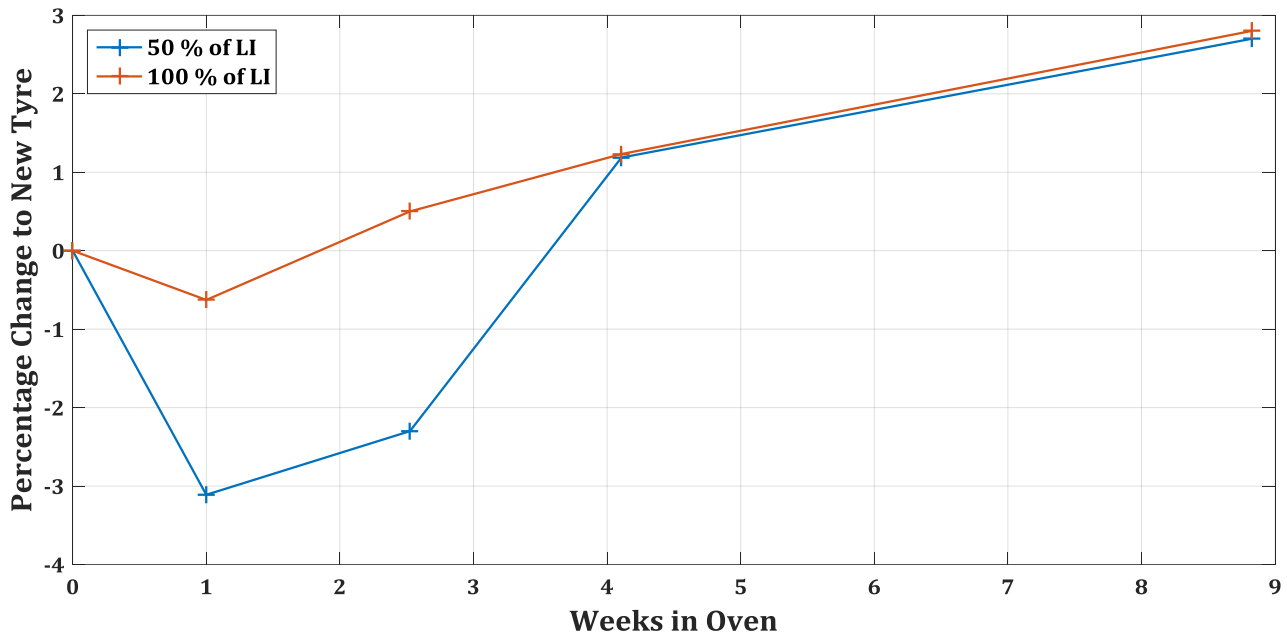


Figure 5.14 - Percentile change in deflection on a longitudinal cleat as the tyre ages

5.5.3 Longitudinal Stiffness

Results of the longitudinal stiffness tests are shown in Figure 5.15. As was evident in Section 4.3.2.3, the errors in the measurement of the longitudinal and lateral forces of the WFT are also evident in Figure 5.15. As a result, the ULP Load Cell data also has been included for the new and fully aged tyre. This provides an additional form of validation.

The P80 Corundum contact surface was used for all tests to create a high friction coefficient and thus a large longitudinal displacement prior to the tyre slipping. Figure 5.15 shows inconsistent results as the longitudinal stiffness appears to soften after the first week of aging. Thereafter, a similar trend to the vertical stiffness is observed. In the region where the WFT has been assumed to record forces correctly (longitudinal forces less than 1200N in this case) the maximum percentile change in deflection was calculated to be 4.16% at 1000N of longitudinal force. This demonstrates good correlation with Figure 5.16 which shows the percentile change in deflection when using the forces from the ULP load cell data.

AGING

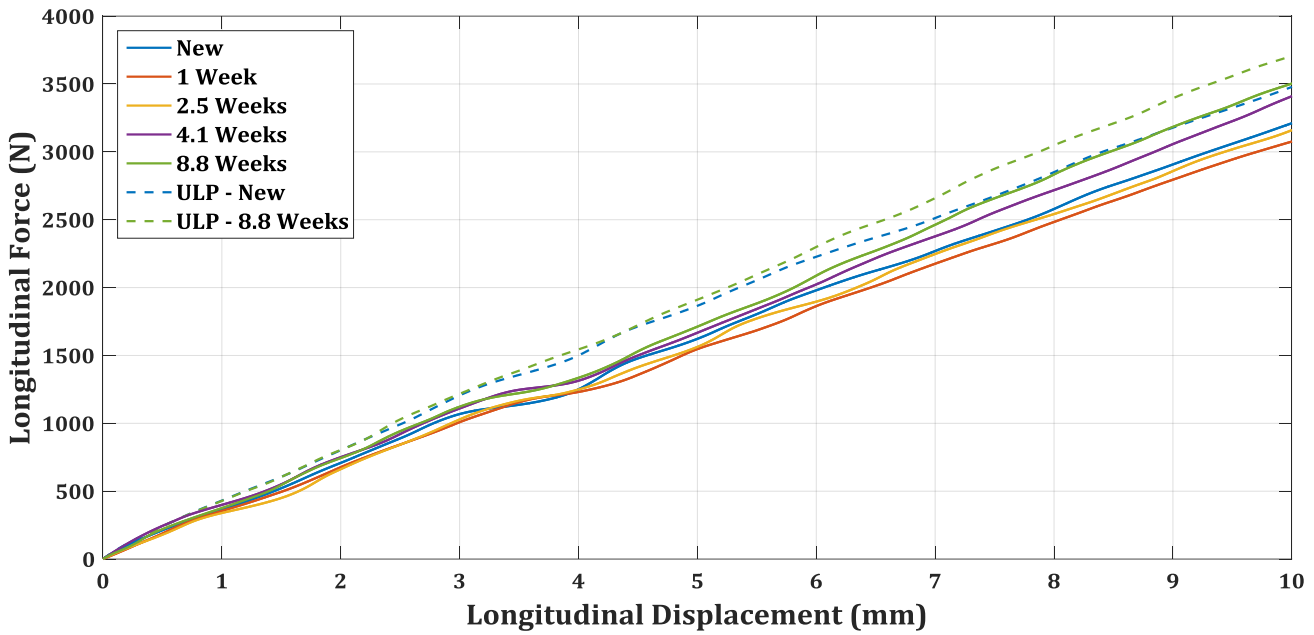


Figure 5.15 - Changes in longitudinal stiffness as the tyre ages

Figure 5.16 shows how the change in percentile deflection is more than 2% larger for the WFT results compared to the ULP results. Nevertheless this change is still significant as it is well beyond the 1% equipment threshold.

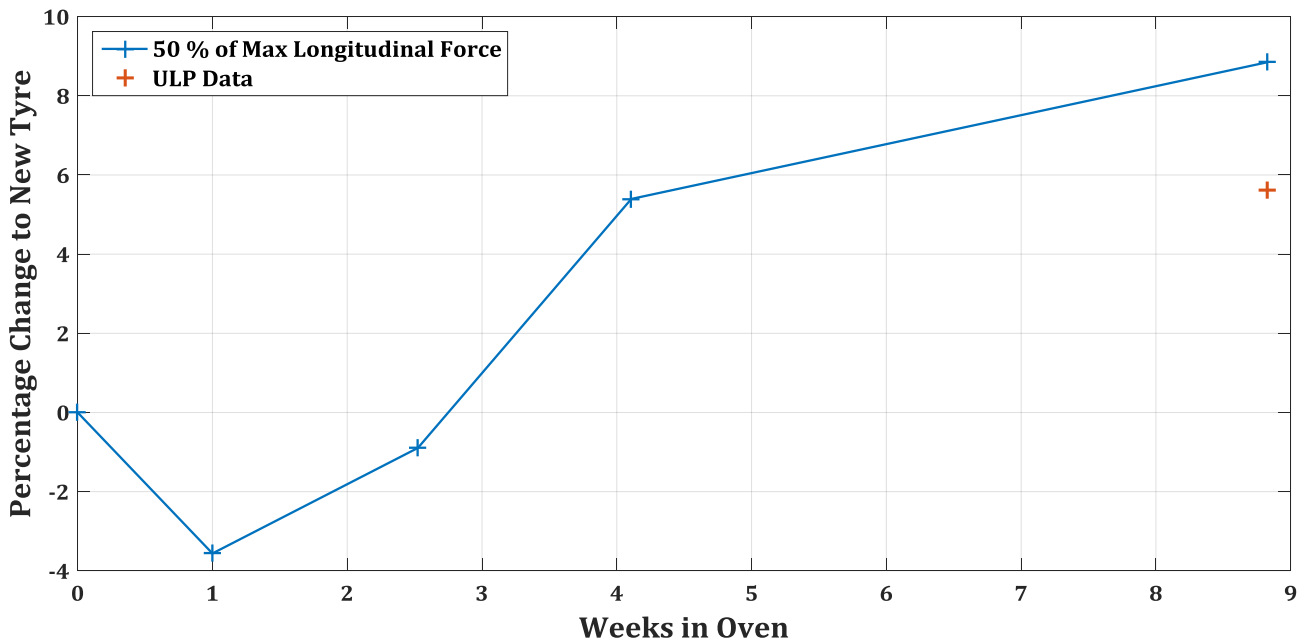


Figure 5.16 - Percentile change in longitudinal deflection as the tyre ages

5.6 DISCUSSION OF RESULTS

The results of the tyre stiffness tests illustrate a variety of changes in the characteristics of the tyre as it ages. Ultimately the comparison between the stiffnesses was conducted through the relative change in the deflection detected at specific loads. All these percentile changes in deflection are summarised in Figure 5.17. The average in percentile deflection at each interval where tests were conducted was also plotted using a linear line of best fit for each of these average data points. The dashed red lines were added for the equipment measuring thresholds of $\pm 1\%$.

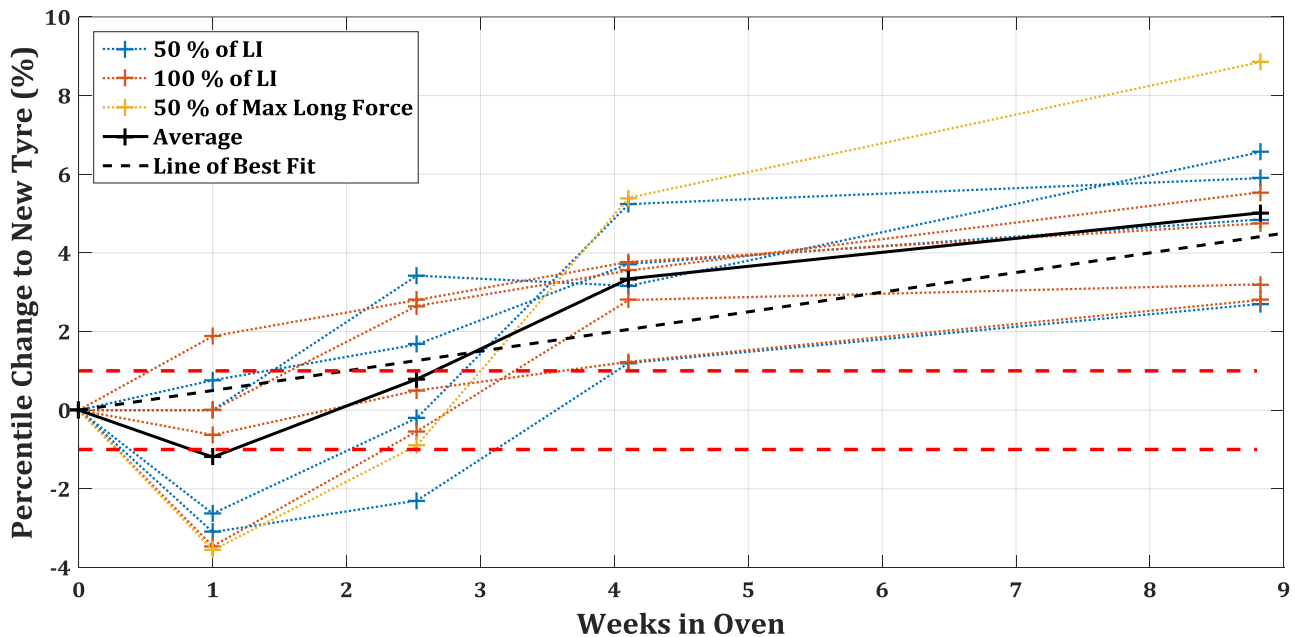


Figure 5.17 - Percentile change in deflection of all test data with averages and a line of best fit

Although very crude, given the wide spread of the data and especially due to the uncertainty around the data after 1 and 2.5 weeks of aging, the linear line of best fit at least provides a good indication of the trend of the aging of the tyre. Bound by $\pm 3\%$ in variation, there is certainly an upward trend, albeit a very small one. Furthermore this upward trend overcomes the equipment threshold in all tests after approximately 4 weeks of aging.

Based on this line of best fit the trend can simply be described by Equation (8):

$$\Delta x = 0.5t \quad (8)$$

In Equation (8), Δx refers to the relative percentage change in deflection and t the time in weeks spent in the oven aging. If the oven temperature was maintained at 65°C , Equation (8) can be translated to the equivalent age of a specimen tyre tested in Phoenix, Arizona in the USA (Baldwin, et al., 2006). This is done by including the acceleration factor calculated in Section 5.2.2, the result of which is shown in Equation (9):

AGING

$$\Delta x = \frac{0.5 \times a_f \times t}{52} \quad (9)$$

Here, the resultant percentile deflection is given as a function of age in years. The acceleration factor, a_f , depends on the oven temperature as well as which choice of reference tyre as this determines the environment and how the tyre was used.

With reference to Chapter 3 and Figure 5.17 it is clear that, especially after 4 weeks in the oven, all the tests illustrated changes larger than that of the testing sensitivity margins of $\pm 1\%$. Prior to this a minority of the results show changes which are negligible compared to this sensitivity.

The most significant and trustworthy result produced in this investigation was that of the stiffness on a longitudinal cleat. A summarised result of this stiffness change is shown in Figure 5.18. Beyond this, as noted at the beginning of this chapter, the two different stiffnesses at 2.5Bar inflation pressure have also been included. The percentile change at the 100% of the LI was also checked at this inflation pressure and also equated to approximately 5% change in deflection as was observed with the 1.5Bar inflation pressure case.

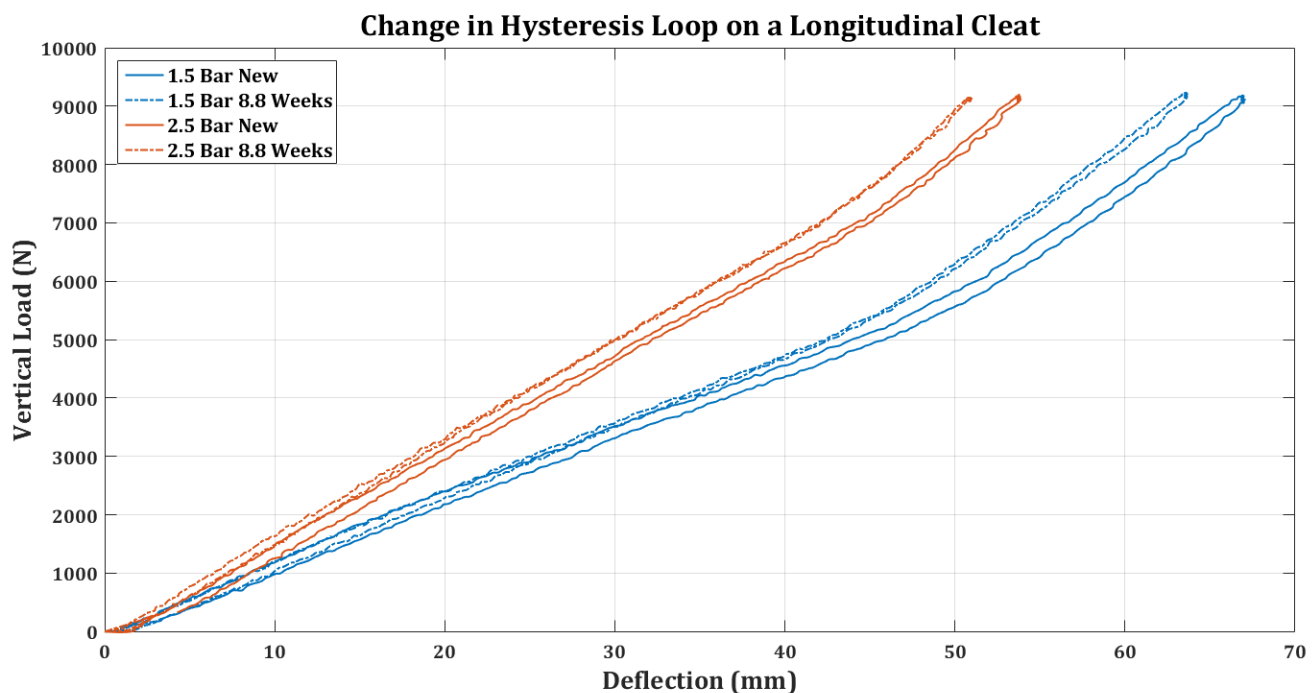


Figure 5.18 - Change in the hysteresis loop on a longitudinal cleat at different inflation pressures as the tyre ages

Of further interest in Figure 5.18 is the noticeable change in the hysteresis loop produced during the loading and unloading cycle whilst testing the tyre. After inspecting this change in all the tests conducted, the most significant change was observed on the longitudinal cleat. This change though is largely dependent on the velocity at which the test was conducted. Unfortunately, for

AGING

these tests a constant cycle frequency was used to load and unload the tyre. This implies that with different displacements, as is clearly evident in Figure 5.18, the velocity for each test differed slightly. This thereby deemed the change in hysteresis data unusable and would require further scrutinising.

5.7 POTENTIAL FTIRE MODEL UPDATES

The intention behind updating the FTire tyre model was built on the idea that an aged tyre would exhibit noticeable changes in stiffness; thereby improving the accuracy of the tyre model should it be updated. Having conducted the investigation above it was clear that in places a noticeable change was observed, however, in others the change was insignificant and judged to be negligible.

In the case where the changes observed were judged to be sufficiently effective a simple method was to be investigated regarding updating the FTire tyre model. In this section the feasibility and usefulness of updating the FTire tyre model using the tread Shore A hardness will be investigated. The chosen method is simple since it avoids retesting the aged tyre as it only involves measuring the tyre rubber tread's Shore A hardness.

5.7.1 Shore A Hardness Update

The original Shore A hardness average around the tread of the tyre was equal to 74.7. As was shown in Figure 5.1, the maximum change in Shore A hardness experienced at the tread was increased by 6. Therefore the FTire tyre model was updated to have a Shore A hardness of 80.7.

In theory, the tread Shore A hardness is a parameter in the FTire tyre model which is only adjusted for the dynamic longitudinal slip test. As a result one can expect a change in this tread stiffness parameter to directly change the nature of the longitudinal slip validation of the tyre model. However, the effect this tread stiffness will have on the other tyre characteristics such as the footprints and vertical stiffnesses, is unknown.

Figure 5.19 shows the change in the footprint validation at 4 degrees camber after the Shore A hardness has been updated in the tyre model. The middle footprint shows this validation and illustrates a very slight change in the area of the footprint. This trend was common amongst all the footprints and this small change does not compare with the drastic change noticed in the actual aged tyre footprint, shown in the right footprint of Figure 5.19. The change in area indicates a small change in stiffness. This was also observed in vertical stiffness changes in the tyre model.

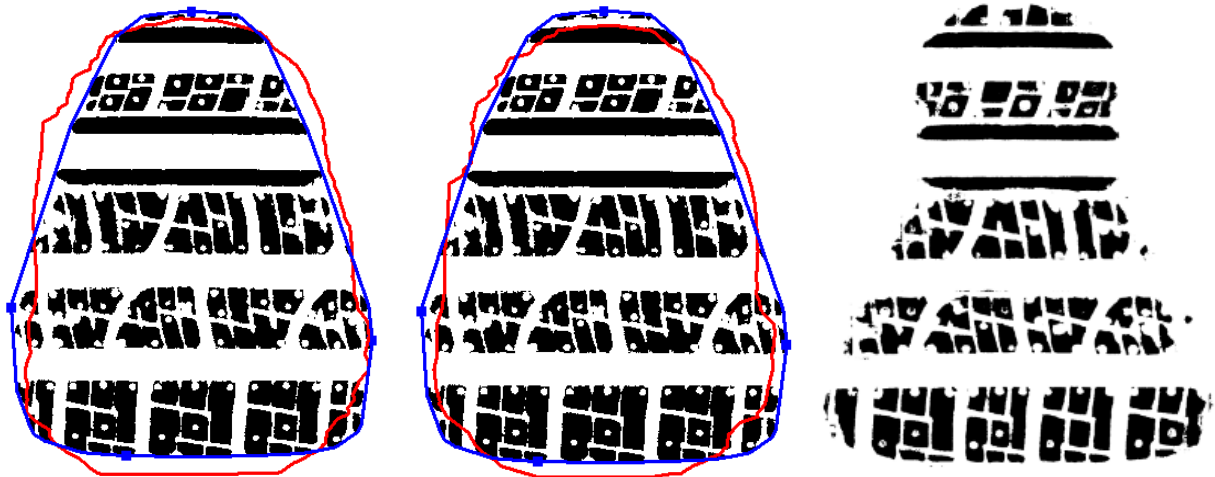


Figure 5.19 - Comparison of the validation of footprints at 4 degrees camber with an update of the Shore A hardness in the tyre model. Left – final validation of new tyre; Middle – validation after Shore A update; Right – actual footprint after aging

Figure 5.20 shows the effect on the tyre model when the Shore A hardness is increased to 80.7. Figure 5.20 (a) shows the vertical stiffness on a flat surface at 0 and -4° camber, Figure 5.20 (b) the vertical stiffness on a transverse cleat at 0° and -4° camber, Figure 5.20(c) the vertical stiffness on a longitudinal cleat and Figure 5.20 (d) the longitudinal stiffness.

Figure 5.20 indicates noticeable but very small changes in the stiffnesses of the tyre model. The changes seen on the vertical stiffness on a flat surface are negligible especially at the high loads. These changes correlate to approximately 0.75 and 0.6% of the original deflection at the 100% of the LI for the 0° and -4° camber respectively.

In the case of the transverse cleat, a more significant change is observed. This correlates to approximately 2% at the LI for both camber cases. The most significant change is observed over the longitudinal cleat with approximately 2.2% change in deflection at the LI. Finally in the longitudinal stiffness the change drops again to around 1% change at 50% of the maximum longitudinal force.

AGING

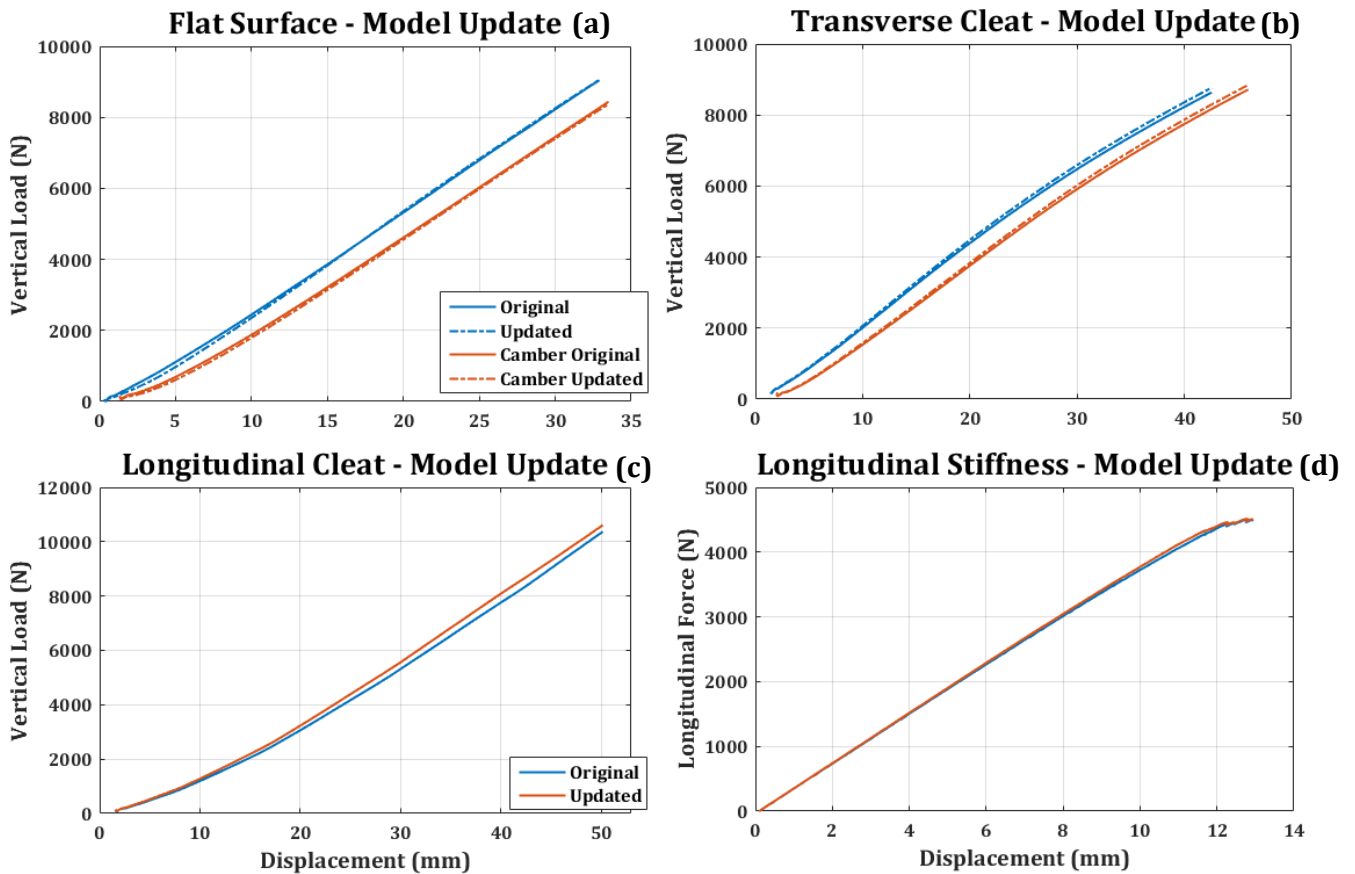


Figure 5.20 - FTire tyre model Shore A hardness update effect on the various stiffness's tested

Recalling the percentile deflection figures discussed previously in this chapter, as well as Figure 5.17, these changes observed in the updated tyre model are slightly conservative. Using the belt twist stiffness which was validated in the original model on the vertical stiffness on a transverse cleat, the updated model is compared in Figure 5.21.

The test on a transverse cleat was used as it displays a comparably large amount of change after the tyre model's Shore A hardness was updated. Furthermore, it was one of the more accurately validated tyre parameters shown in Section 4.3.2.1.2 in Figure 4.10. Thus, should it have been deemed necessary, this parameter would demonstrate one of the larger errors due to a change in stiffness resulting from the aging process.

Immediately clear from Figure 5.21, is that the updated tyre model does not capture the sudden change in vertical stiffness at the lower loads of the case at 0° camber. However, this was already a feature of the validation with the original model and has only been exaggerated here. Nonetheless, the updated model is seen to capture the higher loads well albeit with very little difference in accuracy compared to the original tyre model stiffness.

AGING

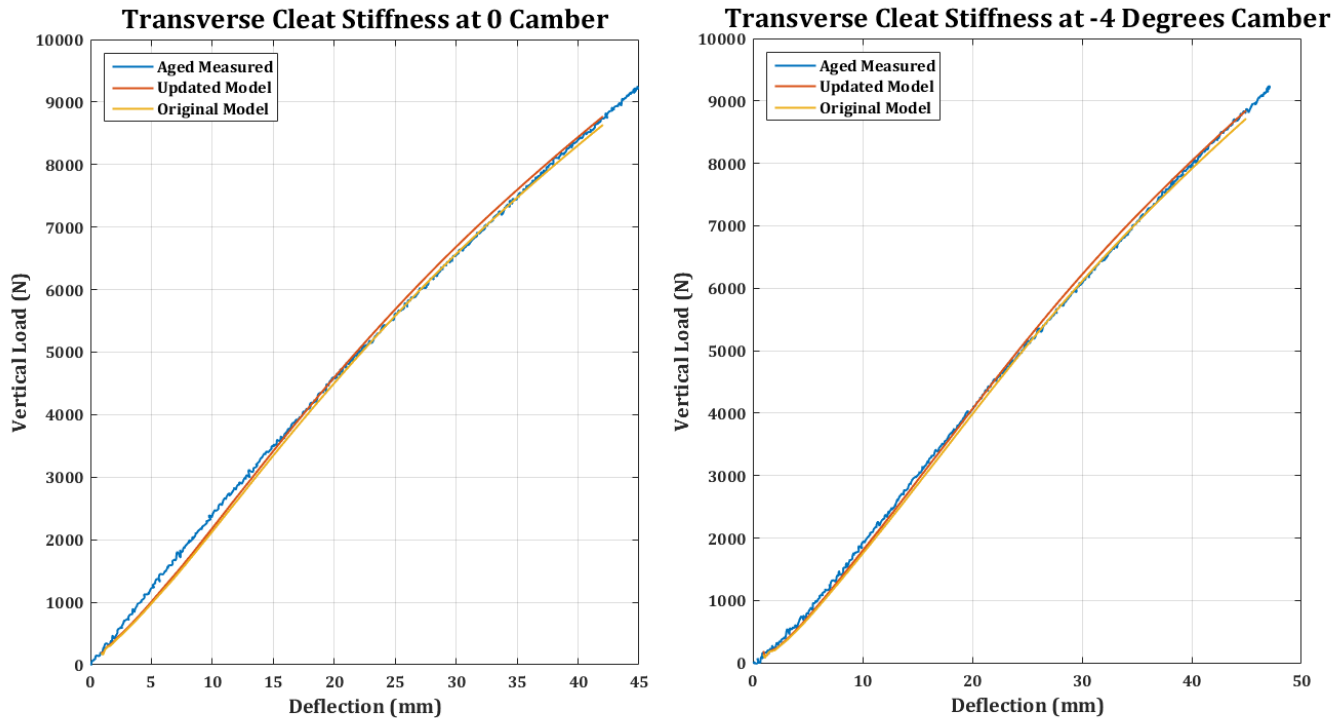


Figure 5.21 - Validation of the Shore A hardness updated tyre model on a transverse cleat at 0 and -4 degrees camber

A similar argument can be made regarding the stiffness at camber in that the actual difference between the original and updated model is in line with the change in stiffness of the test data in that they are both relatively small.

5.8 CONCLUDING REMARKS ON AGING

With the intention of acquiring a tyre model that is an accurate representation of the actual tyre within certain accuracy boundaries, the effect of the tyre age on stiffness properties was to be investigated. The tyre was aged for a total of 8.8 weeks in an oven maintained at 65°C. During this period the tyre was tested on a static test rig 5 times measuring various vertical stiffnesses as well as the longitudinal stiffness. In addition to this the Shore A hardness was measured on the side wall of the tyre as well as the middle of the tread pattern.

Various tyre stiffnesses changed as the tyre aged but the changes were small with average changes of the order of 5%. Stiffness comparisons were completed with test data at 1.5Bar inflation pressure in an effort to improve the isolation of the change in the rubber properties while remaining relevant to the nominal tyre inflation pressure.

The largest changes are evident on the longitudinal cleat. For the remainder of the static data, however, an error less than 5% would be made all the way to approximately 1% with regard to the vertical stiffness test on a flat surface. These smaller changes in the region of 1% can be

AGING

considered negligible as this is also representative of the testing accuracy and repeatability of the test rig.

Despite this overall error margin being very small, updating the FTire tyre model was investigated by adjusting the tread Shore A hardness. Figure 5.1 demonstrated that the Shore A hardness increased as the tyre aged, however, the sidewall changed more significantly compared to the tread. Updating the tyre model had small but noticeable effects on the tyre model stiffnesses. These changes correspond well with the changes measured at the nominal inflation pressure. However, it is difficult to quantify the overall improvement or decline in the accuracy of the model as the changes are simply too small.

In the case of the longitudinal cleat test and the drastic change in the shape of the tyre footprints it was already shown in Chapter 4 that the FTire tyre model could not capture the same behaviour as that which was measured. As a result more work would be required in investigating why this error occurs before the aging effects in this region can be elaborated upon.

Effects of aging are therefore smaller than can sensibly be captured accurately by the tyre parameterisation process and the tyre model.

6 WEAR

6.1 INTRODUCTION

This chapter investigates the effects of the wear on the tyre. A method of wearing the tyre, measuring the change in the tread depth and subsequently testing the tyre to determine the changes in characteristics attributable to wear was conducted.

The tyre was abrasively worn on a dynamic tyre test trailer where tread would be noticeably removed in less than 50km of effective travel of the tyre. This was achieved by applying a combination of periodic longitudinal braking and lateral slip angle sweeping. The profile of the tyre was measured whereby an accurate measurement of the change in the change depth could be acquired after the wearing of the tyre was completed. As a result the tyre was worn and tested consecutively 4 times.

The static test data acquired included basic properties such as the mass and tread depth as well as the Shore A hardness on the sidewall and tread of the tyre. Vertical stiffness on a flat surface and various cleat orientations were tested at 0° and -4° camber. Longitudinal stiffness was also tested on a flat surface.

In order to remove any possible errors in the measurements acquired, the effect of running the tyre in was also investigated. This involved simply loading the new tyre and travelling approximately 20km on it. This tyre was then additionally tested before and after the running in process. The effect of measuring at different locations around the tyre was also investigated. This was particularly important as a severe flat spot occurred on the tyre after the second round of the wearing process.

Finally, the possibility of updating the FTire tyre model was explored in the case where noticeable and relevant changes to the various stiffnesses of the tyre were observed. This involved a simplified method so as to avoid re-parameterising the tyre with a full new set of tyre stiffness data.

6.2 MISCELLANEOUS PROPERTY CHANGES

In this section the changes in the tread profile and mass are discussed as well as a feasible method of quantifying the tread wear as the tyre is systematically worn.

6.2.1 Tread Profile

The tread profile is measured as stated in Section 2.2.3. It is measured on the new tyre as the distance between the top of the tread (or the outside of the tyre) and the bottom of one of the

WEAR

middle tread grooves (or the inner most tread groove). This measurement is not a trivial task when the tread wear is not uniform.

6.2.1.1 Tread Profile Irregularity

The profile was measured at 5 locations around the tyre because uniform wear was not expected due to the abrasive nature of the wearing process. This is clearly demonstrated in Figure 6.1 where the tread profiles at the 5 locations around the tyre are plotted after the final stage of wearing. The profile of the new tyre is included as reference. The tread depth varies by approximately 4mm which relates to almost 50% of the total tread depth. The tread wear for each profile in the lateral direction is also not constant as one side of the tyre is observed to have worn significantly quicker than the other side.

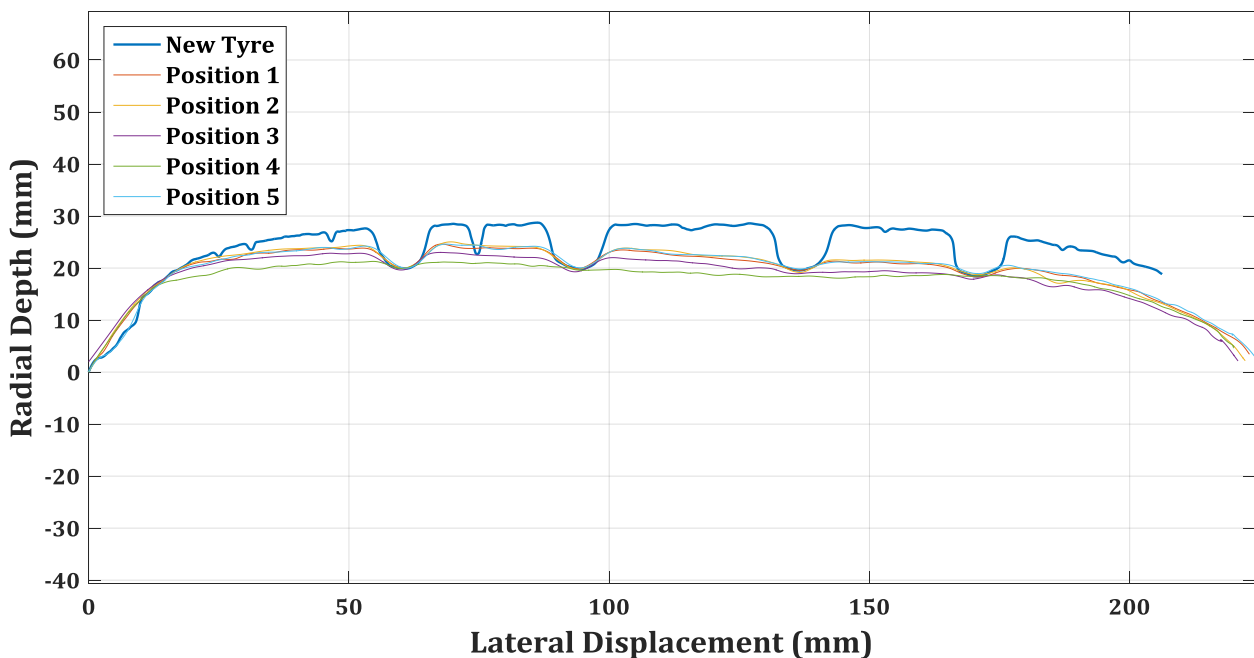


Figure 6.1 - Irregularity in tread profile around the tyre after final process of wearing

The results of Figure 6.1 are not ideal for an investigation into the effects of tread wear on tyre characteristics. Should the tread wear have any noticeable effects on the stiffness of the tyre, this variation may skew the results. Therefore the results presented should be interpreted with caution in that they will not truly represent the characteristics of a tyre with uniform tread depth.

6.2.1.2 Change in Tread Profile

Figure 6.2 shows the change in the tread profile at one location on the tyre as the tyre was worn. The irregularity of the tread depth across the tyre is evident. Also of note is that the amount of tread worn away between the wearing stages was also irregular. After the last round of wear it is also clear that the tread was completely removed in close proximity to the two middle tread grooves which no longer exist.

WEAR

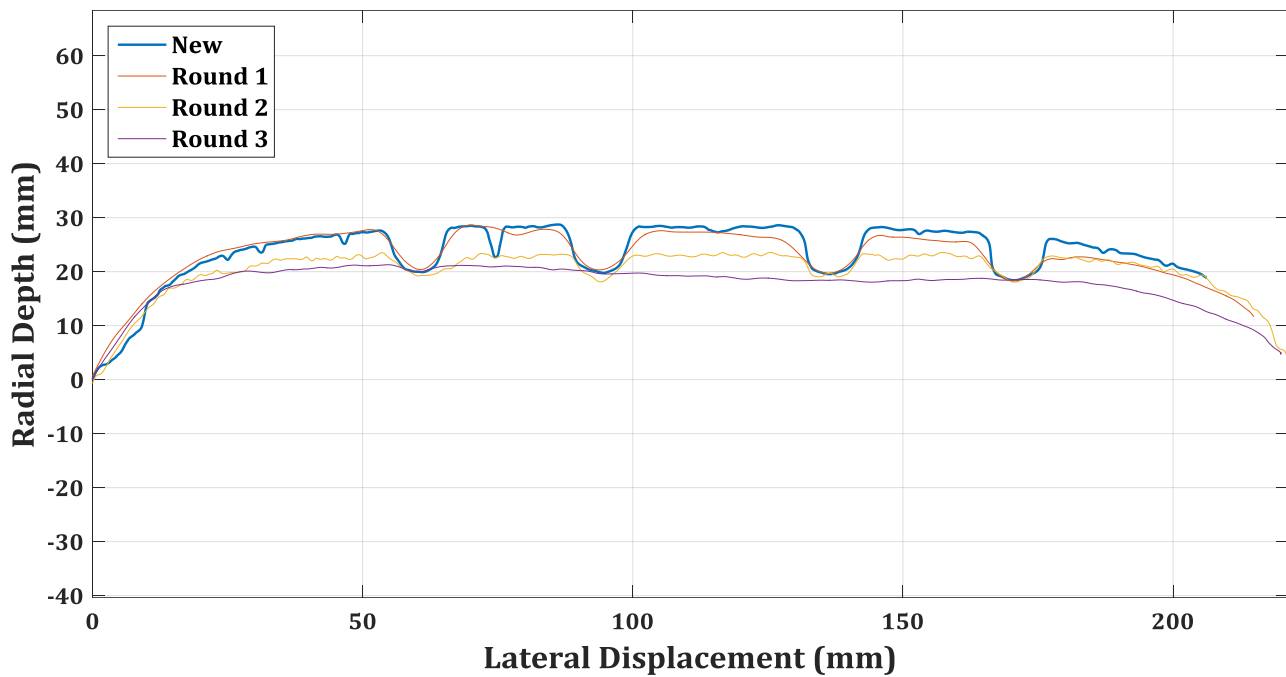


Figure 6.2 - Change in tread profile as the tyre is worn

6.2.2 Mass

In an effort to pin a single value on the tread wear after each stage of wearing the mass of the tyre is incorporated together with the original tread depth. Table 6.1 shows how the tread wear results in a significant change in the mass of the tyre.

Table 6.1 - Change in mass of tyre as the tyre is worn

Round	Tyre Mass (kg)	Δ Tyre Mass (kg)	Percentage of Total Tread Wear (%)
0	13.625	0	0
1	13.025	0.6	28.6
2	12.575	1.05	50
3	11.525	2.1	100

Using Figure 6.2 as a reference it was assumed that after the final stage of wearing the tread depth was equal to zero. Despite severe flat spots and some wear which exposed the carcass of the tyre, there were also sections, as seen in Figure 6.1 that still had 50% of the original tread. Nevertheless, using this assumption the tread wear will be described as in Table 6.1 by a percentage decrease of the original tread. Therefore after the first stage of wearing the tread will be described as being 28.6% less than the original tread and after the second stage as 50% of the original tread. After the final stage it will be described as 100% or fully worn.

WEAR

6.2.3 Tread Wear Assumption Effects

From this assumption it is important to note the effect on the remainder of the analysis of the effect of tread wear. By assuming a uniform distribution of tread, the effects described in this chapter are assumed to be due to the overall decrease in tread around the tyre and not specifically due to the tread wear at the contact patch.

This is important to note since the stiffness can vary due to the actual tread profile at the contact patch in comparison with the rest of the tyre which may have a vastly different tread profile due to, for example, a flat spot. Unfortunately, the actual tread profile at the contact patch was not available and it is thus not possible to state the effects thereof.

6.2.4 Application in FTire

Both the mass and the tread depth are values which can be altered easily in the FTire tyre model. While both can be changed individually, FTire does have a tread wear model. From Gipser (2005), the tread wear model is said to additionally create a time-dependent tread depth when activated and subsequently influences the cross-sectional geometry, radial tread stiffness, tread shear stiffness and tyre mass. Despite its main purpose being for determining how quickly the tyre wears, it indicates that if the mass and/or tread depth are adjusted that they will in turn change the overall stiffness and behaviour of the tyre model. Therefore this exists as a useable property for potentially updating the tyre model should a noticeable effect be found.

6.3 RUN-IN STIFFNESS COMPARISON

To ensure a solid baseline for the results presented in this chapter, an additional test was conducted whereby a new tyre was run-in over a 20km stretch at approximately 6.5kN which relates to around 70% of the LI. This was completed to investigate if the properties, such as vertical stiffness of the tyre, change significantly in the first few kilometres of use. The idea is that the initial stretching and breaking of weak rubber bonds would occur in this initial stage of use and could thus skew the results of the worn tyre tests, should there be any noticeable changes. Sandberg (2008) ran tyres in over a distance of 300km up to a maximum speed of 140km/h prior to any testing was conducted on a tyre. Unfortunately the motivation behind this procedure was not provided and neither was the vertical load of the tyre given.

6.3.1 Stiffness Test Results

Figure 6.3 shows the vertical stiffness of the new tyre compared to the run-in tyre. In this section only a select few stiffness results are shown as the remainder of the stiffness tests exhibit very similar behaviour.

WEAR

6.3.1.1 Vertical Stiffness on a Flat Surface

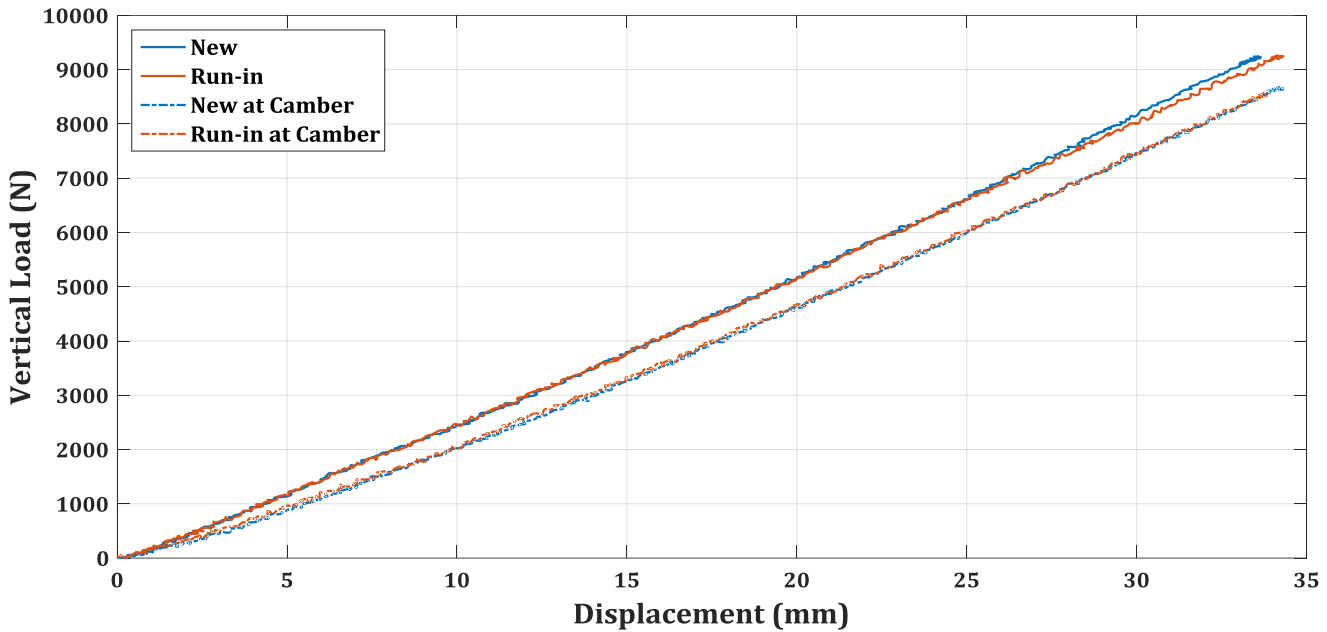


Figure 6.3 - Comparison of vertical stiffness on a flat surface at 0 and -4° camber with a run-in tyre at 2.5Bar

From Figure 6.3, the change in stiffness is negligible especially in the case of the stiffness at -4° camber. Here the stiffnesses visually appear to be exactly the same. At 0° camber, the change is negligible from 0 to approximately 7kN. Above 7kN a small but clear difference in stiffness is noticeable. This change increases such that at the LI the percentage difference in deflection between the two tyres is -1.6%.

6.3.1.2 Vertical Stiffness on a Cleat

When inspecting the stiffness results on a longitudinal and transverse cleat shown in

The most significant changes in stiffness occurred with the longitudinal stiffness. Figure 6.5 shows these stiffnesses as well as the data from the ULP load cell as an additional form of validation. In this case the deviation related to approximately -6.7% at 50% of the maximum longitudinal force acquired. This is a substantial change in stiffness.

Discussion of Results, the same trend was observed. In the case of the transverse cleat tests,

negligible change was observed in the stiffnesses at camber whilst similar changes in deflection were observed at the higher loads of the 0° camber case. This change correlated to approximately -1.8%. In the case of the longitudinal cleat, negligible change exists.

6.3.1.3 Longitudinal Stiffness

WEAR

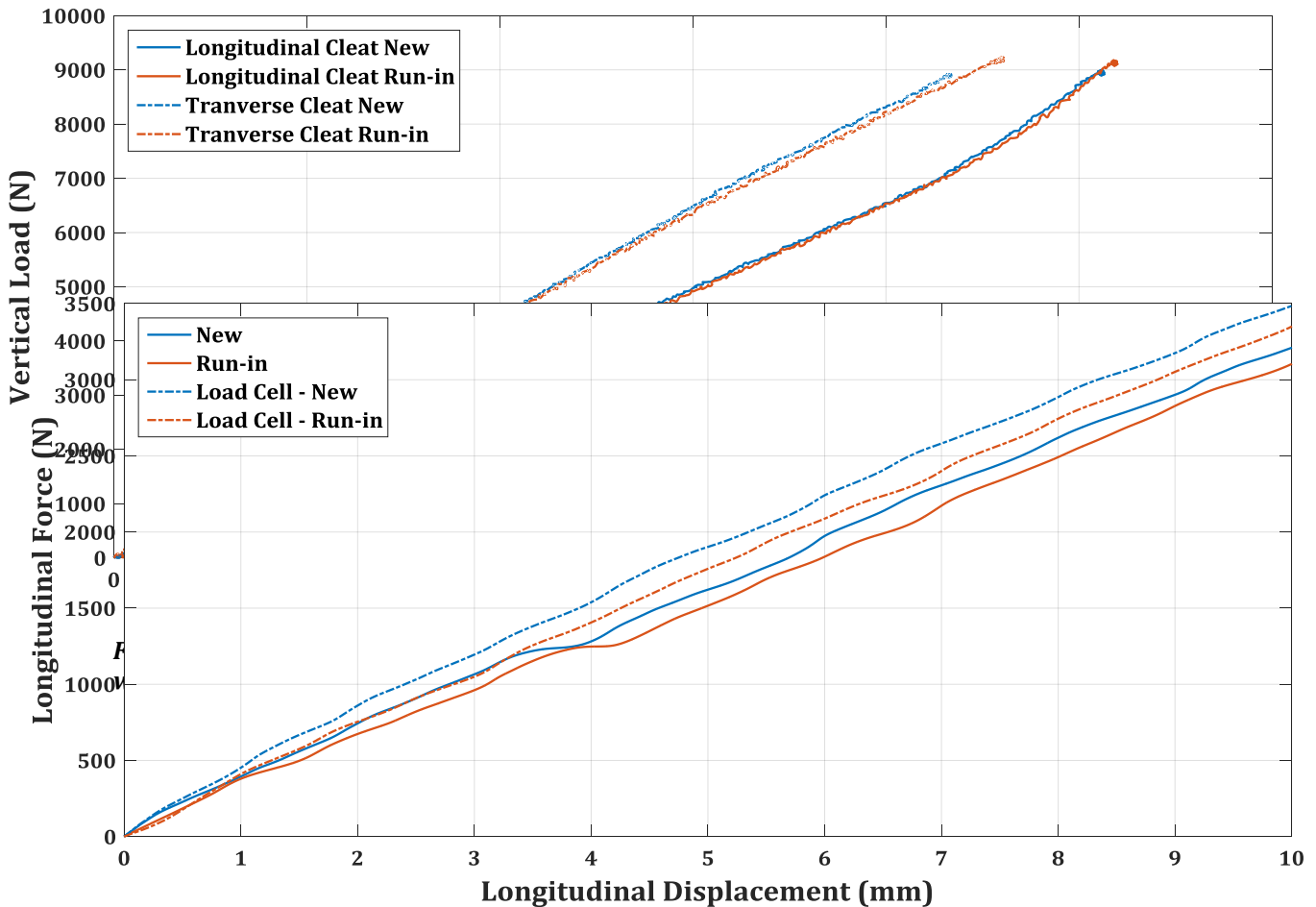


Figure 6.5 - Comparison of longitudinal stiffness with a run-in tyre

The most significant changes in stiffness occurred with the longitudinal stiffness. Figure 6.5 shows these stiffnesses as well as the data from the ULP load cell as an additional form of validation. In this case the deviation related to approximately -6.7% at 50% of the maximum longitudinal force acquired. This is a substantial change in stiffness.

6.3.2 Discussion of Results

The results indicate that the running in period of the tyre has noticeable effects on the various stiffnesses of the tyre. However, these changes are only noticeable at higher vertical loads where the vertical deflection changes in the range of 1.6 to 1.8%. Furthermore these changes only exist on the vertical stiffnesses tested at 0° camber angle. This suggests that the running in period of a tyre's life only influences, but is not limited to, the belt in plane bending stiffness thus implying that the stretching and settling of the steel belts within their surrounding rubber compositions does affect the tyre's overall stiffness. The changes in the remainder of the vertical stiffness tests, such as those at camber, were negligible. However, in the longitudinal direction, substantial changes in stiffness were noted. Since the changes were in the region of a 6% decrease in deflection they cannot go unnoticed.

WEAR

The noted changes in the vertical stiffnesses are just above the testing accuracy threshold of $\pm 1\%$ making them fairly noticeable changes. However, the change to the longitudinal stiffness is well beyond this threshold and can thus be considered a substantial change.

This implies that the changes in vertical deflection at the 100% of the LI and the majority of the deflections in the longitudinal stiffness should initially be accounted for by running in a new tyre before the baseline characteristics are measured.

6.4 FLAT SPOT STIFFNESS COMPARISON

The significant irregularities observed in the tread wear around the tyre during the wear process requires an investigation into the effect the measuring location has on the stiffness results. After the second round of wearing a severe flat spot had developed so this section seeks to determine how important the actual tread wear at the contact patch is and how it can influence the stiffness results.

6.4.1 Stiffness Test Results

Recalling from Figure 6.1, the variation in tread wear around the tyre can be up to $4mm$. In this case the average tread wear difference between the two locations was approximately $2mm$. This relates to just less than 25% of the total available tread. Figure 6.6, shows the vertical stiffness difference on a flat surface at 0° and -4° camber and the effects are clearly noticeable in both cases. The change occurs from approximately $4kN$ in both the 0° and -4° camber cases and eventually relate to a percentile change in vertical deflection at just less than the LI of -2.3 and -2.7% at 0° and -4° camber respectively. This severe difference is also clearly evident in Figure 6.7 which compares the two different contact patches with the tyre at its nominal inflation pressure of $2.5Bar$.

6.4.2 Footprint Comparison

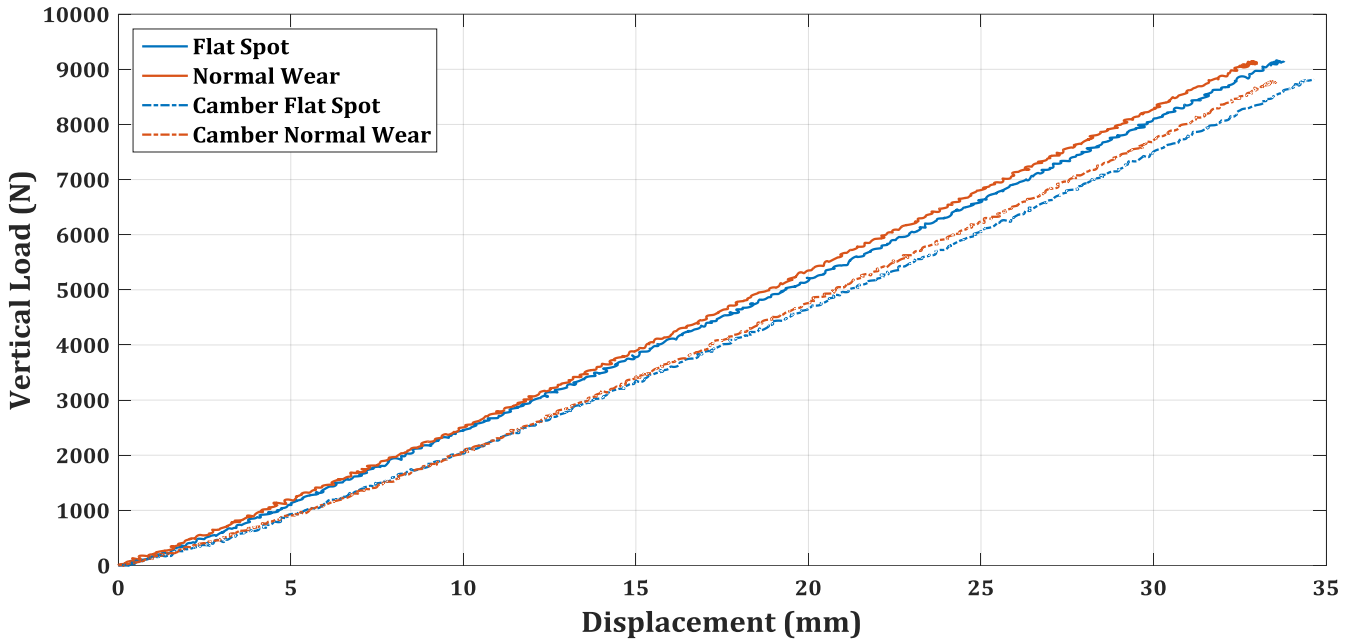


Figure 6.6 - Comparison of vertical stiffness's on a flat surface at 0 and -4° camber between a normally worn contact patch and a flat spot

Figure 6.7 shows the footprints of the tyre after the second round of wearing. The top two footprints are at 0° camber with the left being at the normal wear location around the tyre and the right being at the flat spot as with the test data shown in Figure 6.6. The bottom two footprints are the footprints at -4° camber. This comparison confirms the deviation in stiffnesses shown in Figure 6.6 as the footprints are vastly different due to the presence of the flat spot.

6.4.3 Discussion of Results

These changes in deflection are representative of the worst case scenario where a flat spot has occurred. With regard to the remainder of the test data presented in this chapter, it can be said that it was ensured that none of the tests were made at any flat spot. Nevertheless the differences in tread wear around the tyre are clearly evident as shown in Figure 6.1 and thus, independent of the contact patch location around the tyre, a difference in stiffnesses just due to the tread profile at the contact patch will exist. The maximum expected influence will be 2.7% in deflection at the LI and even so this will only exist if tested at the flat spot.

Both the influences of the irregular tread wear as well as that of the running in of the new tyre must be considered in the stiffnesses results. It is also important to note that in both cases the stiffnesses were decreased. This will assist in the analysis to follow.

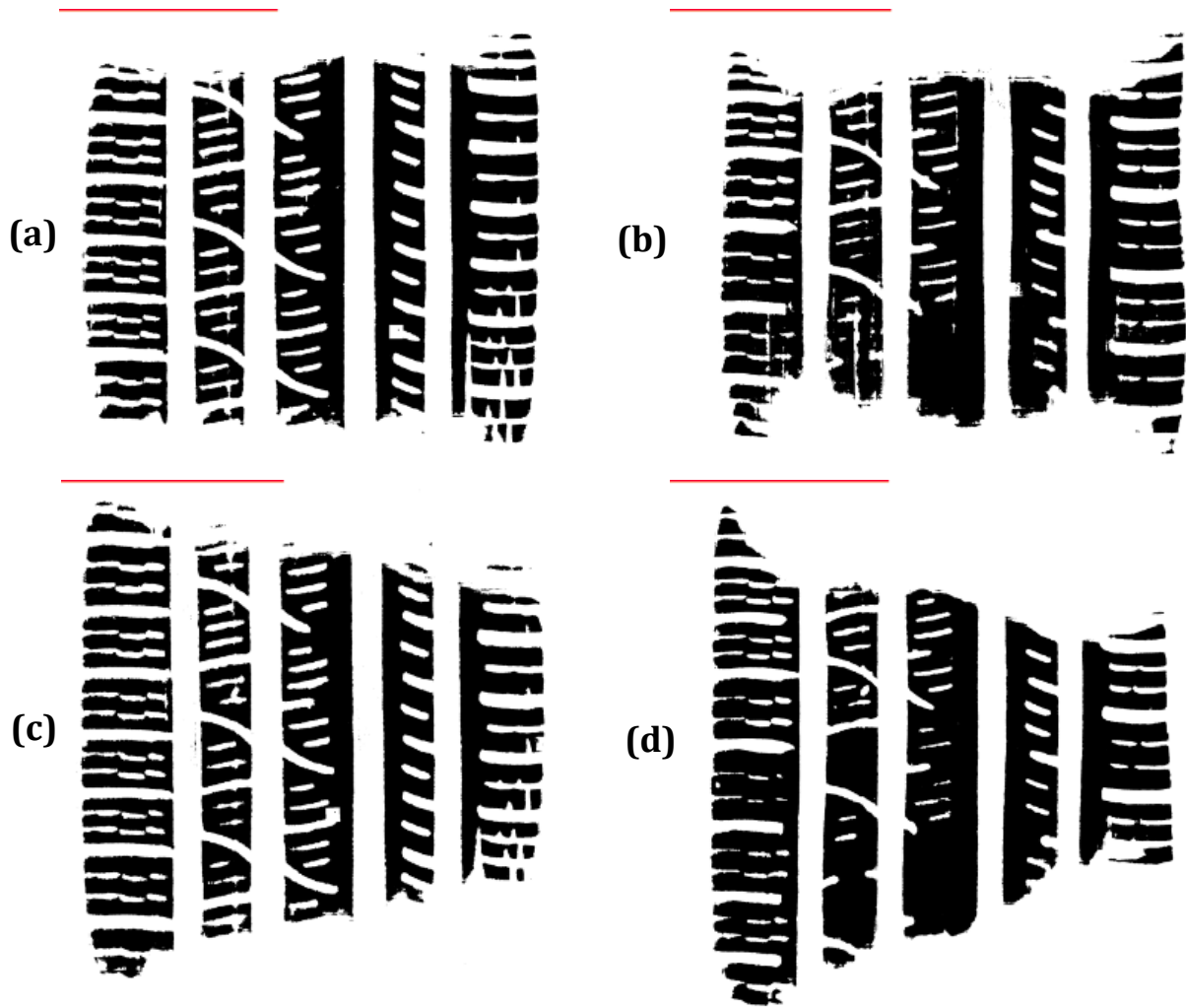


Figure 6.7 - Changes in footprint shape due to flat spot at 0° camber (b) and -4° camber (d), (a) and (c) are the equivalent footprints at another location around the tyre away from the flatspot.

6.5 TREAD WEAR STIFFNESS TEST RESULTS

Stiffness tests performed after each wear round included the following:

- Vertical stiffness on a flat surface at 0° camber
- Vertical stiffness on a flat surface at -4° camber
- Vertical stiffness on a transverse cleat at 0° camber
- Vertical stiffness on a transverse cleat at -4° camber
- Vertical stiffness on a longitudinal cleat at 0° camber
- Longitudinal stiffness on a flat surface

Each of these tests is presented individually using the same method of comparison as was used in Section 5.5 where the percentile vertical deflection at 50 and 100% of the LI is calculated. These values are then graphically depicted. The footprints are discussed in the case of the vertical stiffness tests on a flat surface at 0° and 4° of camber.

WEAR

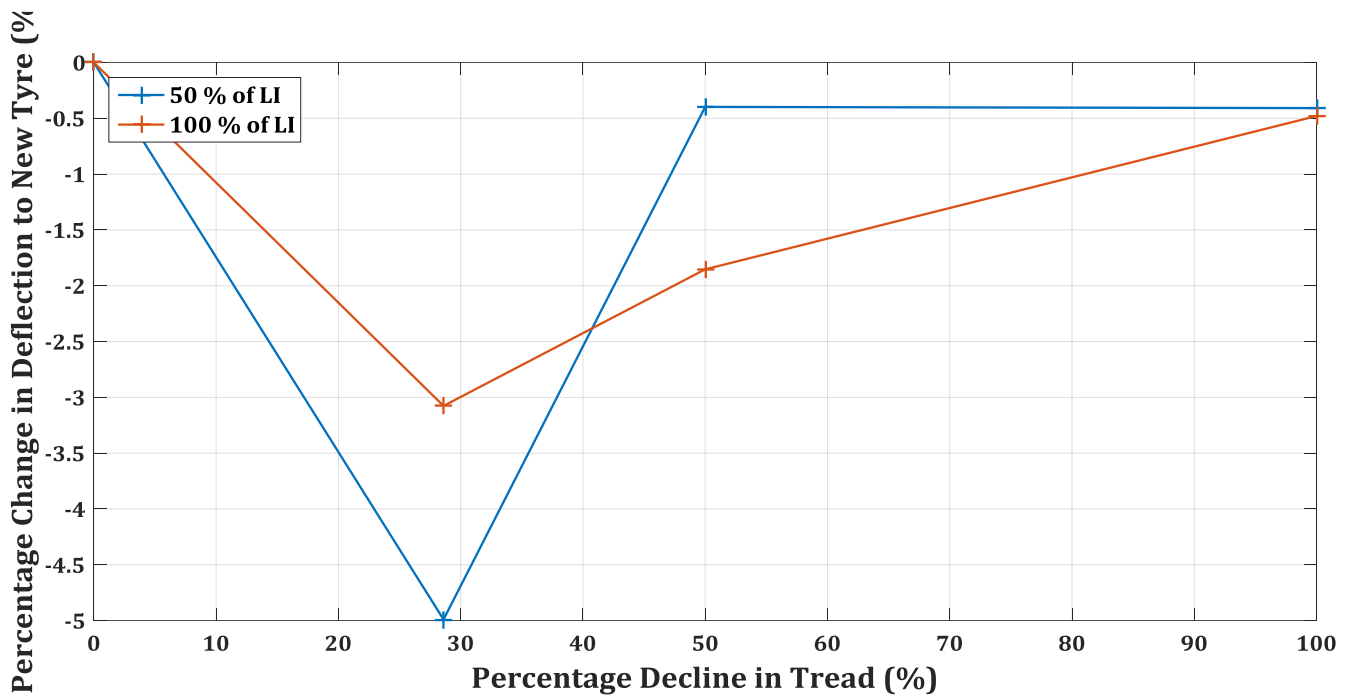


Figure 6.9 - Percentile change in deflection on a flat surface as the tyre is worn

The percentile decline in tread calculated in Section 6.2.2 is used as the basis of this analysis and for the comparison between the various stiffnesses. It should be noted that if these values were to be changed it would not have a large influence on the results as long as the relative difference between them was held constant. The full set of percentile changes in deflection at specific loads is presented in Appendix A.

Finally, the comparisons made will be performed at 1.5Bar inflation pressure. This is done so as to amplify the potential influences on the tyre properties however it should always be kept in mind that the differences at the nominal inflation pressure of 2.5Bar can be slightly less. This will be discussed in greater detail towards the end of the chapter.

6.5.1 Vertical Stiffness on a Flat Surface

6.5.1.1 At 0° camber

Figure 6.8 shows the variation in the vertical stiffnesses on a flat surface at 0° camber as the tyre is worn. From this figure it appears that the influence of wear is very small and irregular. Whilst a comparatively large deviation happens after the first round of wearing, this trend does not continue throughout the remaining set of tests. Here the stiffness comparatively increases back to original stiffness of the new tyre. This is also evident in Figure 6.9 for the changes in vertical deflection at 50 and 100% of the LI. In both cases the deflections initially decrease and then increase again tending towards the original deflection.

WEAR

This initial drop in relative deflections can be accounted for as the run-in period of the tyre however the percentile changes are a few times larger than that of the run-in comparison. Thus this trend would still exist even if the tyre originally tested was run-in. The sudden increase after the first round of tests could be accounted for if the tests at 28.6% tread wear were conducted on a flat spot or section of the tyre with a different tread profile. The remaining tests at 50 and 100% tread wear show no dependence on the tread of the tyre as they do not exceed the testing accuracy threshold of $\pm 1\%$.

The footprints were made at the same contact patch as that which was shown in the test data

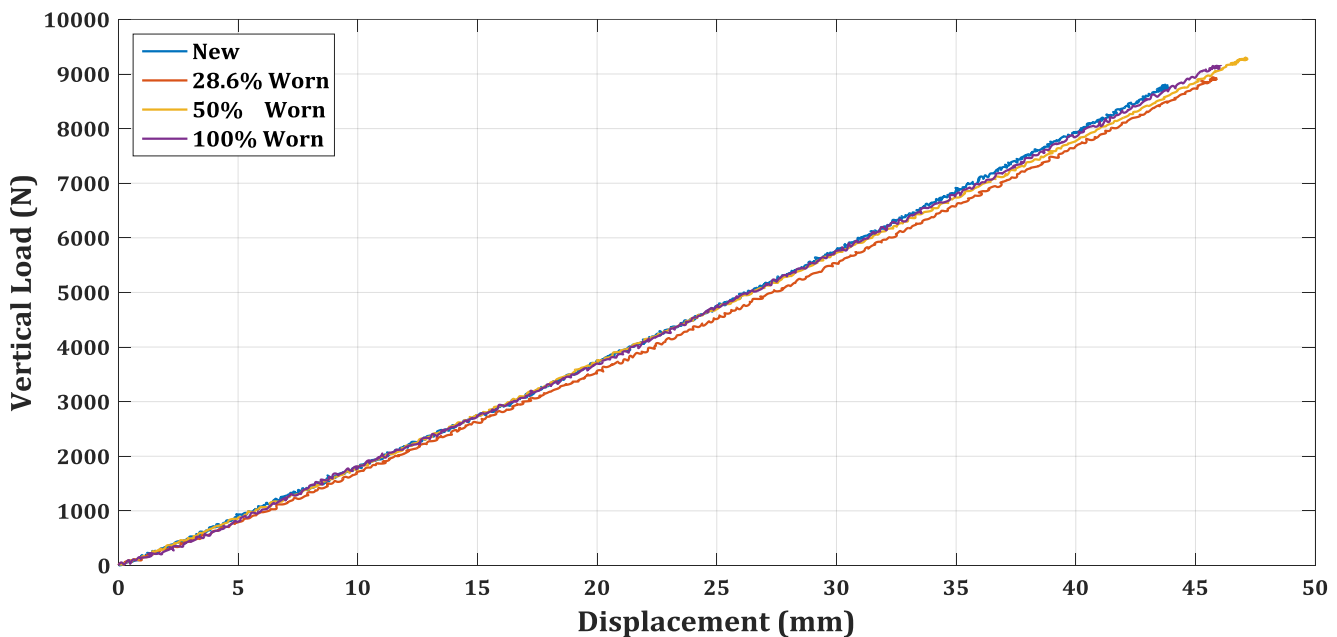


Figure 6.8 - Changes in vertical stiffness on a flat surface as the tyre is worn

above. However, potentially evident from is that the same contact patch was not used between tests after each round of wearing. This could still be misinterpreted as the tyre did not wear uniformly during these stages.

While it is unfair to directly compare the footprints due to the fact that the same vertical load wasn't necessarily used to acquire each footprint, the distinctly clear change in shape of the footprint can explain the variations observed in the vertical stiffness plots of Figure 6.8. The footprints show uneven wear between the stages of wearing and clearly show that one side of the tyre was worn away much quicker than the other. This could change the initial stiffness of the tyre as the outer most side of the tyre makes contact with the ground prior to rest, however, this characteristic is not evident in the stiffness.

The extremity of the abrasiveness of the wearing process is evident in the footprint made after the final stage of wearing. The discontinuities in the tread rubber are depicted well here as well

WEAR

as the feathering of the tread and subsequently add to the uncertainty of the results presented in this chapter.

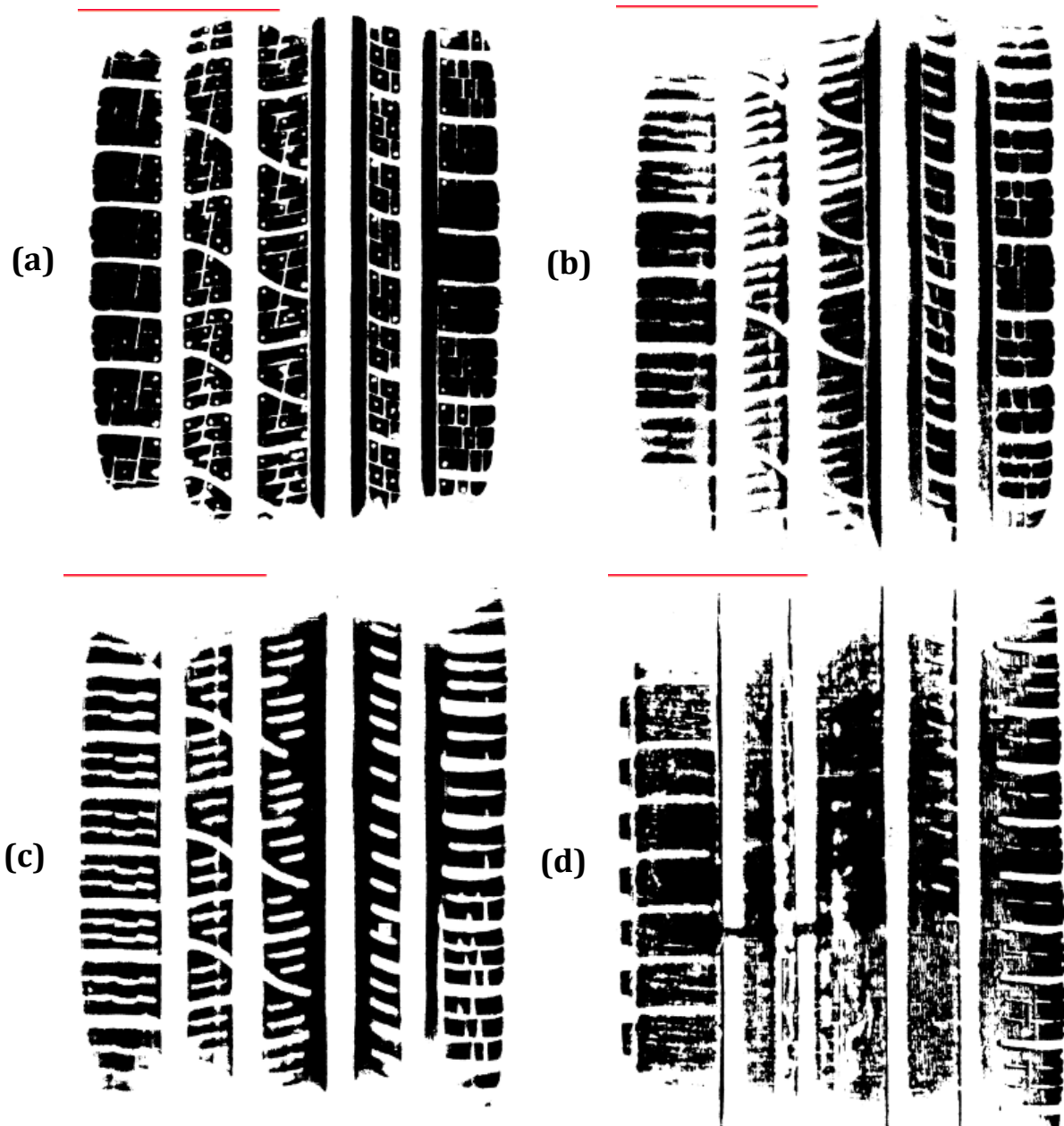


Figure 6.10 - Change in footprint at 0° camber as the tyre is worn - new to fully worn from (a) to (d)

6.5.1.2 At 4° Camber

The stiffness at 4° camber illustrates additionally irregular results. As seen in Figure 6.11 and Figure 6.12, the trend of an initial decrease in stiffness followed by a sudden increase, is more prominent, to such an extent that the stiffness of the fully worn tyre is noticeably stiffer than that of the original tyre.

WEAR

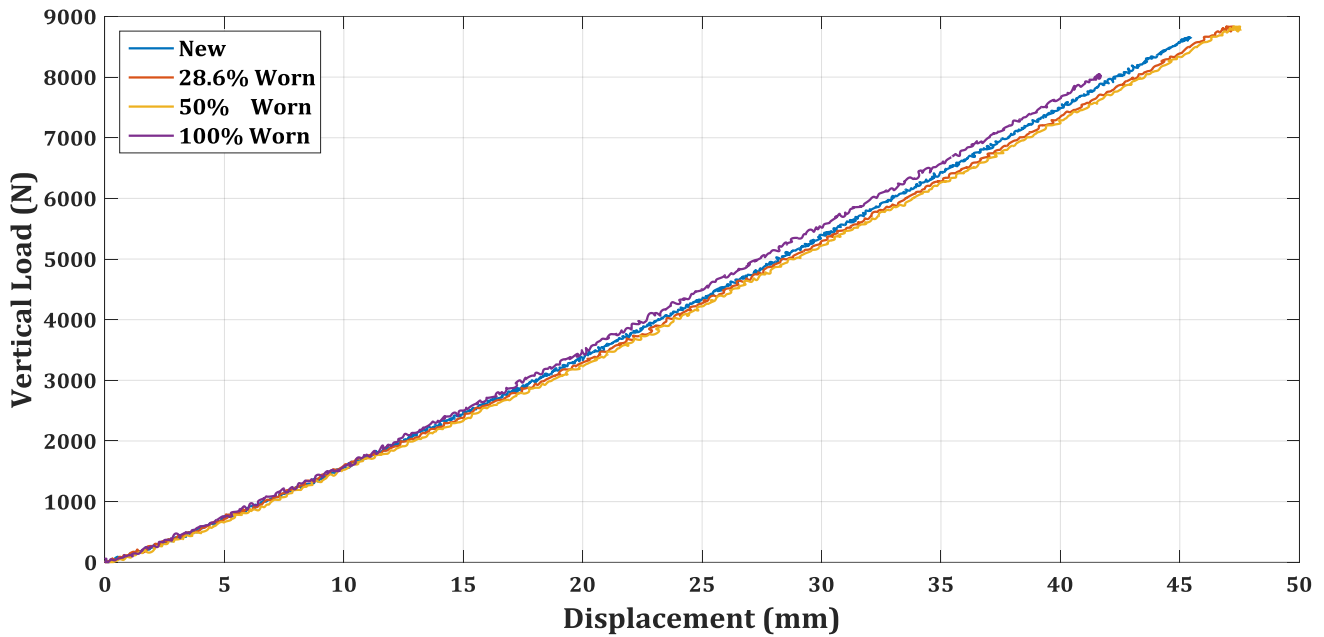


Figure 6.11 - Changes in vertical stiffness on a flat surface at -4° camber as the tyre is worn

This set of stiffness data demonstrates slightly smaller deviations in stiffness, though, compared to Figure 6.3. The effects of running the tyre in were not as apparent with the test at camber over that at 0° camber. Thus these changes can only be accounted for by irregular tread at the contact patch or as being an actual phenomenon of the tyre as it is worn.

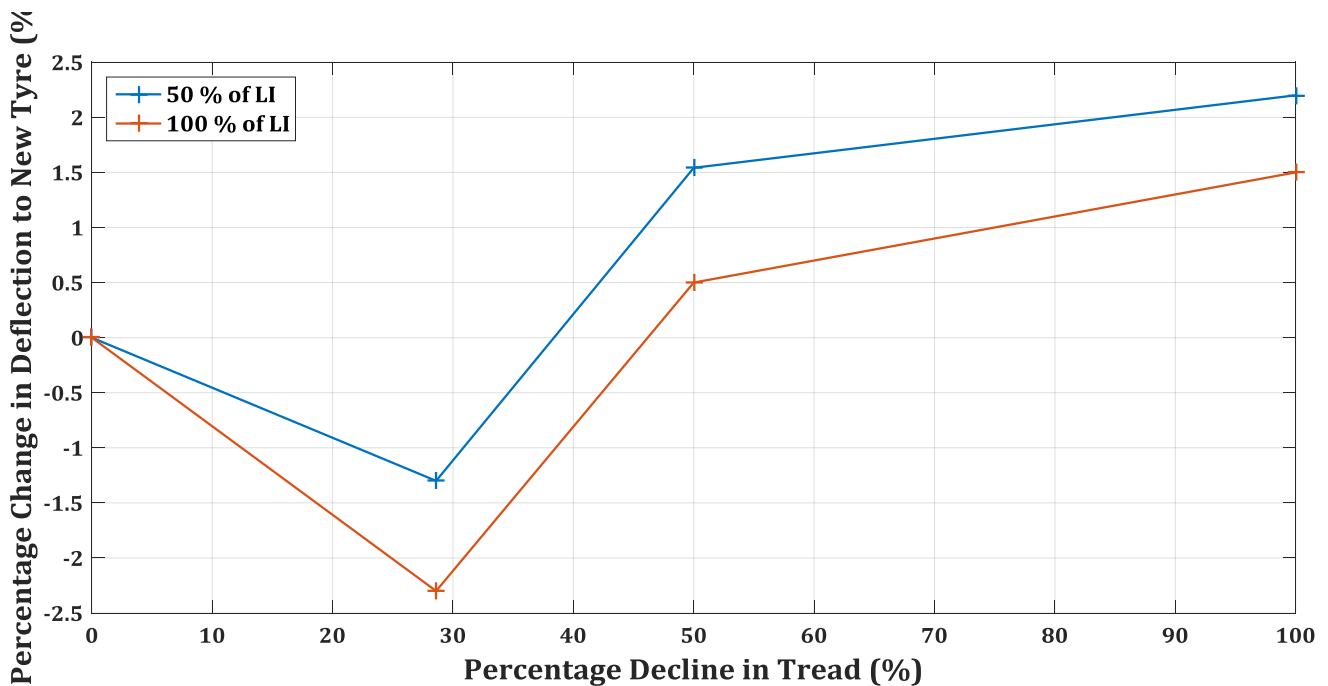


Figure 6.12 - Percentile change in deflection on a flat surface at -4° camber as the tyre is worn

The footprints shown in Figure 6.13 show how the area of the footprint varies from one stage of wearing to the next. Due to the uneven wear across the tyre, the camber angle appears to have less and less of an effect on the shape of the footprint. This information provides useful insight

WEAR

into why the stiffness at this camber angle increased significantly even though a lot of tread was lost in between testing. Unfortunately it removes the value in the test data as the tyre appears to start behaving more like it is on a flat surface at 0° camber.

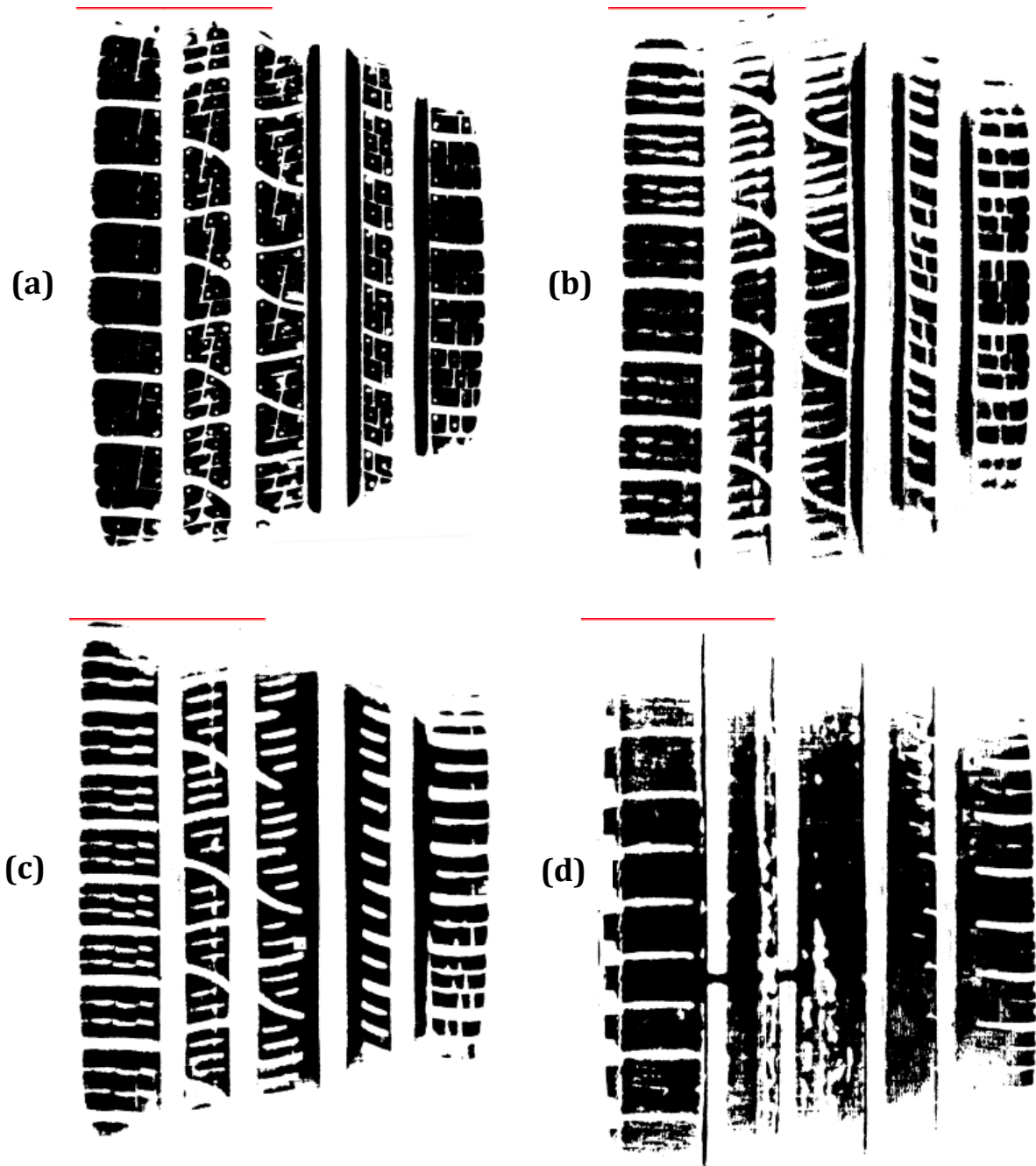


Figure 6.13 - Changes in footprint at -4° camber as the tyre is worn - newest to fully worn, (a) to (d)

6.5.2 Vertical Stiffness on a Cleat

The vertical stiffness tests on a cleat included three cleat orientations: the first is the transverse cleat testing vertical stiffness at 0° and -4° camber and the second is the longitudinal cleat only at 0° camber.

WEAR

6.5.2.1 *Transverse Cleat*

Recalling from Section 6.3.1.2 which decreases the effects of the running in period of a tyre, it was noted that with the transverse cleat at 0° camber the drop in percentile deflection at the LI was approximately 1.8%. In the case of the transverse cleat at camber, however, the change was negligible.

Moreover, from the footprints of Section 6.5.1.2, it is clear that the uneven wear across the tyre reduces the effect of camber on the vertical stiffness. These points will be considered in the discussion below.

6.5.2.1.1 At 0° camber

Figure 6.14 illustrates more predictable stiffness results as a function of the tread wear. Each test appears to slightly lower the stiffness of the tyre. Taking into account that the tyre is run-in through this wearing process 1.8% of the vertical deflection figures should be added to the values shown in Figure 6.15.

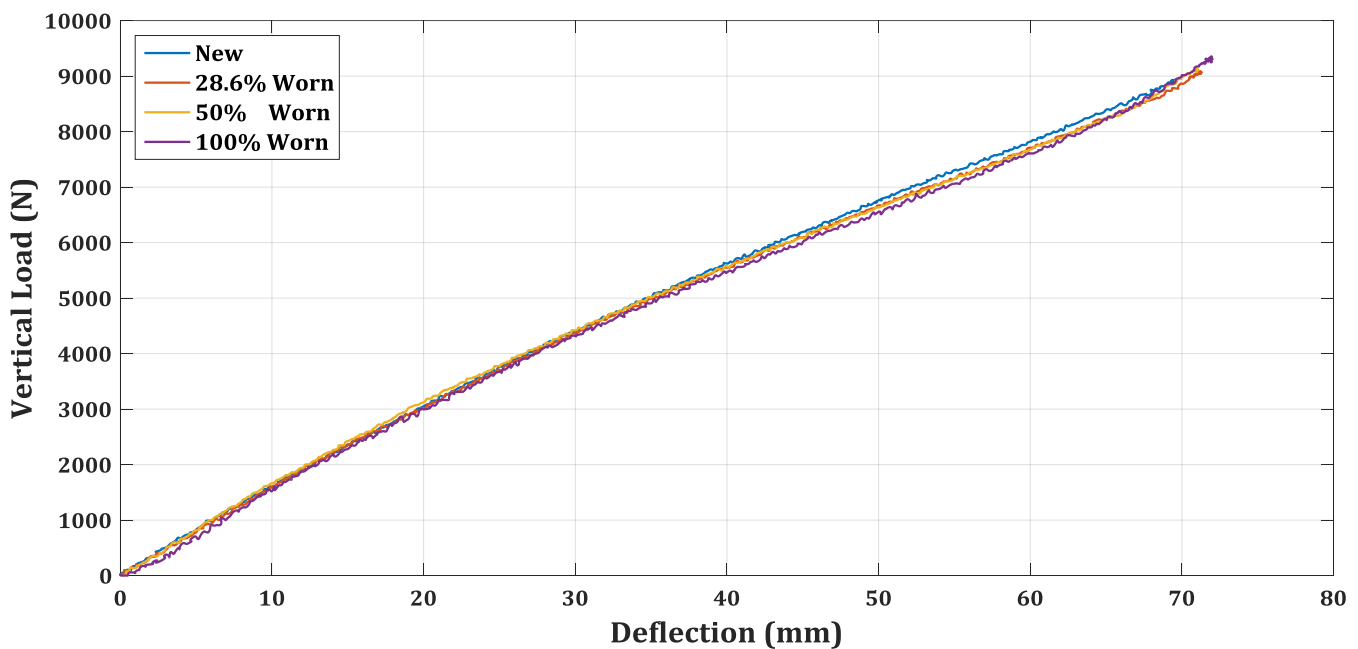


Figure 6.14 - Changes in vertical stiffness on a transverse cleat as the tyre is worn

Another point of interest from Figure 6.14 is that when dealing with the 100% worn case there is a distinctly lower initial stiffness which is evident until approximately 8mm of deflection. This occurs due to the irregular tread profile and uneven wear on the tyre. Contact is initially only made with the section of the tread which is still prevalent in tread depth before contact is made with the rest of the tread. The result is an apparently lower stiffness until the rest of the tyre is in contact with the surface.

WEAR

In the case of the 100% worn tread there appears to be contact with the surface upon which the cleat is mounted at a lower deflection compared to the other stiffnesses. This can be attributed to it being the softer of the stiffnesses and thus requiring more deflection to reach the same load.

Figure 6.15 demonstrates irregular behaviour in the changes of the deflection at 50% of the LI however the changes are very small. A more consistent trend is observed in the case at 78% of the LI but if the run-in tyre effects are considered by adding the aforementioned 1.8% deflection change, the effects solely due to tyre wear are far less significant than those observed with the changes at 50% of the LI.

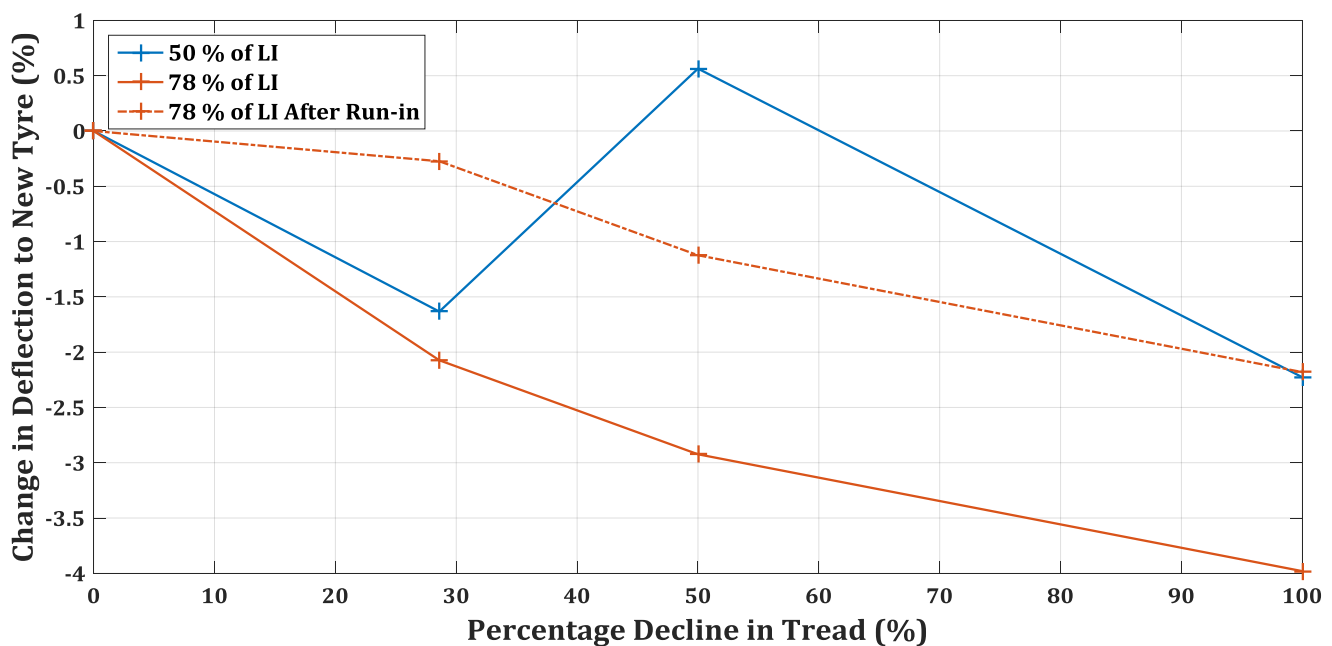


Figure 6.15 - Percentile change in deflection on a transverse cleat as the tyre is worn

6.5.2.1.2 At 4° Camber

Once again the results at camber are more inconsistent due to the uneven wear across the tyre resulting in the stiffness appearing more like it is not at a camber angle. This is clearly evident in Figure 6.16 of the vertical stiffness on the transverse cleat at -4° camber where the stiffnesses noticeably increase as the tyre is worn.

With the effects of the run-in period not evident at a camber angle with the transverse cleat it can be concluded that the slight decrease in stiffness of the 100% worn tread, compared to the 50% worn tread, is an actual trait of the tyre as it is worn. Still, these results are not usable due to the uncertainty surrounding the tread profile and uneven wear.

These trends are confirmed in Figure 6.17 and are decidedly not representative of the tyre as it is worn.

WEAR

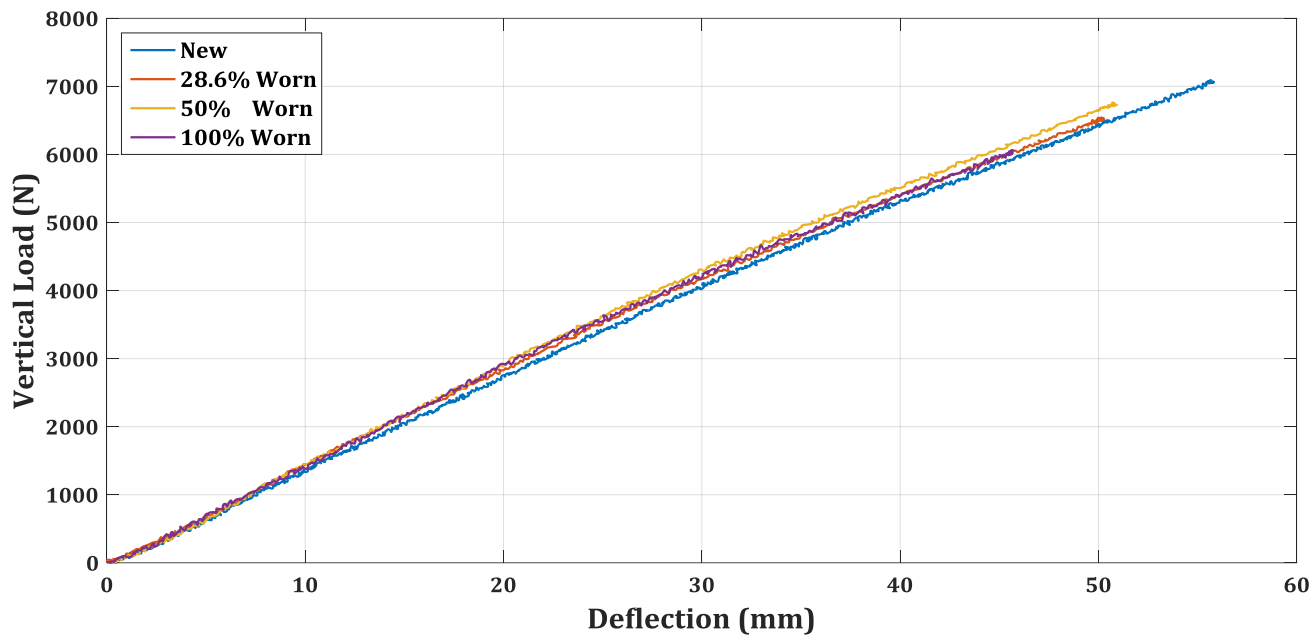


Figure 6.16 - Changes in vertical stiffness on a transverse cleat at -4° camber as the tyre is worn

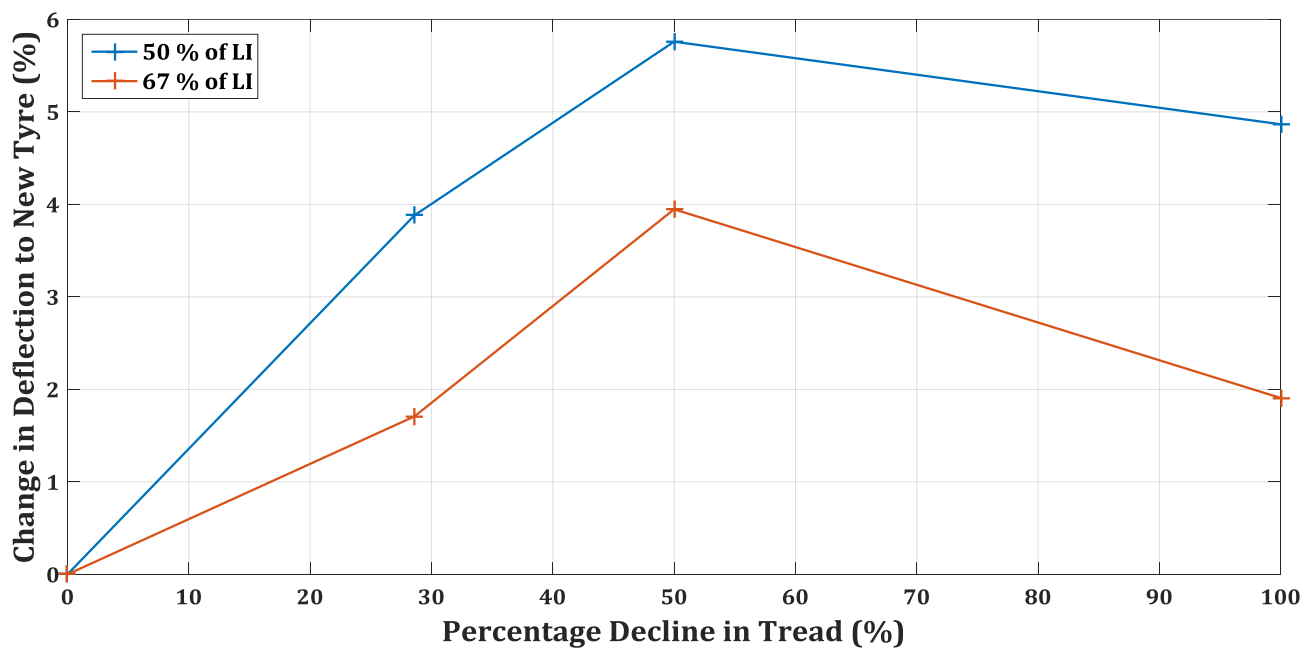


Figure 6.17 - Percentile changes in deflection on a transverse cleat at -4° camber as the tyre is worn

6.5.2.2 Longitudinal Cleat

The vertical stiffness tests on a longitudinal cleat are presented in Figure 6.18 and illustrate some interesting trends as the tyre is worn. By far the largest deviations in stiffness are observed between the new and fully worn tyre at just less than 50% of the LI. However, this expected trend changes after the rest of the tyre makes contact with the mounting surface. Although the fully worn tyre is still shown to be slightly less stiff, the deviation is less significant as was observed prior to the nick point in the stiffnesses.

WEAR

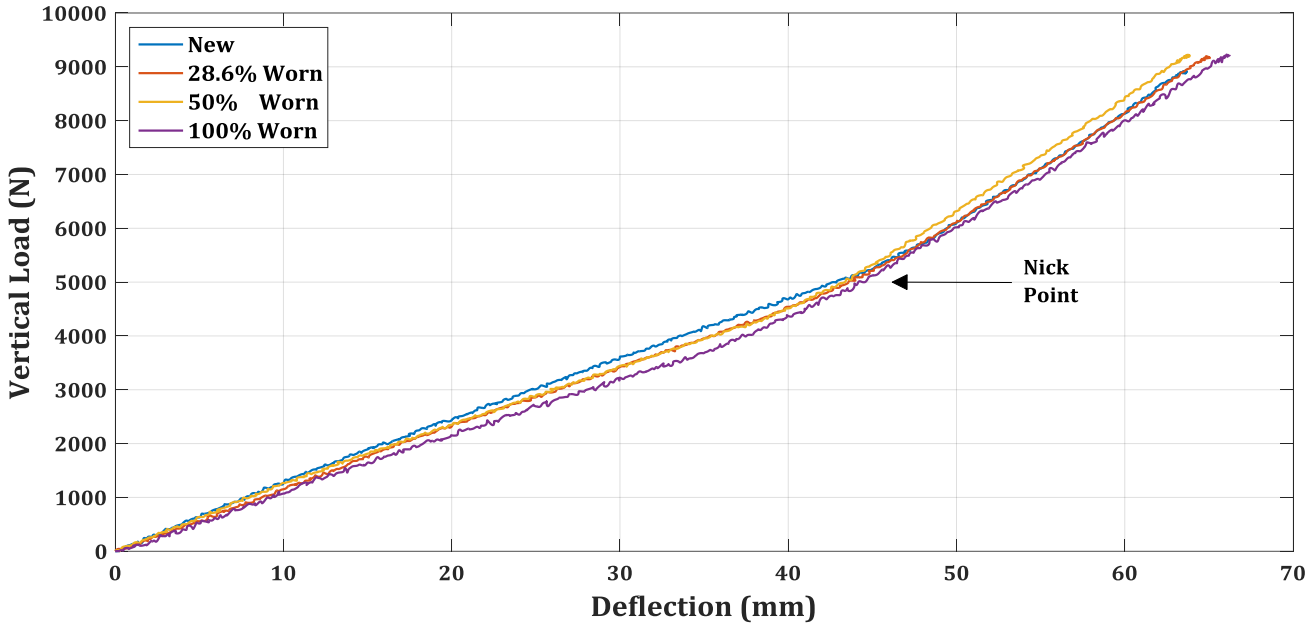


Figure 6.18 - Changes in deflection on a longitudinal cleat as the tyre is worn

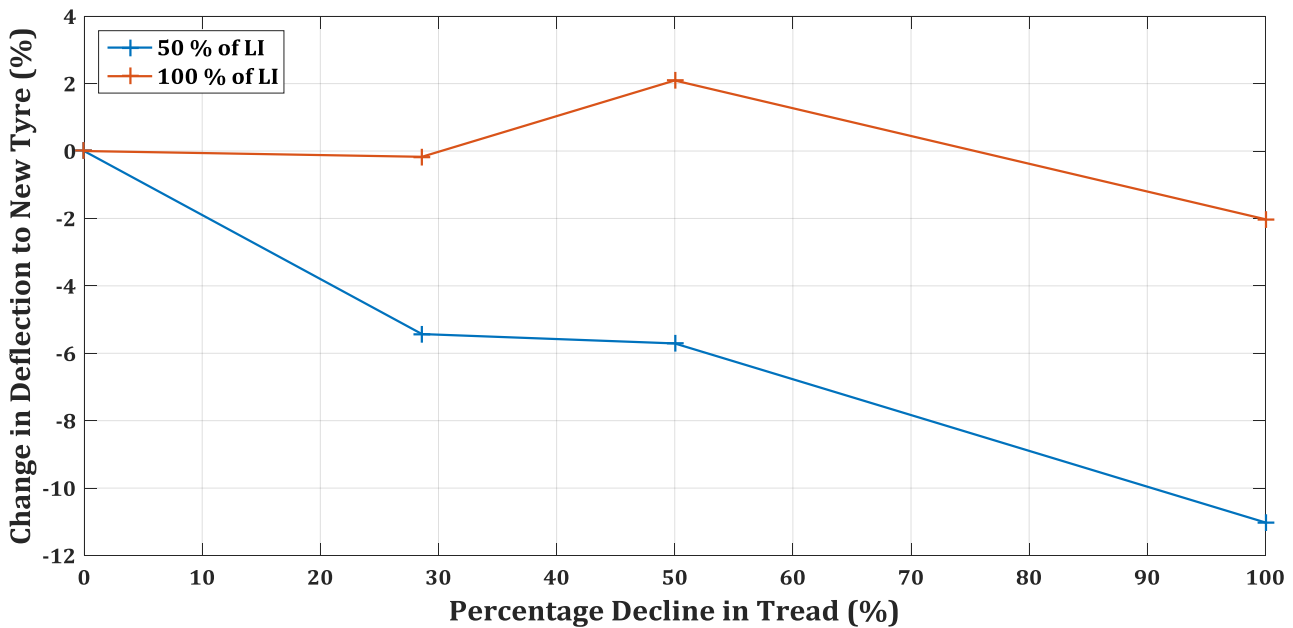


Figure 6.19 - Percentile change in deflection on a longitudinal cleat at 50 and 100% of the LI as the tyre is worn

These trends are clearly evident in Figure 6.19 where the expected trend of a decrease in stiffness with a decrease in the tread occurs at the 50% of the LI deflection values. The sudden change observed after the nick point at around 5kN could simply be due to the irregular tread profile at the contact patch. While the tread around the contact patch is not as dominant a contributing factor when it is only in contact with the cleat, it appears to have much more of an influence when it makes contact with the mounting surface.

WEAR

6.5.3 Longitudinal Stiffness

Figure 6.20 shows the change in the longitudinal stiffness as a function of the wear of the tyre. Clearly evident from this figure are significantly larger deviations in the stiffnesses than previously seen in this investigation. Once again the data from the ULP load cell is used to validate the stiffness data of the WFT for forces larger than 1200N. The results are summarised in Figure 6.21 and it is quite clear from this figure that the percentile changes are almost double those values previously seen.

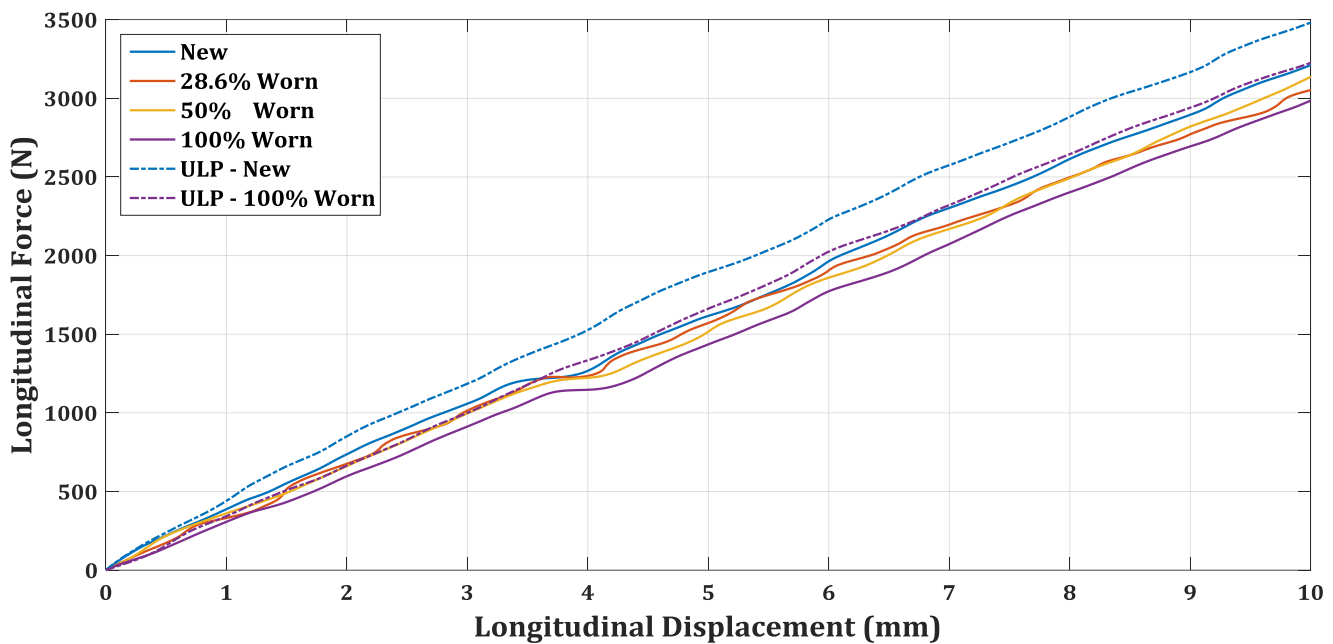


Figure 6.20 - Changes in the longitudinal stiffness as the tyre is worn

It is of utmost importance to recall the large discrepancies in longitudinal deflection noticed between the new and run-in tyre of Section 0. Here percentile changes in longitudinal deflection were shown to be -6.7% at around 2kN (or 50% of the maximum longitudinal force acquired). Once the values in Figure 6.21 are updated to include the effects of the run-in period of the tyre, the deviations drop significantly. This resultant graph does show an initial increase in the deflection yet this could be due to the tyre not having done the same run-in time or distance as that of the run-in test tyre.

Nevertheless, there still appears to be a trend in the lowering of the longitudinal stiffness of the tyre only due to wear. These updated values are more in line with the deviations previously seen in this investigation.

Additionally, the trend evident in the ULP load cell percentile deflection data correlates to an extent with that of the WFT data but is just slightly lower. It could be argued that the reason for this trend in deviations is due to the fact that the longitudinal stiffness is much less dependent on

WEAR

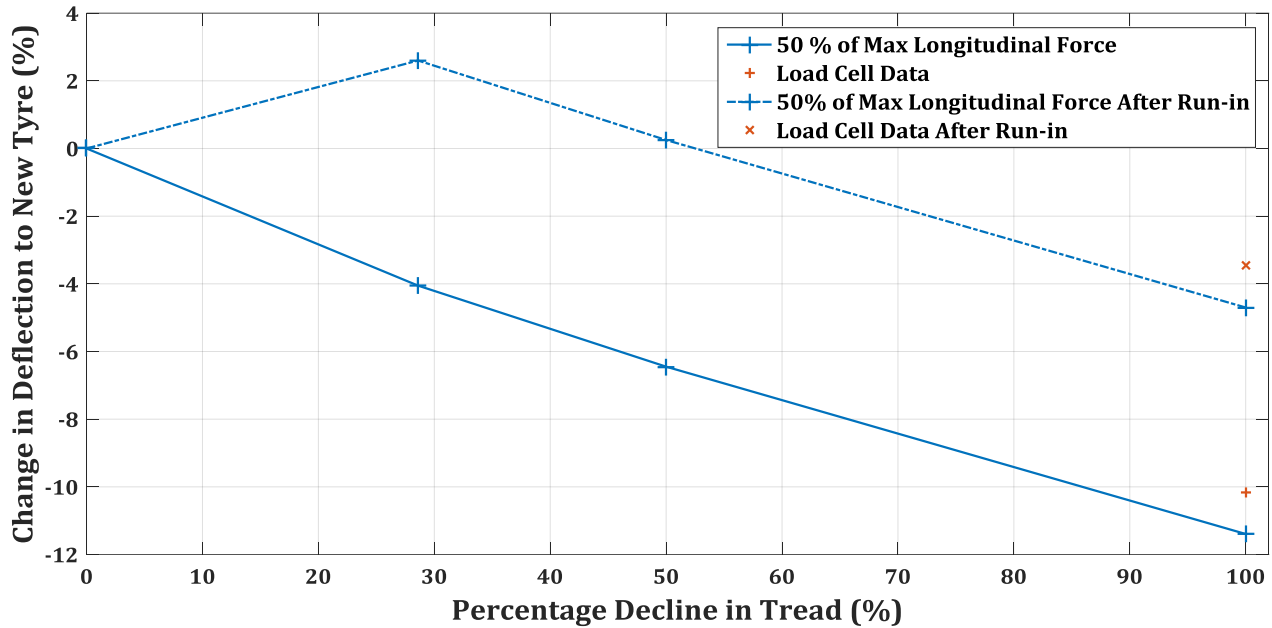


Figure 6.21 - Percentile change in deflection at 50% of the maximum longitudinal force acquired

the tread profile at the contact patch and more a function of the longitudinal stiffness of the tyre as a whole.

6.6 DISCUSSION OF RESULTS

Figure 6.22 gives a good summation of the percentile change in deflection results presented in this chapter so far. The red threshold lines for the equipment measuring accuracy are easily exceeded on almost all accounts, however, no trend has been formed from the full set of data. The completely scattered behaviour of the results obtained demonstrate that further investigation is required on this topic with a much improved method of realistically wearing the tyre.

6.7 POTENTIAL FTIRE MODEL UPDATES

The effects due to the wear on a tyre were presented in the sections above. A single trend through all the stiffnesses tested was not clear. Irregularities in the tread profile are mainly to blame for this. One trend that did emerge is the distinction at 0° camber between a new and run-in tyre. This distinct feature was particularly noticeable in the vertical and longitudinal stiffness but a run-in tyre can only be distinguished from a new tyre by the mileage it has covered.

FTire does not account for such a feature and it would thus be recommended to either validate the tyre model such that the applicable stiffnesses are adjusted by the aforementioned percentage in deflection lower than the test data of a new tyre. Alternatively, the tyre should be run-in prior to conducting the parameterisation tests.

WEAR

Nevertheless, methods of updating the tyre model due to tread wear do exist. A method using the mass and tread depth will be investigated in this section as a means for updating the tyre model. The changes noticed in the tyre model stiffnesses will be held in the same light as the changes observed above.

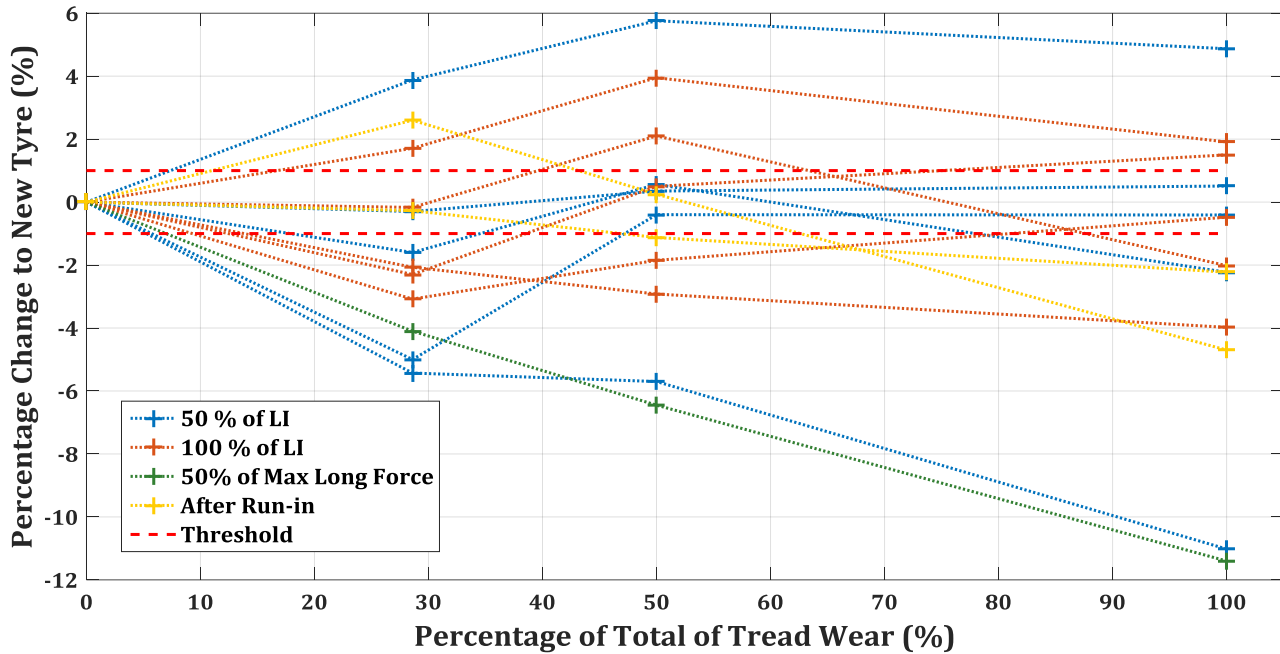


Figure 6.22 - Percentile change in deflection of all test data

6.7.1 Mass and Tread Depth Update

The most sensible parameters which can be used to update the FTire tyre model are the mass and tread depth of the tyre. These two parameters are directly linked and should thus be adjusted accordingly. There are several means of simply acquiring this data. Firstly the mass of the tyre can be measured when the tyre is new and again when the model is being updated. In the case where a new tyre isn't or wasn't available a tread depth gauge can be used to measure average depth of the tread. Knowing either of these and the outermost diameter of the tyre both values can be approximated using the density of the rubber. With the exact value of the density not being easy to acquire it would require the user to use a combination of the tread wear measured as well as the mass of the tyre.

In this case the change in mass is known to be 2.1kg from the new tyre to the full worn tyre. While this mass will be used, an average tread depth of 2mm will be used opposed to 0mm due to the fact that the wear was so uneven across and around the tyre.

WEAR

Figure 6.23 shows the change in footprint of the tyre model. It has not been compared to the footprint produced after wearing due to the irregular tread wear that was prevalent during this process. Figure 6.23 indicates that FTire predicts a noticeable decrease in the area of the tyre model's footprint. This is interesting as it would imply that the tyre has become stiffer whereas from the results shown above it is expected for the tyre to become less stiff.



Figure 6.23 - Changes in the footprint at 0° camber after model update of mass and tread depth - Left is the original model, Right is the updated model

If anything, the opposite of all the stiffnesses tested is demonstrated in Figure 6.24. Here the stiffnesses on a flat surface and on a transverse cleat at 0° and -4° camber are shown with the stiffness on a longitudinal cleat and finally the longitudinal stiffness. In all cases, where a noticeable change has occurred, there was a decrease in the stiffness.

Major variation is observed in both cases where a camber angle was introduced as seen in Figure 6.24 (a) and (b). This change appears due to a significantly lower initial stiffness followed by a sudden change and then a stiffness very similar to that of the original tyre. This is a trend usually seen with the longitudinal cleat where the sudden change in gradient is due to the rest of the tyre making contact with the surface on which the cleat is mounted. However, in this case, especially with the flat surface test at camber, this does not occur.

A similar trend is evident in the test with the longitudinal cleat. Here the stiffness is perceived to be initially almost negligible. This is highly unusual behaviour and is not thought to be representative of the actual tyre. The FTire tyre model does not appear to accurately capture the

WEAR

change in the tread depth for this test. However, with the inaccurate test results due to irregular tyre wear it cannot be said whether this is or isn't representative of the tyre behaviour.

Lastly, with regard to the longitudinal stiffness where the most reliable test data based on the wear of the tyre was acquired, the hypothesised result is observed with the updated tyre model.

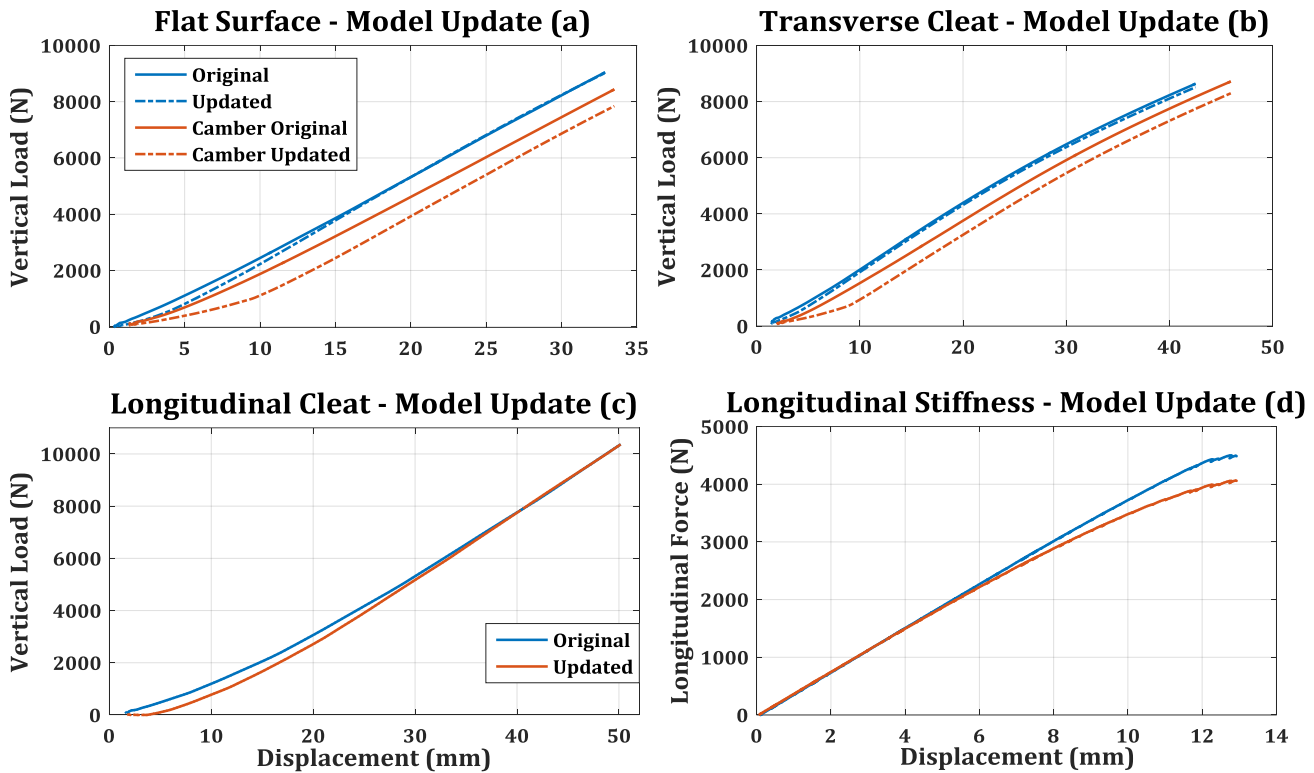


Figure 6.24 - FTire tyre model mass and tread depth update effect on various stiffnesses tested

Here the stiffness decreases with an increase in longitudinal forces. Validation of this updated model was completed with the longitudinal stiffness tested on the fully worn tyre and is shown in Figure 6.25.

It is important to keep in mind the decrease in stiffness due to the run-in period of the tyre. This will shift the fully worn measured stiffness line by approximately 0.4mm to the left in Figure 6.25. Despite it being an error prone measurement, the gradients correlate quite well despite the obvious offset.

WEAR

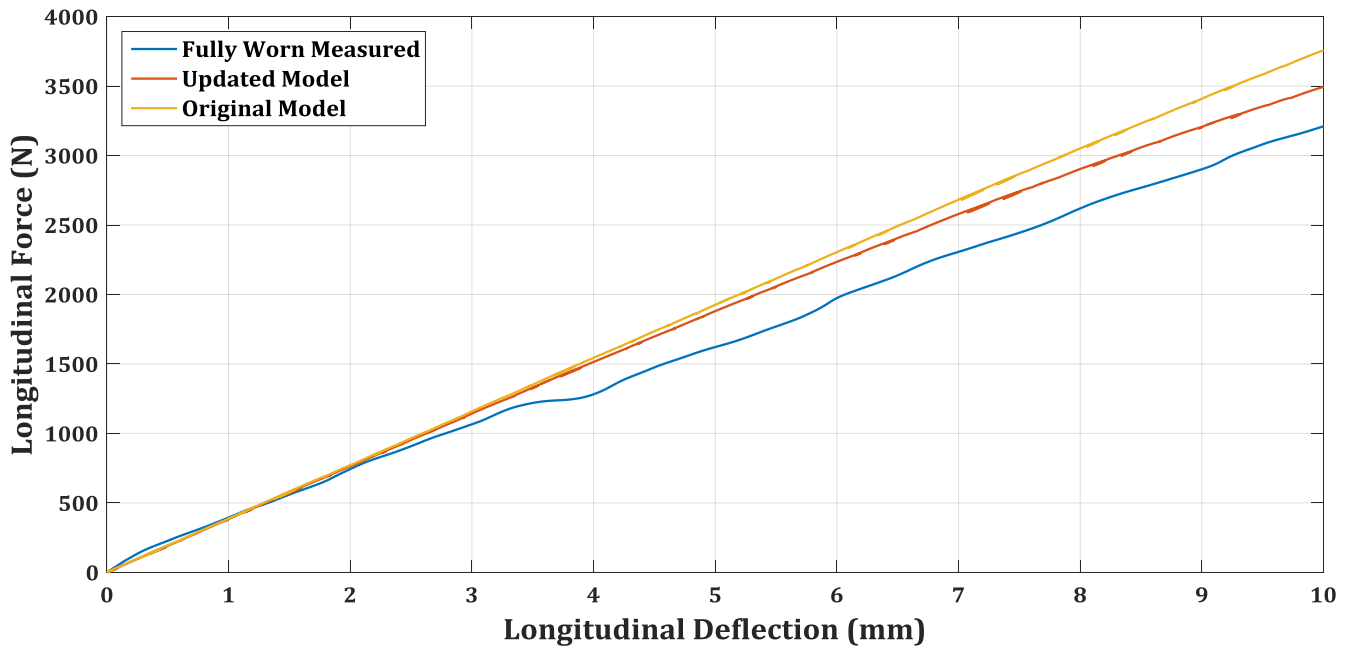


Figure 6.25 - FTire tyre model update validation with measured longitudinal stiffness after wearing

6.8 CONCLUDING REMARKS

The investigation above illustrates a variety of changes in the tyre characteristics as the tyre is worn. Unfortunately, not all data captured and presented is reliable due to severe uneven wear across and around the tyre. The effects of uneven wear around the tyre, such as flat spots, were shown to produce at worst a 2.7% difference in the deflection at the LI. Furthermore, the effect of uneven wear across the tyre (in the lateral direction) was illustrated in the footprints. Here, a camber angle appeared to have been induced on the tyre despite the test being conducted on a flat surface.

As a result of these inconsistencies, a specific trend attributable to the wear of the tyre was not apparent. A very clear trend was apparent in the comparison between the new tyre and the one that had been run-in. These effects were clear on tests at 0° camber on a flat surface and with the transverse cleat as well as most noticeably with the longitudinal stiffness. These changes were shown to be sufficient to motivate a model update, however, it is a very difficult parameter or adjustment to quantify and resultantly update in the FTire tyre model. The simplest method of updating the tyre model would be to adjust the new tyre measured stiffnesses by the percentile deflection figures shown in Section 6.3.1. Alternatively, the tyre would need to be tested after a run-in period has been completed with the tyre.

Due to the irregularities in tread wear mentioned above, it was found that the longitudinal stiffness test demonstrated the most consistent results based on the wear of the tyre. After accounting for the run-in period of the tyre it showed a consistent decrease in percentile deflection at 50% of the maximum longitudinal force acquired which was furthermore well above

WEAR

the testing accuracy threshold. The consistency of this test is arguably due to its independency from the tread profile at the contact patch.

Based on this longitudinal stiffness test the largest potential error being made by not updating the tyre model due to severe wear on the tyre of concern is just larger than 4% in longitudinal deflection. Further investigation is required, however, to confirm this for the other vertical stiffnesses which indicate a clear dependency on the tread profile at the contact patch.

Finally, the FTire tyre model shows some potential in accurately predicting these changes in tyre characteristics due to wear by simply adjusting the mass and tread depth of the tyre appropriately. It requires further validation with test data on an evenly worn tyre but the link between a lack of tread and a softening in the overall tyre stiffness certainly exists.

7 CONCLUSION AND RECOMMENDATIONS

7.1 CONCLUSION

The investigations carried out in this dissertation successfully quantified the effects of aging and wear on the stiffnesses of a tyre. An initial sensitivity analysis was presented on the accuracy of the static test setup and testing procedure. This produced a threshold value by which any effects later observed in the tyre stiffnesses would need to overcome to become noteworthy.

In general this threshold of $\pm 1\%$ was commonly exceeded by the aging and wearing effects presented. However, some additional influences were also presented which also demonstrated noticeable changes to the tyre stiffnesses. Most significant of these influences was that of a run-in tyre. This proved to be a period in the operational life of the tyre which needs to be accounted for if percentile changes in deflection more accurate than 1.5% in the tyre model are desired.

Ultimately, the largest possible error between a severely aged tyre and a tyre model based on a new tyre is approximately 5%. In the case of the wear investigation irregularities in the wearing procedure made it difficult to identify a trend and specifically quantify the effects. The most noticeable effect was observed with the longitudinal stiffness due to its potential independence from the tread at the contact patch. Here a maximum error of 4% would be made if the wear of a tyre is ignored in the tyre model. However, this feature requires further investigation.

In addition to this, an FTire model was fully parameterised with the test data that was acquired. Successful validation was obtained between the test data and that of the tyre model. This tyre model was then used to check its ability on adapting to the changes observed in the aging and wear analysis. A simple method such as measuring the Shore A hardness of the tread was used to update the tyre model for a change in the age of the tyre. This showed promising results as it certainly had an overall impact on all the stiffnesses of the tyre.

This method was combined with altering the tread depth and mass of the tyre to update the tyre based on the wear it had experienced. These also demonstrated promising results, however, the actual test data acquired based on the wear of the tyre was too irregular and inconsistent to validate these changes.

The collective effort of a well validated FTire tyre model, a critically quantified static tyre testing procedure accuracy and both noticeable and negligible changes in static tyre stiffnesses due to the wear and age of a tyre were thoroughly scrutinised and presented together with the potential of simply updating the tyre model conclude a successful investigation.

CONCLUSION AND RECOMMENDATIONS

The changes in tyre properties due to aging and wear were quantifiably small and can be neglected for most purposes. Methods of updating the tyre model demonstrated noticeable influence but were unnecessary given the small changes due to age or wear. Running in the tyre before testing is expected to result in a better tyre model with little effort or cost.

7.2 RECOMMENDATIONS

Despite the overall success of the investigation, there are several areas which require further analysis, they include:

- The same wear investigation can be repeated using a far less abrasive wearing method such as buffing or normal road use in a controlled environment. This is to ensure that a uniform wear is created around and across the tyre as this severely influences the static test data of the tyre. This should be followed by validating the method of updating the FTire tyre model using the change in mass and tread depth.
- A combined effort of wearing and aging a tyre can also be investigated; this gives a more realistic version of the aged tyre test.
- A thorough investigation is warranted into the effects of the run-in period of a tyre. This can include the minimum vertical load and distance required to replicate the properties of a run-in tyre.
- Further scrutinising can be completed on the effects to the hysteresis loop of the vertical stiffness of a tyre as it is worn and aged. This may also become evident if the damping properties are properly acquired on the worn and aged tyre. The effect of locking the wheel against having it freely rotate on the static test setup can further validate the accuracy of the testing procedure.
- For the FTire model, a consistent and trustworthy method of acquiring the dynamic cleat tests should be considered. This allows the user to validate the damping properties of the tyre which can be crucial to the wear and age research.
- Investigate effects in large off-road tyres where big tread blocks may have larger effects due to wear.
- Further investigate the roll over moment of the tyre and the unusual WFT data acquired for the longitudinal and lateral stiffness of the tyre. Examine whether or not it is a potential phenomenon of the tyre due to its asymmetric tread pattern.

8 REFERENCES

Acuity [Online] // Acuity Laser. - Acuity, 2016. - 1 11 2016. - <http://www.acuitylaser.com/products/item/ar700-laser-displacement-sensor>.

Assaad M C and Ebbott T G Mechanics of Cord-Rubber Composite Materials [Book Section] // The Pneumatic Tire / book auth. Administration National Highway Traffic Safety. - Washington DC : U.S Department of Transport, 2006.

Baldwin J M Accelerated Aging of Tires, Part 1 [Journal] // American Chemical Society. - Cleveland : American Chemical Society, 2003.

Baldwin J M and Bauer D R Rubber Oxidation and Tire Aging - A Reivew [Report]. - Farmington Hills : Exponent Failure Analysis Associates, 2008.

Baldwin J M, Bauer D R and Ellwood K R Accelerated Aging of Tires, Part 2 [Journal]. - Dearborn : Rubber Chemistry and Technology, 2005. - 2 : Vol. 78. - p. 336.

Baldwin J M, Bauer D R and Ellwood K R Accelerated Aging of Tires, Part 3 [Journal]. - Dearborn : Rubber Chemistry and Technology, 2005. - 5 : Vol. 78. - 767.

Baldwin J M, Bauer D R and Ellwood K R Rubber Aging in Tires. Part 1: Field results [Journal]. - Dearborn : Polymer Degradation and Stability, 2006. - 103 : Vol. 92. - 109.

Baldwin J M, Bauer D R and Hurley P D Field Aging of Tires, Part 2 [Journal]. - Dearborn : Rubber Chemistry and Technology, 2005. - 5 : Vol. 78. - p. 754.

Bauer D R, Baldwin J M and Ellwood K R Correlation of Rubber Properties between Field Aged and Laboratory Aged Tires [Journal]. - Dearborn : Rubber Chemistry and Technology, 2005. - 5 : Vol. 78. - 777.

Blundell M and Harty D The Multibody Systems Approach to Vehicle Dynamics [Book]. - Oxford : Elsevier, 2004.

Botha T R and Els P S Digital image correlation techniques for measuring tyre-road interface parameters: Part 1 and 2 [Journal]. - Pretoria : Journal of Terramechanics, 2014. - 87-112 : Vol. 61.

Ellwood K. R. J, Baldwin J. and Bauer D. R. A Finite Element Model for Oven Aged Tires [Journal]. - Dearborn : Tire Science and Technology, 2004. - 2 : Vol. 33. - pp. 103-119.

Els P S [et al.] Comparison of Tire Footprint Measurement Techniques [Conference] // IDETC2016-59944. - Charlotte : ASME, 2016.

REFERENCES

- Gent A N** Mechanical Properties of Rubber [Book Section] // The Pneumatic Tire / book auth. Administration National Highway Traffic Safety. - Washington DC : U.S Department of Transport, 2006.
- Gillespie T D** Fundamentals of Vehicle Dynamics [Book]. - Warrendale : Society of Automotive Engineers, Inc., 1992.
- Gipser and Hofmann** FTire Parameterization [Report]. - Munich : Cosin, 2016.
- Gipser M and Hoffmann G** FTire - Flexible Structure Tire Model. - Munich : Cosin, 2016. - Vol. 3.
- Gipser M** FTire: a physically based application-orientated tyre model for use with detailed MBS and finite-element suspension models [Journal]. - Esslingen : Taylor and Francis, 2005. - Vehicle System Dynamics : Vol. 43.
- Indian Standard** Passenger car, truck, bus and motorcycle tyres - methods of measuring rolling resistance [Report]. - New Delhi : Bureau of Indian Standards, 2010.
- Kataoka T, Zetterlund P B and Yamada B** Effects of Storage and Service on Tire Performance: Oil Component Content and Swelling Behaviour [Journal]. - Akron : Rubber Chemistry and Technology, 2003. - 1 : Vol. 76. - 507.
- Kerchman V.** Gas Transport in the Tire Aging Test and Intracarcass Pressure Issues [Journal]. - Akron : Tire Science and Technology, 2011. - 2 : Vol. 39. - pp. 95-124.
- LaClair T J** Rolling Resistance [Book Section] // The Pneumatic Tire / book auth. Administration National Highway Traffic Safety. - Washington DC : U.S Department of Transport, 2006.
- McDonel E T** Tire Cord and Cord-to-Rubber Bonding [Book Section] // The Pneumatic Tire / book auth. Administration National Highway Traffic Safety. - Washington DC : U.S Department of Transport, 2006.
- National Highway Traffic Safety Administration** EA00-023: Firestone Wilderness AT Tires [Report]. - [s.l.] : U.S Department of Transportation, 2001.
- National Highway Traffic Safety Administration** FMVSS 139 - New Pneumatic Radial Tires for Light Vehicles [Report]. - Washington DC : U.S Department of Transport, 2006. - TP-139-02.
- National Highway Traffic Safety Administration** NHTSA Tire Aging Test Development Project: Phase 1 - Phoenix, Arizona Tire Study [Report]. - Washington DC : U.S Department of Transportation, 2003. - 07-0496.

REFERENCES

Pottinger M G Forces and Moments [Book Section] // The Pneumatic Tyre / book auth. Administration National Highway Traffic Safety. - Washington DC : U.S Department of Transport, 2006.

Rao S S Mechanical Vibrations [Report]. - Upper Saddle River : Pearson, 2011.

Sandberg U The influence of tyre wear and ageing on tyre/road noise emission and rolling resistance [Report]. - [s.l.] : Swedish Road and Transport Research Institute, 2008.

Unrau H J, Zamow J and Porsche F TYDEX-Format: Description and Reference Manual [Report]. - [s.l.] : Tydex, 1997.

Walter J D Tire Standards and Specifications [Book Section] // The Pneumatic Tyre / book auth. Administration National Highway Traffic Safety. - Washington DC : U.S Department of Transport, 2006.

Yong L [et al.] Analysis of impact factors of tire wear [Journal]. - [s.l.] : Journal of Vibration and Control, 2011. - 833-840 : Vol. 18.

APPENDIX A

8.1 AGING TABLES

Changes in deflection on a flat surface at 50 and 100 % of the LI during aging

Load	50 % of the LI		100 % of the LI	
Weeks in Oven	Δ Deflection (mm)	Δ Deflection (%)	Δ Deflection (mm)	Δ Deflection (%)
1	-0.56	-2.63	-1.46	-3.46
2.5	-0.04	-0.2	-0.23	-0.54
4.1	1.12	5.24	1.19	2.8
8.8	1.26	5.9	1.36	3.2

Change in deflection on a flat surface at camber at 50 and 100% of the LI during aging

Load	50 % of the LI		100 % of the LI	
Weeks in Oven	Δ Deflection (mm)	Δ Deflection (%)	Δ Deflection (mm)	Δ Deflection (%)
2.5	0.82	3.42	1.21	2.65
4.1	0.75	3.16	1.63	3.55
8.8	1.57	6.56	2.54	5.54

Change in deflection on a transverse cleat at 50 and 75% of the LI

Load	50 % of the LI		85 % of the LI	
Weeks in Oven	Δ Deflection (mm)	Δ Deflection (%)	Δ Deflection (mm)	Δ Deflection (%)
1	0.2	0.76	1.17	1.88
2.5	0.45	1.67	1.74	2.8
4.1	1.00	3.72	2.34	3.77
8.8	1.32	4.85	2.95	4.75

APPENDIX A

Changes in deflection on a longitudinal cleat at 50 and 100 % of the LI

Load	50 % of the LI		100 % of the LI	
Weeks in Oven	Δ Deflection (mm)	Δ Deflection (%)	Δ Deflection (mm)	Δ Deflection (%)
1	-1.04	-3.1	-0.4	-0.63
2.5	-0.77	-2.3	0.35	0.5
4.1	0.4	1.2	0.78	1.23
8.8	0.9	2.7	1.77	2.8

Changes in longitudinal deflection at 50% of the maximum longitudinal force

Load	50 % of Maximum Longitudinal Force		Longitudinal Load Cell at 50 %	
Weeks in Oven	Δ Deflection (mm)	Δ Deflection (%)	Δ Deflection (mm)	Δ Deflection (%)
1	-0.28	-3.56		
2.5	-0.07	-0.9		
4.1	0.42	5.4		
8.8	0.69	8.85	0.4	5.61

8.2 WEARING TABLES

Changes in deflection on a flat surface at 50 and 100% of the LI whilst the tyre is worn

Load	50 % of the LI		100 % of the LI	
Tread Wear (%)	Δ Deflection (mm)	Δ Deflection (%)	Δ Deflection (mm)	Δ Deflection (%)
28.6	-1.06	-5.0	-1.24	-3.08
50	-0.08	-0.4	-0.75	-1.85
100	-0.09	-0.41	-0.2	-0.48

APPENDIX A
Changes in deflection on a flat surface at -4° camber at 50 and 100% of the LI whilst the tyre is worn

Load	50 % of the LI		100 % of the LI	
Tread Wear (%)	Δ Deflection (mm)	Δ Deflection (%)	Δ Deflection (mm)	Δ Deflection (%)
28.6	-0.3	-1.3	-0.97	-2.3
50	0.35	1.5	0.2	0.5
100	0.51	2.2	0.64	1.5

Changes in deflection on a transverse cleat at 50 and 78% of the LI as the tyre is worn

Load	50 % of the LI		78 % of the LI	
Tread Wear (%)	Δ Deflection (mm)	Δ Deflection (%)	Δ Deflection (mm)	Δ Deflection (%)
28.6	-0.44	-1.6	-1.08	-2.07
50	0.15	0.56	-1.52	-2.92
100	-0.6	-2.23	-2.07	-3.98

Changes in deflection on a transverse cleat at -4° camber at 50 and 67% of the LI as the tyre is worn

Load	50 % of the LI		67 % of the LI	
Tread Wear (%)	Δ Deflection (mm)	Δ Deflection (%)	Δ Deflection (mm)	Δ Deflection (%)
28.6	1.15	3.88	0.79	1.71
50	1.7	5.76	1.82	3.95
100	1.44	4.87	0.88	1.91

Changes in deflection on a longitudinal cleat at 50 and 100% of the LI as the tyre is worn

Load	50 % of the LI		67 % of the LI	
Tread Wear (%)	Δ Deflection (mm)	Δ Deflection (%)	Δ Deflection (mm)	Δ Deflection (%)
28.6	-1.82	-5.43	-0.11	-0.17
50	-1.91	-5.7	1.32	2.1
100	-3.7	-11.02	-1.28	-2.02

APPENDIX A
Changes in longitudinal deflection at 50% of the maximum longitudinal force as the tyre wears

Load	50 % of Maximum Longitudinal Force		Longitudinal Load Cell at 50 %	
Tread Wear (%)	Δ Deflection (mm)	Δ Deflection (%)	Δ Deflection (mm)	Δ Deflection (%)
28.6	-0.25	-4.1		
50	-0.4	-6.45		
100	-0.7	-11.4	-0.55	-10.15